In vivo study of the role of the cytoskeleton and fungal Golgi in hyphal tip growth of *Aspergillus nidulans*

A Thesis submitted to the College of
Graduate Studies and Research
In Partial Fulfillment of the Requirements
For the Degree of Master of Science
In the Department of Biology
University of Saskatchewan
Saskatoon

By
Michelle Hubbard

Keywords: *Aspergillus nidulans,* hyphae, polar growth, microtubules, Golgi

PERMISSION TO USE

In presenting this thesis in partial fulfillment of the requirements for a postgraduate degree from the University of Saskatchewan, I agree that the libraries of this university may make it freely available for inspection. I further agree that permission for copying of this thesis in any manner, in whole or in part, for scholarly purposed may be granted by the professors who supervised my thesis work or, in their absence, by the Head of the Department or Dean of the college in which my thesis work was done. It is understood that any copying or publication or use of this thesis or parts thereof for financial gain shall not be allowed without my written permission. It is also understood that due recognition shall be given to me and to the University of Saskatchewan in any scholarly use which may be made of any material in my thesis.

Requests for permission to copy or to make other use of material in this thesis in whole or in part should be addressed to:

Head of the Department of Biology
University of Saskatchewan
Saskatoon, Saskatchewan S7N 5E2

ABSTRACT

Filamentous fungi, such as *Aspergillus nidulans*, are composed of tubular, highly polarized, multinucleate cells called hyphae. Polar growth involves secretion specifically at the hyphal tip. Secretion involves intracellular transport and co-ordination of the cytoskeleton and the endomembrane system.

Intracellular transport is likely mediated by cytoskeletal elements, which, in fungal cells consist primarily of actin and microtubules (MTs). An *A. nidulans* strain transformed with green fluorescent protein (GFP) tagged α-tubulin was utilized in the investigation of relationship between cytoplasmic MT arrays and hyphal growth rate. *A. nidulans* MTs were observed to be long and flexuous and to run roughly parallel to the long axis of hyphae. No correlation between relative MT abundance and hyphal growth rate was observed, although non-growing hyphae had a lower relative MT abundance than growing hyphae. Actin depolymerization decreased hyphal growth rate while MT depolymerization did not. MT stabilization increased hyphal growth rate. Ethanol, the solvent in which the MT and actin inhibitors were dissolved, increased both average overall growth rate and growth rate variability for individual hyphae. Taxol appeared to interact with irradiation to decreased growth rate during imaging.

Golgi are involved in secretion and potentially in polar growth. An *A. nidulans* α-coatomer protein (COP)I homolog (α-COPI), tagged with GFP, was used to investigate the role(s) of fungal Golgi in polar growth. α-COPI-GFP co-localized with the known Golgi marker, α-2, 6-sialyltransferase (ST), tagged with red fluorescent protein (RFP), in untreated hyphae. Based on this observation, I propose that α-COPI-GFP can be used as a proxy for fungal Golgi localization. Fungal Golgi were more abundant at hyphal tips than subapically. Fungal Golgi forward (tipward) velocity correlated with hyphal growth rate. Fungal Golgi forward velocity was, on average, approximately ten times greater than average hyphal growth rate. Actin depolymerization reduced fungal Golgi forward velocity while MT depolymerization did not. However, MT stabilization increased fungal Golgi forward velocity.

Polymerized MTs do not appear to be essential for hyphal growth but do appear to be involved in hyphal growth rate variability. MTs also appear to play some role in the

movement of fungal Golgi. The distribution and movement of fungal Golgi is clearly related to polarity.

ACKNOWLEDGMENTS

This thesis is the results of two years of work whereby I have been accompanied and supported by many people. It is with pleasure that I now have the opportunity to express my gratitude for all of these people.

The first person I would like to thank is my supervisor Dr. Susan Kaminskyj for her academic guidance, project design and patience with my studies. I am thankful to my supervisory committee members, Drs. Sean Hemmingsen, Federica Brandizzi and Larry Fowke for their advice and help during my studies. I would also like to thank Brenda Haug for her assistance with Western blots and Liz and Berl Oakley, Ohio State University, for the LO1022 strain.

I would also like to express my warmest gratitude to my parents, my partner Rob Moroz and friends for their support over the past two years.

This thesis work is supported by a University of Saskatchewan Dean's Scholarship and a National Science and Engineering Research Council (NSERC) Masters Canada Graduate Scholarship. The Canada Foundation for Innovation provided funding for the purchase of the Zeiss META510 confocal microscope used in work for this thesis.

TABLE OF CONTENTS

LIST OF FIGURES

LIST OF ABBREVIATIONS

ARF	ADP-ribosylation factor
BFA	brefeldin A
CM	complete media
COPI	coatomer protein I
ER	endoplasmic reticulum
GEF	GDP exchange factor
GFP	green fluorescent protein
MBC	methyl benzimidazole-2-ylcarbamate
MT	microtubule
RFP	red fluorescent protein
sod^{VI}C	*s*uppression *o*f *d*isomy of chromosome VI
ST	α-2, 6-sialyltransferase
TEM	transmission electron microscopy

CHAPTER 1: Introduction

1-1. Cell polarity

1-1.1. General features of cell polarity

Polarity can be broadly defined as the generation and maintenance of specialized regions. It is found in taxonomically diverse biological systems. Filamentous fungi are highly polarized (reviewed in Bartnicki-Garcia 2002; Harris 2006; Heath 1990a, 1994) and hence are exemplary model systems for studying polar growth. The generation and maintenance of specialized regions involves targeted secretion of materials needed for cell growth such as cell wall and membrane constituents (reviewed in Bartnicki-Garcia 2002). Targeted secretion requires co-ordination of cellular machinery (reviewed in Bartnicki-Garcia 2002; Heath 1990a), including the cytoskeleton (reviewed in Heath 1994, 1995) and the endomembrane system (reviewed in Heath 1994). Polarity is complex. Thus, it is useful to break the phenomenon of polarity down into more easily studied components rather than attempting to study polarity as a whole. This thesis presents insight into certain aspects of polarity relating to the cytoskeleton and endomembrane system in the model filamentous fungus *Aspergillus nidulans.*

1-1.2. Cell polarity in filamentous fungi

Fungi are eukaryotic, heterotrophic organisms that reproduce by spores (Kendrick 2000). Fungi are composed of long, multinucleate, walled tubular cells called hyphae (Kendrick 2000). Hyphae are divided into compartments by cross walls called septa (Bessey 1950). The individual compartments have some developmental autonomy, for example regarding sporulation, but the septa are perforate (Buller 1933; Moore and McAlear 1962) to allow continuity at least of turgor pressure, and likely of passage of small metabolites.

Fungal hyphae are highly polarized cells (reviewed in Bartnicki-Garcia 2002; Heath 1990a) in that growth takes place only at tips or at branch sites accompanied by no or minimal lateral growth (Kendrick 2000). Thus fungal hyphae are extremely polar in that they do more than generate and maintain specialized regions. Filamentous fungi are experimentally tractable in that they possess small genomes compared to other eukaryotes (Cavalier-Smith 1985), few vegetative cell types, short life cycles and haploid

vegetative cells (Kendrick 2000). In addition, in some well-studied organisms, such as *A. nidulans*, many biological tools such as temperature sensitive mutant alleles and genes fused with DNA sequences encoding fluorescently proteins exist. A more detailed discussion of some of these biological tools will follow.

1-1.3. Suitability of *Aspergillus nidulans* as a model fungal system in which to study polarity

The genus *Aspergillus* is likely the fungal genus that is both the most useful and the harmful to humans. *Aspergillus nidulans* is related to species important to humans including human pathogens, crop spoilage and food production agents such as *A. fumigatus* (Denning 1998; Patterson et al. 2000), *A. flavus* (Moss 1998) and *A. sojae* respectively (Abe 2006; FAO/WHO 1987). Other *Aspergillus* species include *A. niger, A. terreus* and *A. oryzae.* These species have biotechnological relevance. For example, *A. niger* can be used in the manufacture of citric acid by fermentation of molasses (Ali 2006), *A. terreus* can be used in ethanol fermentation (Pushalker and Rao 1995, 1998) and *A. oryzae* has been used for hundreds of years in the production of soy sauce, miso and sake (Abe 2006). The genomes of *A. nidulans, A. fumigatus, A. niger, A. flavus A. terreus* and *A. oryzae* have all been sequenced (Board Institute).

The dual modes of fungal propagation, asexual anamorph and sexual telomorph, have been known since approximately 1861 (reviewed in Weresub and Pirozynski 1979). *Emericella nidulans* is the telomorph of *Aspergillus nidulans* (Kendrick 2000). *A. fumigatus, A. niger, A. flavus A. terreus* and *A. oryzae* have no known telomorph stages (Kendrick 2000). The existence of a sexual stage in *A. nidulans* facilitates sexual crosses, and hence more convenient genetic study; in the absence of known sexual stages, genetic crosses involving other *Aspergillus* species are more difficult. The anamorphs, or asexual forms, of *Aspergillus* species are difficult to distinguish from one another without a great deal of practice (Raper and Fennel 1965). This morphological similarity illustrates how closely related members of the *Aspergillus* genus are and suggests that biological properties found in one species may be extrapolated to apply to other species. Phylogenetic classification of *Aspergillus* species can be made on DNA sequence and/or on morphological data. Phylogenetic classification based on 18S rRNA sequences

indicated that *A. flavus*, *fumigatus*, *terreus, niger* and *nidulans* represent a monophyletic group (Verweij et al. 1995). In addition, a comparison to the whole genomes of *A. flavus* and *A. oryzae* shows a high degree of similarity (Payne et al. 2006).

The biology of *Aspergillus nidulans* has been thoroughly studied (e.g. Martinelli 1994). Its genome is sequenced (Broad Institute) and its life cycle and reproduction has been characterized (Adams et al. 1998; Champe et al. 1994; Doonan 1994; Timberlake and Clutterbuck 1994). Also, many genetic tools are available in *A. nidulans* such as morphological mutants and fluorescently tagged gene products (Fernández-Abalos et al. 1998; Suelmann et al. 1997) and morphogenesis mutant alleles (Kaminskyj and Hamer 1998; Malavazi et al. 2006; Shaw and Upadhyay 2005).

1-1.3.1. *HypA1* morphogenesis mutant allele

Morphogenesis mutants are used to identify loci involved in various processes related to polarity (e.g. Kaminskyj and Hamer 1998; Malavazi et al. 2006; Shaw and Upadhyay 2005). The *hypA1* mutant allele is part of a family of *A. nidulans* mutants known as the *hyp* for *hyp*ercellular mutant family (Kaminskyj and Hamer 1998). The *hyp*ercellular mutant family is characterized by having aberrant patterns of septation and showing defects in polarity establishment and tip growth (Kaminskyj and Hamer 1998). However, they have normal nuclear division cycles and can complete the asexual growth cycle at restrictive temperature (Kaminskyj and Hamer 1998). The *hypA1* mutant allele contains a nonconservative amino acid change resulting in a temperature sensitive phenotype (Kaminskyj and Hamer 1998; Shi et al. 2004). Temperature sensitivity is a useful tool in that even potentially lethal temperature sensitive mutants can be maintained and can complete their lifecycle at the permissive temperature (e.g. Harris et al. 1999). Also, temperature sensitive mutants facilitate the alteration of morphology of cells by changing the temperature from permissive to restrictive or vice versa (Harris et al. 1999; Kaminskyj and Hamer 1998; Shi et al. 2004). In *hypA1* mutant strains, hyphal growth resembles wildtype at 28˚C, but at 42˚C the *hypA1* mutation leads to defects in polarity (Kaminskyj and Hamer 1998; Shi et al. 2004). When growth temperature is changed from 42˚C to 28˚C, *hypA1* mutant cells regain the polarized wildtype morphology. The *hypA1* mutant phenotype defects include proliferation of nuclei in subapical cells and

decreased polarity characterized by delayed spore germination, increased hyphal diameter and reduced hyphal elongation (Kaminskyj and Hamer 1998; Shi et al. 2004). The *hypA1* mutant phenotype may affect the morphology of fungal Golgi and other components of the secretory system (Kaminskyj and Boire 2004; Shi et al. 2004).

1-2. Fungal cytoskeleton and polarity

The eukaryotic cytoskeleton is a coordinated meshwork of filamentous polymers permeating the cytoplasm (reviewed in Heath 1994). The cytoskeleton is important in the spatial organization of organelles and other intracellular structures (reviewed in Heath 1994). The main structural components of the cytoskeleton are microtubules (MTs), actin and intermediate filaments (reviewed in Heath 1994). This thesis will deal exclusively with MTs and actin.

1-2.1. Microtubules (MTs)

Microtubules (MTs) are a highly conserved component of the eukaryotic cytoskeleton. MTs are composed of α-tubulin and β-tubulin protein subunits that assemble to form heterodimers. These heterodimers in turn assemble, along with MT-associated proteins, into long, polar, dynamic filaments called protofilaments. Typically, the protofilaments arrange themselves in an imperfect helix with one turn of the helix containing 13 tubulin dimers each from a different protofilament (Fig. 1-1a; reviewed in Howard and Hyman 2003; Ledbetter and Porter 1964). MT filaments are polar in that α-tubulin is at one end, the (-) end, while β-tubulin is at the opposite, or (+) end (Fig. 1-1a). MT filaments are dynamic in that they exhibit dynamic instability, which involves slow growth (polymerization) and rapid shrinkage (depolymerization), *in vivo* (Fig. 1-1b; reviewed in Howard and Hyman 2003; Mitchison and Kirschner 1984). A third type of tubulin monomer, γ-tubulin, is involved in MT nucleation (Horio et al. 1991; Oakley et al. 1990). In addition, γ-tubulin is a component of the spindle-pole-body that is essential for MT organization and function in *Aspergillus nidulans* (Fig. 1-1b; Oakley et al. 1990). The spindle-pole-body acts as a cap of the (−) end while MT growth continues at the (+) end.

MTs are required for mitosis and nuclear migration (Morris and Enos 1992; Morris et al. 1995; Plamann et al. 1994; Suelmann and Fischer 2000b). While the roles of actin in fungal tip growth have been relatively clearly established (e.g. Heath 1994), the role(s) of MTs beyond nuclear migration and mitosis require further investigation and clarification. Because of this lack of clarity, I chose to undertake a study of the role(s) of MTs in tip growth in *Aspergillus nidulans*. MTs seem likely to contribute to tip growth in that *A. nidulans* MTs are mostly parallel to the long hyphal axis (Meyer et al. 1987; Ovechkina et al. 2003; Sampson and Heath 2005), suggesting long-distance tracks for transport of materials needed for tip growth and morphogenesis. However evidence to support this is largely circumstantial.

1-2.1.1. Benomyl

Benomyl inhibits the assembly of MTs both *in vitro* and *in vivo* in some fungi, including *Aspergillus nidulans* (Davidse and Flach 1977, 1978; Harris et al. 1994; Howard and Aist 1977, 1980; Momany and Hamer 1997). Benomyl is an important fungicide because it appears to inhibit the assembly of the MTs in pathogenic fungi, while having little impact on the plants on which the fungi grow (reviewed in Davidse 1986). On a molecular level, benomyl breaks down to methyl benzimidazole-2-ylcarbamate (MBC) (reviewed in Davidse 1986). MBC binds the tubulin dimer and prevents polymerization of MTs (Davidse and Flach 1977). MBC binds β-tubulin by interacting with amino acids 6, 165, and 198-200 (Jung and Oakley 1990; Jung et al. 1992). The interaction of benomyl and related compounds to amino acid 6 is likely hydrophilic and binding at amino acid 200 appears to be blocked by the polar OH group on tyrosine (Jung et al. 1992).

1-2.1.2. Taxol

Taxol prevents MT depolymerization by stabilizing existing MTs (Schiff et al. 1979). Because of the dynamic nature of MTs, prevention of depolymerization leads to disruption of dynamic instability and increased polymerization of the MT population. On a molecular level, taxol binds at the taxol-binding site on β-tubulin (Combeau et al. 1994; Rao et al. 1992) in polymerized MT filaments, preventing depolymerization by an

unknown mechanism, involving the interaction between α and β-tubulin (Nogales et al. 1995). Rao et al. (1994) found the taxol-binding site to be located in the N-terminal 31 amino acids of β-tubulin. In addition, Nogales et al. (1995) showed that the taxol-binding site is near the inter-protofilament contact point (Fig. 1-1c). Consistent with the known stoichiometry of taxol in MTs (Díaz and Andreu 1993), Nogales et al. (1995) showed the existence of one taxol-binding site per tubulin heterodimer (Fig. 1-1c).

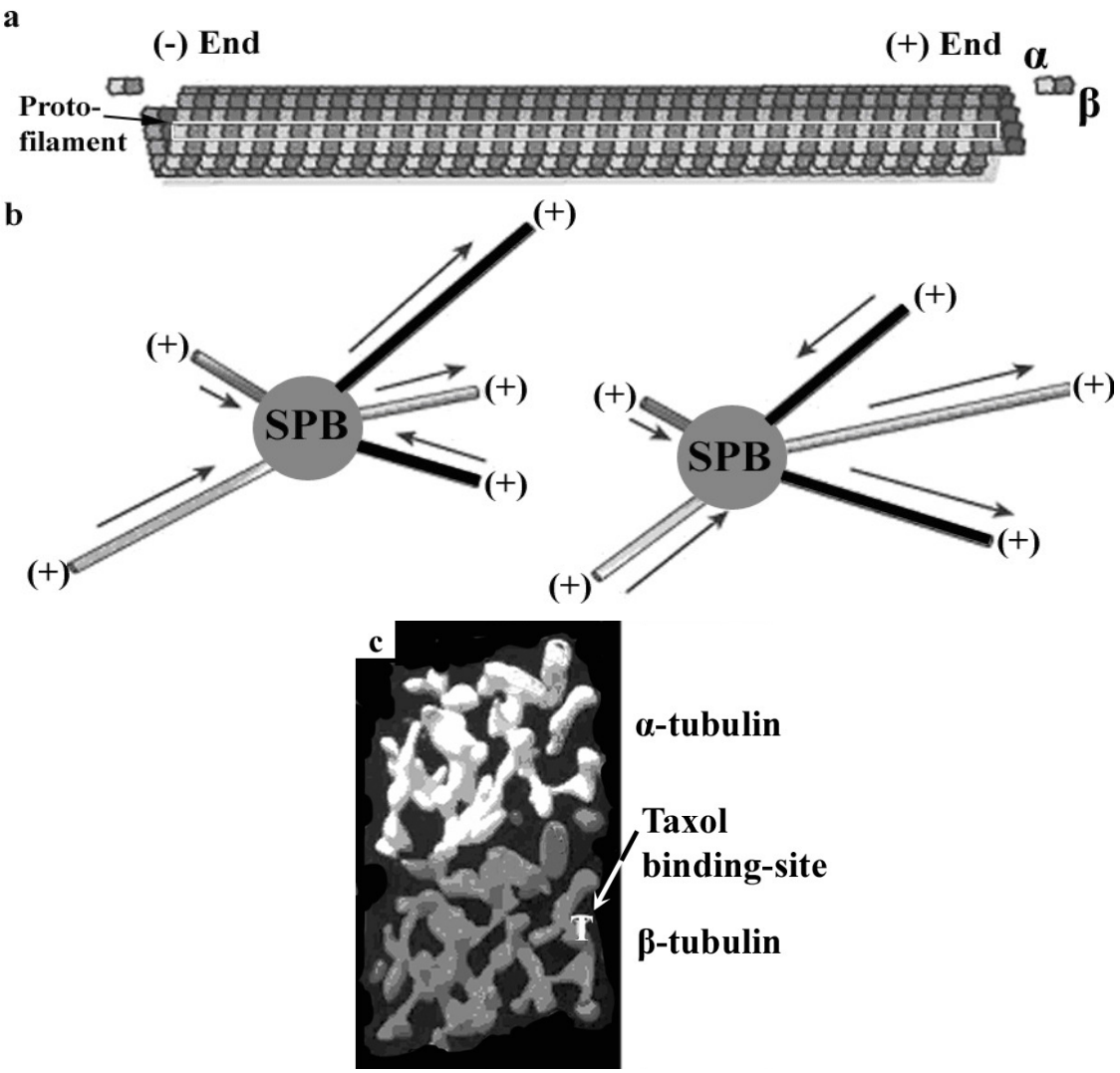

Figure 1-1. Microtubule (MT) structure, dynamics and taxol binding. a) Cartoon of a MT showing the (+) and (-) ends and the α and β subunits and the bundling of protofilaments. b) Spindle-pole-body (SPB) nucleating dynamic instability. Arrows pointing away form the spindle-pole-body indicate polymerizing MTs, while arrows pointing towards the spindle-pole-body indication depolymerization. The two MTs shown in black undergo a shift from polymerization to depolymerization, or a shift from depolymerization to polymerization. Adapted from Figure 2a Howard and Hyman (2003). c) A tubulin heterodimer with α-tubulin shown in white and β-tubulin in grey. Arrow and T indicate the approximate position of the taxol-binding site. The taxol binding site does not appear to interfer with the contact point between α- and β-tubulin. Adapted from Figure 3a of Nogales et al. (1995).

1-2.2. Actin

Actin polymers, often referred to as F-actin, are composed of globular protein monomers, often referred to as G-actin (reviewed in Carlier 1991; Korn 1982). F-actin filaments have +/- polarity; polymerization is more rapid at the plus end.

In fungi, actin is involved in tip-localized extension of the cell wall and plasma membrane and migration of the cytoplasm towards the advancing tip (Bachewich and Heath 1999; reviewed in Heath 1994). Actin, or actin binding proteins such as tropomyosin (Maytum 2000), also appear to be involved in the migration of organelles (Shepherd et al. 1993) and vesicles (Lui and Bretscher 1992; Novick and Botstein 1985) presumed to be carrying material needed for tip growth through the cytoplasm towards the tip (reviewed in Heath 1994; Heath et al. 2000). Actin is abundant at growing hyphal tips, often in the form of a cap next to the apical plasma membrane (Bartnicki-Garcia 2002; Heath et al. 2003). This actin cap has been implicated in tip morphology and shown to be present in growing tips and absent in non-growing tips (Heath 1994; Jackson and Heath 1990a, 1990b, 1993a). Actin inhibition has been shown to reduce tip growth in *Aspergillus nidulans* (e.g. Sampson and Heath 2005) as well as *Saprolegnia ferax* (Bachewich and Heath 1997; Gupta and Heath 1997).

1-2.2.1. Latrunculin B

Latrunculin is produced by *Latrunculia magnigicans*, a Red Sea sponge (Nèeman et al. 1975). Two related latrunculin compounds, latrunculin A and latrunculin B have been shown to depolymerize actin structures *in vitro* and *in vivo* (Kashman et al. 1980; Spector et al. 1983). The inhibitor latrunculin B binds actin monomers and prevents assembly into filaments by inducing a conformational change (Morton et al. 2000). These changes in the structure of actin are limited to specific regions (Morton et al. 2000). Latrunculin A and/or B binding blocks actin polymerization by interfering with the ATP-binding site on actin monomers (Morton et al. 2000).

1-3. The fungal secretory system and polarity

The components of the secretory pathway include the endoplasmic reticulum (ER), fungal Golgi, Spitzenkörper and vesicles. Because polarized secretion is involved in polar growth (reviewed in Bartnicki-Garcia 2002) it is possible that the fungal secretory system contributes to polarity.

1-3.1. Fungal endoplasmic reticulum (ER)

The ER is a network of interconnected tubules, vesicles and sacs that function in synthesis of both integral membrane proteins and proteins destined for secretion, sequestration of calcium, and insertion of membrane proteins. The ER is a dynamic structure. In the ectomycorrhizal basidiomycete fungus *Pisolithus tinctorius* the ER forms reticulate tubules throughout the hyphae (Cole et al. 2000). Proteins synthesized in the ER subsequently progress to the Golgi (Caro and Palade 1964).

1-3.2. Fungal Golgi

Golgi are involved in the sorting of proteins for secretion or transport to intracellular locations (reviewed in Farquhar and Palade 1981, 1998; Mogelsvang and Howell 2006; Palade 1975). In *Aspergillus oryzae* the putative Golgi marker, FmanIBp:GFP, was observed under fluorescence microscopy as punctate structures distributed through the hyphal cytoplasm (Akao et al. 2006). *A. nidulans* and *P. tinctorius* fungal Golgi consist of single, multilobed cisterna (Beckett et al. 1974; Cole et al. 2000). Consistent with observations in *A. oryzae,* in *P. tinctorius*, many fungal Golgi are observed in each cell (Cole et al. 2000). Kaminskyj and Boire (2004) observed *A. nidulans* fungal Golgi to be single, multilobed cisterna occupying a roughly horseshoe shaped area. These observations were made in relatively young *hypA1 A. nidulans* cells, grown at the restrictive temperature, but containing relatively non-aberrant endomembrane arrays because of the cells' youth.

GFP tagged *sod*^{VI}*C* (suppression *o*f *d*isomy of chromosome VI) (Whittaker et al. 1999; discussed in more detail in section 1-3.3.2., page 12) appear to localize preferentially to numerous small structures in each *A. nidulans* hypha (Figs. 3-2, 3-3, 3-4 inset) as could be expected, based on the appearance of fungal Golgi in the literature

(Akao et al. 2006; Beckett et al. 1974; Kaminskyj and Boire 2004). Thus it is possible that GFP tagged *sod*^{VI}*C* could be used as a reasonable a proxy for fungal Golgi.

1-3.3. Vesicles

The maintenance of specialized functions of membrane-bound components of the secretory system requires distinct protein and lipid compositions. These proteins must be sorted within and between membrane-bound compartments or organelles. Transport within and between organelles is facilitated by the budding of vesicles from a donor membrane, followed by the transport of the vesicles to a recipient membrane and subsequent fusion of the vesicle and recipient membranes (reviewed in Lee et al. 2004; Palade 1975; Rothman and Wieland 1996). Vesicle transport can be anterograde or retrograde (reviewed in Lee et al. 2004). Anterograde vesicle transport can be defined as transport progressing in the direction of secretion, such as from the ER to the Golgi (reviewed in Lee et al. 2004). Thus, retrograde vesicle transport is transport progressing in the opposite direction to secretion, such as from the Golgi to the ER (reviewed in Lee et al. 2004).

1-3.3.1. The vesicle coatomer protein (COP)I

Vesicle formation employs membrane-associated protein skeletons, which in fungi are composed of coatomer protein assemblies called COPI and COPII (Serafini et al., 1991). Retrograde transport from the Golgi to the ER is mediated by COPI (Letourneur et al. 1994; Rothman 1996; Fig. 1-2), which consists of eight subunits: ADP-ribosylation factor (ARF) and seven COP proteins known as α, β, β́, γ, δ, ε and ζ (Gayner et al. 1998; Serafini et al. 1991; Waters et al. 1991). Activation of ARF by a Golgi-localized GDP exchange factor (GEF) causes ARF-GTP to bind the Golgi membrane which leads to the recruitment of COPI coatomer (Rothman and Wieland 1996). ARF-GTP-COPI reshapes the donor membrane, leading to budding of a vesicle (Rothman and Wieland 1996).

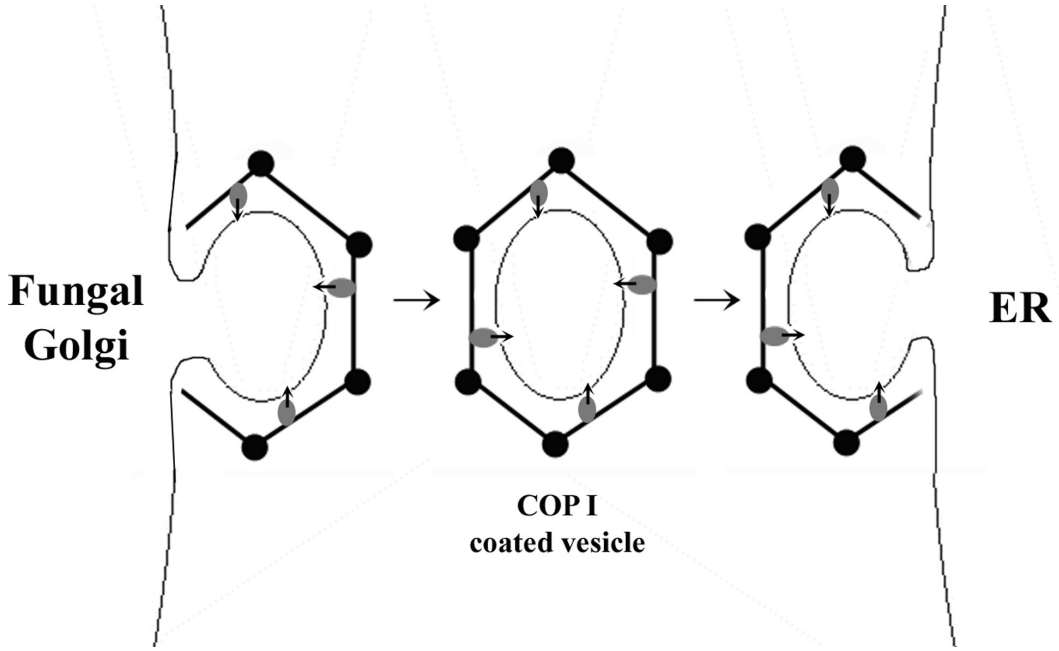

Figure 1-2. Golgi to ER via COPI coated vesicles. Coatomer protein (COP)I coats vesicles involved in retrograde transport. COPI coated vesicles bud from the *cis* Golgi and subsequently fuse with the rough endoplasmic reticulum (ER). COPI coatomers are made up of eight subunits: COPs α, β, β́, γ, δ, ε and ζ (shown collectively as circles and rods) and ADP-ribosylation factor (ARF). The grey circle and black arrow represent ARF and an exposed N-terminal myristate, respectively. When ARF exchanges GDP for GTP (not shown; promoted by an ARF-specific GDP exchange factor (GEF)) the N-terminal myristate is exposed on ARF. This in turn promotes binding of COPI to the Golgi membrane. Vesicle fusion occurs at the ER when ARF-GTP is hydrolyzed via endogenous phosphatase activity of ARF. Adapted from Figure 1.1 of Yang (2003).

1-3.3.2. The *Aspergillus nidulans* α-COPI homolog: suppression of disomy of chromosome VI (*sod^{VI}C*)

Suppression of disomy prevents the genetic abnormality characterized by the presence of two copies of a given chromosome, in this case chromosome VI, instead of the single copy normally found in the haploid genome of *Aspergillus nidulans*. Surprisingly, given its role in prevention of disomy of chromosome VI, the protein encoded by the *A. nidulans* gene *sod^{VI}C* has 71% amino acid sequence similarity to the *Saccharomyces cerevisiae* α-coatomer protein (COP)I protein (Gerich et al. 1995; Letourneur et al. 1996; Whittaker et al. 1999). Because of this, *A. nidulans sod^{VI}C* will hereafter be referred to as α-COPI.

A mutation of α-COPI, known as *sod^{VI}C1*, leads to abnormal growth and morphology in *A. nidulans* at the restrictive temperature, 42ºC, while permitting apparently wildtype growth at 30ºC, albeit at a reduced rate (Lee et al. 2002; Whittaker et al. 1999). When grown at 42ºC, *sod^{VI}C1* mutants show almost zero percent germination (Whittaker et al. 1999). When grown at 30ºC before being transferred to 42ºC, *sod^{VI}C1* mutants exhibited reduced growth rate and defects in nuclear division at 42ºC (Whittaker et al. 1999). Many *sod^{VI}C1* cells showed signs of lysis when incubated at 42ºC for longer than 8 h (Whittaker et al. 1999). The impacts of the *sod^{VI}C1* mutation in α-COPI on morphology (Lee et al. 2002; Whittaker et al. 1999) suggest than COPI function is required for wildtype morphology of *A. nidulans*.

1-3.4. The Spitzenkörper

The Spitzenkörper was originally discovered in living hyphae in 1957 (Girbardt 1957) and can be described as a phase-dark, usually spherical body (López-Franco and Bracker 1996) that is found in growing hyphal tips and represents an accumulation of secretory vesicles (reviewed in Bartnicki-Garcia 2002). The Spitzenkörper is spatially coincident with the vesicle supply center (reviewed in Bartnicki-Garcia 2002). Spitzenkörper have been found in over 30 species of fungi (López-Franco and Bracker 1996). Spitzenkörper position and trajectory have been shown to correlate with the direction of hyphal growth in living *Neurospora crassa* hyphae (Riquelme et al. 2000). The establishment of a new growth direction correlated with a sustained shift in

Spitzenkörper trajectory (Riquelme et al. 2000). Similarly, Bracker et al. (1997) found that manipulation of the Spitzenkörper trajectory with laser tweezers resulted in an alteration in the direction of hyphal growth. Thus, the Spitzenkörper is important in hyphal growth.

1-3.5. The inhibitor brefeldin A (BFA)

Brefeldin A (BFA) is a toxin produced by organisms such as the fungus *Eupenicillium brefeldianum*. BFA is an inhibitor of COPI-mediated Golgi derived vesicle budding *in vivo* (Donaldson et al. 1991). Fujiwara et al. (1988) found that BFA treatment of animal cells for 60 min resulted in disassembly of the Golgi complex and accumulation of secretory proteins in the ER. Similarly, Sciaky et al. (1997) found that BFA induced tubulation of the Golgi within 10 min and subsequent fusion with the ER in another 5-10 min in animal cells. Treatment with BFA leads to the disassembly of the Golgi apparatus in plant cells (e.g. Ritzenthaler et al. 2002). In the fungus *Pisolithus tinctorius* brefeldin A reduces growth, disrupts the Spitzenkörper, reduces the number of apical vesicles, redistributes and mildly dilates the ER, and increases the size of Golgi bodies (Cole et al. 2000).

BFA inhibits vesicle transport by inducing the release of COPI coatomers from Golgi complex membrane derived vesicle buds (Donaldson et al. 1990, 1992; Helms and Rothman 1992; Klausner et al. 1992; Robinson and Kreis 1992). This occurs because BFA inhibits the ARF GEF involved in facilitating COPI vesicle budding (Morinaga et al. 1996; Peyroche et al. 1996). Thus, BFA is a potentially useful tool for studying Golgi dynamics in fungi.

1-4. Fluorescent proteins as tools in cell biology

Green fluorescent protein (GFP) is derived from the jellyfish *Aequorea victoria*. GFP fluoresces green when exposed to blue light (Prendergast and Mann 1978; Tsien 1998). The use of GFP as an *in vivo* tag fused to other proteins of biological interest has revolutionized fluorescence microscopy (Yuste 2005). GFP fusion proteins permit protein localization in living cells and visualization of the structure and function of living tissues (reviewed in Brandizzi et al. 2004; Yuste 2005). The introduction of GFP fusion

proteins to fungal cell biology represented a major advance in this field (Cormack 1998). GFP fusion proteins have been used in *Aspergillus nidulans* (e.g. Fernández-Ábalos et al. 1998; Horio and Oakley 2005; Sampson and Heath 2005; Suelmann et al. 1997) and other filamentous fungi, such as *Neurospora crassa* (Fuchs et al. 2002).

The *Discosoma* red fluorescent protein, DsRed, has also been used in *A. nidulans* (Dou et al. 2003). However, DsRed requires tetramer formation and maturation over several days for fluorescence, making it inappropriate for many applications (Baird et al. 2000). Campbell et al. (2002) developed a monomeric red fluorescent protein (mRFP) which matures quickly. In *A. nidulans*, mRFP fusion proteins have been used successfully (Toews et al. 2004).

1-4.1. Green fluorescent protein (GFP) tagged α-tubulin

Tagging of α-tubulin with GFP permits the observation of MT profiles (an estimate of MT abundance described in Material and Methods, section 2-3.3., page 21) and distribution *in vivo*. The GFP tagged α-tubulin used was under the control of a constitutive promoter, *tub*A, rather than the *alc*A promoter that has been used with previous constructs. The use of the constitutive promoter *tub*A is a major advance in the study of MTs as it facilitates the observation of fluorescent MTs in cells grown on glucose rather than ethanol or threonine.

1-4.2. Green fluorescent protein (GFP) tagged α-COPI

An *A. nidulans* strain possessing GFP tagged α-COPI (provided by the Assinder group; Whittaker et al. 1999) was used to observe α-COPI dynamics *in vivo.* GFP tagged α-COPI is under the control of the *alc*A promoter (Whittaker et al. 1999).

1-4.3. The red fluorescent protein (RFP) tagged Golgi marker α-2,6-sialyltransferase (ST)

The mammalian enzyme α-2,6-sialyltransferase (ST) contains a transmembrane domain that is important in Golgi retention (Munro 1991). ST has been shown to localize to the animal (Munro 1991), plant (Wee et al. 1998) and *S. cerevisiae* Golgi (Schwientek et al. 1995). Brandizzis' group provided an ST-monomeric red fluorescent protein

(mRFP) plasmid under the control of the cauliflower mosaic virus 35S promoter. This promoter has been shown to induce expression of genes under its control in plants (Jefferson et al. 1987; Odell et al. 1985), ascomycete yeast (Hirt et al. 1990) and filamentous fungi such as *Uromyces* (Li et al. 1993), *Ganoderma lucidum* and *Pleurotus citrinopileatus* (Sun et al. 2002) and *Pleurotus ostreatus* (Xu et al. 2004). Because cauliflower mosaic virus 35S promoter can induce expression in yeast and filamentous fungi, both of which are somewhat closely related in *Aspergillus nidulans*, it was possible that the cauliflower mosaic virus 35S promoter will also drive gene expression in *A. nidulans*.

1-5. Objectives

1-5.1. Objectives for chapter 2 entitled "Growth rate of *Aspergillus nidulans* hyphae is largely independent of cytoplasmic microtubule abundance".

1) To examine and describe cytoplasmic microtubule populations in living *Aspergillus nidulans* hyphae.

2) To examine the relationship between hyphal growth rate and relative MT abundance in untreated *A. nidulans* hyphae.

3) To examine the effects of actin- and MT-selective inhibitors and solvent controls on relative MT abundance and hyphal growth rate.

4) To examine hyphal growth rate variability and the effects of actin- and MT-selective inhibitors and solvent controls on hyphal growth rate variability in *A. nidulans*.

1-5.2. Objectives for chapter 3 entitled "The distribution and movement of fungal Golgi are related to growth rate and the cytoskeleton in *Aspergillus nidulans* hyphae".

1) To determine whether the Golgi marker ST-RFP co-localizes with the putative fungal Golgi marker α-COPI-GFP.

2) To investigate the impact of BFA on α-COPI-GFP and ST-RFP particle morphology.

3) To investigate the distribution of *sod*^{VI}*C*-GFP in *hypA1 A. nidulans* hyphae at restrictive (42°C) and permissive (28°C) temperatures.

4) To investigate the relationship between the temperature at which *hypA1 A. nidulans* hyphae are grown and the average forward velocity of fungal Golgi and growth rate in the same cells.

5) To investigate the relationship between hyphal growth rate and forward velocity of fungal Golgi.

6) To investigate the impact of MT and actin targeting drugs on the average forward velocity of fungal Golgi and hyphal growth in the same cells.

CHAPTER 2: Growth rate of *Aspergillus nidulans* hyphae is largely independent of cytoplasmic microtubule abundance.

2-1. Summary

Roles for the microtubule (MT) cytoskeleton in fungal growth include mitosis and nuclear migration, but otherwise are less clearly understood. Confocal microscopy was used to quantify MT abundance and growth rate in hyphae of an *Aspergillus nidulans* strain containing GFP-α-tubulin. There was no correlation between growth rate and MT abundance for 112 growing hyphae in an untreated population. However, the 109 non-growing hyphae had a lower average MT abundance than did their growing counterparts. Results for untreated cells were compared to cells treated for 30-120 min with the MT drugs taxol and benomyl, the actin drug latrunculin B, and with solvents used for the drug treatments. Taxol was dissolved in DMSO and benomyl and latrunculin were dissolved in ethanol. Compared to their respective controls, MT abundance was significantly increased by DMSO, significantly reduced by benomyl, and moderately increased by latrunculin, but was unaffected by ethanol. Growth rates were significantly increased by ethanol and taxol, significantly reduced by latrunculin, and unaffected by DMSO. Average hyphal growth rate in the first 30-120 min following 1 μg/mL benomyl treatment was statistically similar to untreated cells, despite the absence of visible MTs after 2 min of treatment, but growth rate was significantly reduced by 2.5 μg/mL benomyl over the same time period, implying there were ancillary effects from this treatment. For individual hyphae in each treatment, growth rates varied over short time periods; treatment with 0.1 % ethanol substantially increased growth rate variability, as well as overall growth rate. Notably, growth rates of taxol treated hyphae decreased significantly following fluorescence observation, suggesting a possible application to cancer chemotherapy.

2-2. Introduction

The actin and microtubule (MT) cytoskeletons have many roles in polarized growth of filamentous fungi (Bartnicki-Garcia 2002, Heath 1990a, 1994, 1995). Filamentous actin arrays are concentrated in areas of active cell extension and cell wall deposition (Heath 1990a, 1990b, 1994, 1995). In *Aspergillus nidulans,* cytoplasmic actin arrays have documented roles in hyphal extension and morphogenesis (Harris et al. 1994; Sampson and Heath 2005; Torralba et al. 1998), septation (Momany and Hamer 1997), and mitochondrial motility (Suelmann and Fischer 2000a). A class I myosin is essential in *A. nidulans* and is enriched at hyphal tips (McGoldrick et al. 1995). The SEPA formin important in actin organization is enriched at *A. nidulans* hyphal tips (Sharpless and Harris 2002). A chitin synthase in *Ustilago maydis*, *mcs1*, was shown to have an N-terminal myosin class V-like domain (Weber et al. 2006), a novel link between the actin cytoskeleton and cell wall deposition that might in future be related to chitin synthase localization and *Aspergillus* septum deposition (Ichinomiya et al. 2005). Taken together, Heath (1990b) and Heath et al. (2000) provide abundant evidence that actin is of primary importance in hyphal tip growth and morphogenesis, which is supported in *A. nidulans* by Harris et al. (1994), Sampson and Heath (2005), and Torralba et al. (1998).

There is abundant evidence that MTs are required for mitosis and for nuclear migration in filamentous fungi (Heath 1994, 1995; Morris and Enos 1992; Morris et al. 1995; Plamann et al. 1994; Suelmann and Fischer 2000b). However, unlike actin, roles for MTs specifically in hyphal growth are less consistent. Cytoplasmic MTs support rapid, long term, and/or morphologically wildtype growth in fungi including *Aspergillus* (Horio and Oakley 2005; Konzack et al. 2005; Ovechkina et al. 2003; Sampson and Heath 2005), *Neurospora* (Mouriño-Pérez et al. 2006, Riquelme et al. 2002), and *Ustilago* (Fuchs et al. 2005, Schuchart et al. 2005). However, *A. nidulans* conidia can germinate in the presence of the MT-depolymerizing agent benomyl (Oakley and Morris 1980). *A. nidulans* hyphal growth continues during mitosis, during which most cytoplasmic MT depolymerize (Riquelme et al. 2003; Trinci and Morris 1979); for contrary results, see Sampson and Heath (2005). *A. nidulans* temperature-sensitive *nud* mutants form hyphae under restrictive conditions, despite defects in MT-associated motor proteins (Morris et al. 1995). Many fungi with tip growing cells show dramatic growth

rate fluctuations on the order of a few seconds (López-Franco et al. 1994; Sampson et al. 2003) whereas comparable quantitative changes in *A. nidulans* MT arrays require much longer times (Ovechkina et al. 2003; Sampson and Heath 2005).

The number and arrangement of cytoplasmic MTs vary significantly even between filamentous ascomycetes, further complicating development of a general description of their role(s) in hyphal tip growth. For example, in *A. nidulans*, MTs are relatively few in number and are predominantly in the central cytoplasm (Meyer et al. 1987; Ovechkina et al. 2003; Sampson and Heath 2005), whereas in *N. crassa* MTs are relatively numerous and are found in the both central and peripheral cytoplasm (Freitag et al. 2004; Mouriño-Pérez et al. 2006). *A. nidulans* MTs are mostly parallel to the hyphal axis (Meyer et al. 1987; Ovechkina et al. 2003; Sampson and Heath 2005), whereas *N. crassa* MTs are mostly parallel to the axis near the hyphal tip but more randomly oriented in basal compartments (Freitag et al. 2004).

Until recently, it was not possible to probe the dynamic relationship between MT arrays and tip growth rate, since MTs had to be visualized in fixed cells using immunofluorescence or electron microscopy. The development of *A. nidulans* strains with constitutive GFP-α-tubulin (Horio and Oakley 2005) allows investigation of MT dynamics in living hyphae. Horio and Oakley (2005) and Sampson and Heath (2005) showed that benomyl- and methyl benzimidazole-2-ylcarbamate (MBC)-induced MT disassembly led to decreased growth rate. However, using an *alcA*-regulated GFP-MT strain, Ovechkina et al. (2003) found that mitosis-induced MT disassembly in individual hyphae did not reduce growth rate. This lack of consistency indicates the need for further investigation into the roles of MTs in hyphal growth.

We used an *A. nidulans* strain with constitutively-tagged GFP-α-tubulin described in Horio and Oakley (2005) to study the quantitative relationship between cytoplasmic MTs and growth rate in large numbers of individual hyphae. Our study differs from reports by Horio and Oakley (2005) and Sampson and Heath (2005) in several ways: 1) We used a haploid strain (LO1022) grown on nutrient-rich medium rather than a diploid strain (LO1052) grown on minimal medium. Most *A. nidulans* experimental strains are haploid, as are those isolated from nature. 2) We collected data on large numbers of hyphae chosen for their similar morphology, and then restricted

analyses to hyphae that were shown to be growing. 3) We used both equivalent and lower concentrations of benomyl and latrunculin B, and compared them to solvent-only controls. In addition: 4) We estimated relative MT abundance using a quantitative index. 5) We present the first data on the *in vivo* effect of taxol on *A. nidulans* MT abundance and growth rate.

Surprisingly, MT index and growth rate were not correlated for large numbers of individual untreated hyphae, although the average MT index for growing hyphae exceeded that of non-growing ones. Similarly, when groups of hyphae were treated with the cytoskeleton-selective drugs benomyl, latrunculin B and taxol, or with comparable concentrations of carrier solvents, average growth rate and microtubule index varied independently following different treatments.

2-3. Materials and Methods

2-3.1. *Aspergillus nidulans* growth conditions.

A. nidulans strain LO1022 (GFP-α-tubulin; *pabaA1; wA2; cnxE16, sC12; veA1*) was maintained at 28 ºC on complete medium (CM; Kaminskyj 2001) supplemented with methionine. LO1022 is ideal for this type of study since it is haploid, like *A. nidulans* strains in nature and the majority of the strains studied experimentally, and can be grown on rich medium for optimal growth rate. For confocal microscopy, freshly harvested spores were inoculated onto sterile dialysis tubing overlying CM agar (Kaminskyj 2000), and grown for at least 24 h at 28 ºC. The dialysis tubing and overlying hyphae were lifted from the CM agar, mounted in a microscope slide chamber (Heath 1988) in ~100 µL of liquid CM, containing solvent and inhibitors as required, and allowed to recover for 30 min before observation. Mounting induced transient hyphal tip swelling that made a convenient marker for treatment initiation. Observations were terminated after 120 min.

2-3.2. Cytoskeletal inhibitors

Benomyl, paclitaxel (trade name, Taxol®), and anhydrous dimethyl sulphoxide (DMSO) were obtained from Sigma (www.sigmaaldrich.ca). Latrunculin B (hereafter, latrunculin) was obtained from Molecular Probes (www.molecularprobes.com). All other

chemicals were obtained from VWR (www.vwrcanlab.ca). Inhibitors were diluted from stock solutions with room temperature liquid CM immediately before use.

Benomyl was stored at 4 °C as a 10 mg/mL stock in 100% ethanol, and used at 1 μg/mL in 0.01 % ethanol or 2.5 μg/mL in 0.025% ethanol. Latrunculin B (hereafter, latrunculin) was stored as a 25 mg/mL stock in 100% ethanol at -20 ºC, and used at 5 μg/mL in 0.02 % ethanol or 20 μg/mL in 0.08 % ethanol. Taxol was stored at -20 ºC as a 2 mM stock in 100 % DMSO and used at 50 μM in 0.25 % DMSO. DMSO was purchased as 1 mL ampoules of dry solvent, and the stock was stored in aliquots, over desiccant. The ethanol control concentration was 0.1 %, at the top of the range used in preliminary experiments, and similar to previously published studies (Harris et al. 1994; Kaminskyj 2000), but higher than used for the benomyl and latrunculin data presented. The inhibitor concentrations were similar to or lower than those used in the literature (benomyl and latrunculin) or were the lowest for which a response was detected (taxol).

2-3.3. Confocal microscopy

Aspergillus nidulans hyphae were imaged with a Zeiss META 510 laser scanning confocal microscope (www.zeiss.com) using a Plan Apochromat 63 x, N.A. 1.2, multi-immersion objective equipped with differential interference contrast (DIC) optics. GFP-α-tubulin fluorescence was imaged with 488 nm excitation from an Argon laser, with emission controlled by a BP505-530 filter. Excitation intensity was 5 - 10 % from a laser current of 5.9 amps. Eight or 16 scans per pixel at 0.6-2.5 μs/pixel were used to improve signal to noise ratio. Optical sections were 1.2 μm thick, and chosen to be near-median focal level.

Hyphae were chosen for analysis if they were located at the colony margin, had an even profile, a smoothly tapered tip, and had grown out from the characteristic mounting-induced morphology, that is, a swollen tip or an abrupt change in growth direction. Hyphae that had not responded in this way to mounting were assumed to be non-growing, and were not selected for analysis. However, whether a particular hypha was actually growing, and at what rate, was not determined until after the data were collected. For each tip, 5-20 images were collected over 60-300 s. For observation of relative MT abundance and hyphal growth rate, we did not use cells whose nuclei were in

mitosis at any time during the observation period. DIC images used to measure hyphal growth rates were captured simultaneously with the fluorescence images used to quantify MT profiles. Minor photobleaching was detected by the end of longer imaging sessions, but MT index values and hyphal growth rates were not noticeably affected.

MTs containing GFP-α-tubulin cannot be precisely counted using fluorescence microscopy, even with optimal confocal settings employed here. The theoretical resolution of our confocal system was 230 nm, whereas the width of a fluorescent MT is about 25 nm plus the GFP decoration. Fluorescent objects are self-luminous, which enhances detection but does not improve resolution. Williamson (1991) showed that fluorescence images of fixed MTs in plant cells underestimated number and overestimated continuity compared to serial reconstruction transmission electron microscopy (TEM). Sampson and Heath (2005) reported "approximate correlations" between numbers of MTs containing GFP-α-tubulin visualized by fluorescence and MTs in the same *A. nidulans* cells following chemical-fixed TEM. Precise correlations are simply not possible given the inevitable chemical fixation-induced cytoplasmic movements (Kaminskyj et al. 1992). Other factors confounding MT quantification include that a MT grazing the confocal optical volume may not be detected, and GFP-tubulin dimers, protofilaments or MTs shorter than the resolution limit would contribute to background cytoplasmic fluorescence. Thus, our MT index values described below reflect relative rather than absolute abundance. Regardless, strains with constitutive GFP-α-tubulin are a major advance.

MT bundling in *A. nidulans* hyphae further complicates quantification. A freeze-substitution, cross section, serial reconstruction TEM analysis of an *A. nidulans* hypha revealed about half of the cytoplasmic MTs were in bundles of two or three, typically at least one MT-width apart (R. Roberson, *personal communication*). Confocal microscopy cannot resolve individual MTs within bundles, nor unambiguously distinguish MT bundles from singletons, although occasionally we could infer bundling from abrupt changes in brightness, as did Mouriño-Pérez et al. (2006) in *N. crassa*. Thus some of the drug effects presented herein may be due to MT bundling / unbundling as well as polymerization / depolymerization.

To compare relative MT abundance between hyphae or treatments, we developed the MT index using near-median confocal optical sections encompassing about 25 % of the hyphal volume. The MT index for a hypha was defined as the sum of MT profile counts at 5 μm, 10 μm, 15 μm and 20 μm from the hyphal tip. Counts for MT index used 12-bit Zeiss confocal images. Figure 2-1 shows Adobe Photoshop 8-bit images of typical cells, presented in reverse contrast to facilitate MT visualization.

To assess growth rate, the tip position imaged using DIC was marked at the beginning and the end of the analysis period. Growth rate was the difference in hundredths of μm between the initial and final tip position divided by the difference in time in decimal seconds (both generated by the LSM510 software) and expressed as μm/min.

2-3.4. Statistical and graphical analysis

Data are expressed as the mean ± standard error of the mean. Statistical analyses used the 2000 version of Microsoft Excel with data analysis add-ins, or Statview SE+Graphics 1.01, both of which generate probability values. Statistical comparisons between treatments used one-way, single factor ANOVA, and post-*hoc* comparisons used Fisher PLSD. Numerical data are presented using Cricket Graph 1.0. Images are presented using Adobe Photoshop 7.0.

Comparisons were made only between groups with similar variances. Data for MT indexes was collected in groups of 10-20 hyphae per treatment, followed by MTs indexes from 10-20 hyphae from another treatment. Hyphal growth rates were collected after MT indexes had already been recorded. Individual hyphae were selected arbitrarily from a field of view containing numerous apparently growing (ie hyphae with a tapered tip profile).

2-4. Results

2-4.1. Cytoplasmic microtubules in *Aspergillus nidulans* hyphae

In untreated *A. nidulans* hyphae, cytoplasmic MTs are long and flexuous, and run generally parallel to the long axis of the cell (Fig. 2-1a). Over seconds to minutes, MT position varied but MT index remained consistent. MTs arrays were not affected by

ethanol (Fig. 2-1b), whereas all detectable MTs were lost within 2 min of treatment with benomyl (Fig. 2-1c). MT arrays were relatively unaffected by latrunculin (Fig. 2-1d) consistent with its cytoskeletal target being actin microfilaments rather than MTs. *A. nidulans* MT arrays were relatively unaffected by DMSO (Fig. 2-1e) or taxol (Fig. 2-1f) whereas taxol-treated cells appeared to have coarser arrays, perhaps due to MT bundling.

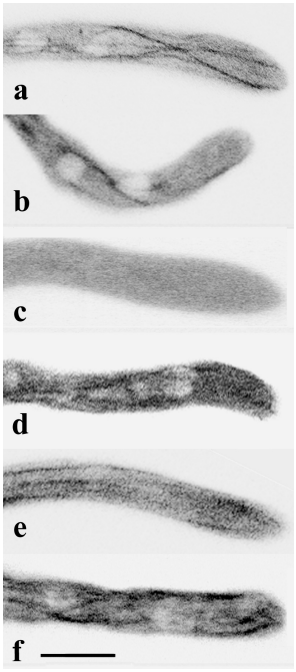

Figure 2-1. Representative images of *Aspergillus nidulans* hyphae containing GFP-α-tubulin. Hyphae were visualized using confocal epifluorescence microscopy of single near-median sections. Images are shown with inverted contrast so microtubules are seen as dark lines. Hyphae were a) untreated, or treated with b) 0.1 % ethanol, c) 1 μg/mL benomyl in 0.01 % ethanol, d) 5 μg/mL latrunculin B in 0.02% ethanol, e) 0.25% DMSO, f) 50 μM taxol in 0.25% DMSO. Treatments including taxol give the impression of inducing microtubule bundling, but individual microtubules cannot be resolved with fluorescence microscopy. Bar = 5 μm, for all images.

2-4.2. Growth rate and relative microtubule abundance in untreated *Aspergillus nidulans* hyphae

Tagging of α-tubulin with GFP does not alter hyphal growth rate as compared to the hyphal growth rates in A28, a wildtype *A. nidulans* strain lacking α-tubulin tagged with GFP (Fig. A-1). MT profile numbers were counted for 1.2 μm thick near-median optical sections of 112 growing *A. nidulans* hyphae. The average number of MT profiles at 5 μm, 10 μm, 15 μm and 20 μm behind the tip was 2.73±0.07, 3.06±0.06, 3.09±0.07 and 3.07±0.06, respectively. There were significantly fewer MTs 5 μm behind the tip than further back (P=0.001). In *A. nidulans,* cytoplasmic MTs are nucleated from nucleus associated organelles, so this result is consistent with the typical position of the nucleus nearest the hyphal tip (Fig. 2-1).

Tip growth rate and MT index (relative MT abundance) for 221 untreated *A. nidulans* hyphae are shown in Fig. 2-2. Some data points overlap, particularly for the 109 non-growing hyphae. The average MT index of growing hyphae (11.75 ± 0.73) was higher than for non-growing hyphae (7.72 ± 0.28) (P<0.0001), but there was no significant correlation between MT index and growth rate amongst the growing hyphae. Occasionally, even rapidly-growing hyphae had a low MT index: two cells with growth rates close to 1 μm/min had MT index values of 6.

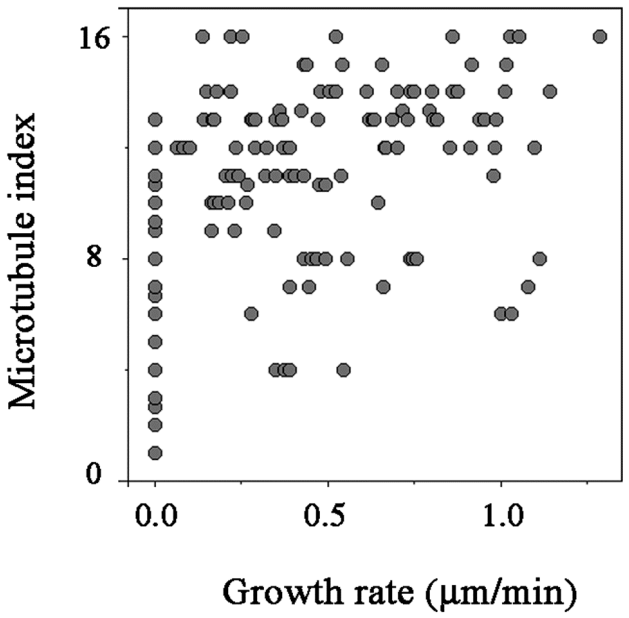

Figure 2-2. The correlation between relative microtubule abundance and hyphal growth rate. Microtubule index, an estimate of relative microtubule abundance, is shown for untreated *Aspergillus nidulans* hyphae containing constitutively tagged GFP-α-tubulin. See Methods for calculations of microtubule index and growth rate. Some data points overlap, particularly for the 109 non-growing cells. The average microtubule index was significantly lower for the non-growing cells (7.74 ± 0.28) than the 112 growing cells (11.76 ± 0.28) ($P<0.05$, *t*-test), but otherwise microtubule index did not correlate with the growth rate variation.

2-4.3. Effect of cytoskeleton-selective drugs on relative microtubule abundance and hyphal growth rate

Our preliminary data from untreated *A. nidulans* hyphae showed that growth rate was not correlated with MT index amongst growing cells, although overall there was a difference between the MT index of growing and non-growing hyphae. To explore the relationship between growth rate and MT index we used well-characterized drugs, benomyl and latrunculin B, known to affect hyphal tip growth in *A. nidulans* (Horio and Oakley 2005; Sampson and Heath 2005) targeting MTs and filamentous actin, respectively. In addition, taxol has been shown to induce polymerization of *A. nidulans* MTs *in vitro* (Yoon and Oakley 1995) but to our knowledge had not been studied *in vivo*. If there were treatment-related differences between groups of hyphae, we might yet discern broad relationships between relative MT abundance and hyphal growth rate.

Cytoskeleton drugs are sparingly soluble in aqueous solutions, and are used at low concentrations, so treatment solutions are diluted into growth medium from stocks prepared in ethanol or DMSO (e.g. Harris et al. 1994; Kaminskyj 2000). *A. nidulans* grows well in medium containing 1 % ethanol as a sole carbon source (Fernández-Ábalos et al. 1998; Palmer et al. 2004) and it tolerates 1 % DMSO without noticeable morphological effects. Average MT index and growth rate for populations of untreated, 0.1 % ethanol treated, and 0.25 % DMSO treated *A. nidulans* hyphae are shown in Fig. 2-3a. The 0.1 % ethanol treatment significantly increased hyphal growth rate ($P=0.0001$) but did not affect MT index ($P>0.1$); most of the ethanol-treated hyphae were growing compared to half of the untreated cells (Fig. 2-3a). In contrast, 0.25 % DMSO treatment significantly increased the average MT index ($P=0.0001$), but not the hyphal growth rate ($P >0.05$). Half of the DMSO-treated hyphae were growing, similar to untreated hyphae. Thus, low solvent concentrations caused significant effects on *A. nidulans* cytoplasmic MT abundance or on hyphal growth rate, but not on both parameters.

Benomyl treatments to depolymerize cytoplasmic MTs were 1 μg/mL and 2.5 μg/mL dissolved in 0.01 % and 0.025 % ethanol, respectively. Both concentrations were effective (Fig. 2-3b); one MT found in 76 hyphae after 1 μg/mL benomyl, and none in 27 hyphae after 2.5 μg/mL benomyl. Unexpectedly, a third of the hyphae in each benomyl-treated population continued to grow at least during the first 2 h following

benomyl application (Fig. 2-3b). For 1 μg/ml benomyl, the average growth rate was statistically similar to the ethanol control treatment (Fig. 2-3b), whereas 2.5 μg/mL benomyl caused a significant growth rate reduction ($P<0.001$). Benomyl blocks *A. nidulans* nuclei at metaphase (Oakley and Morris 1981) and the mitotic cycle is about 100 min. By the end of 2 h in 1 μg/mL benomyl essentially all nuclei had metaphase spindles, so hyphal growth rate studies for benomyl treatments ended at 60 min. Overnight treatment with 1 μg/mL benomyl induced the formation of multiple apical branches (Fig. A-4) comparable to Riquelme et al. (1998, 2003). In addition to the immediate effect of 1 μg/mL benomyl on cytoplasmic MTs, higher benomyl concentrations or longer treatment times had additional deleterious consequences on hyphal growth. We were unable to abolish hyphal tip growth by eliminating MTs, implying that the actin cytoskeleton was playing a key role in delivering growth related materials to the hyphal tip over substantial distances.

Latrunculin targets filamentous actin (Bachewich and Heath 1998), whose functions in hyphal tip growth are well established (Bartnicki-Garcia 2002; Harris et al. 1994; Heath 1990b, 1994, 1995; Torralba et al. 1998), but not MTs (Bachewich and Heath 1998). Our latrunculin concentrations were chosen to reduce tip growth rate (5 μg/mL) or to match the concentration (20 μg/mL) used previously on *A. nidulans* (Sampson and Heath 2005). Both latrunculin concentrations significantly reduced average growth rate ($P<0.01$), and there was a clear dose relationship (Fig. 2-3c). By 120 min, latrunculin treatment caused apical swelling and/or branch initiation (not shown). All these effects were expected. Latrunculin also reduced the proportion of growing cells compared to the ethanol control (Fig. 2-3c), but only to a level comparable to untreated cells (Fig. 2-3a). We were surprised to find that both latrunculin treatments were associated with higher MT index values than the ethanol control (Fig. 2-3c) although the increase was marginal ($P=0.08$). Increased MT index following actin perturbation implies interdependence between the actin and MT cytoskeletal systems.

Taxol has been shown to induce polymerization of *A. nidulans* MTs *in vitro* (Yoon and Oakley 1995), but to our knowledge this is the first *in vivo* study in this species. We used 50 μM taxol in DMSO, which Yoon and Oakley (1995) had found effective *in vitro* although they also used higher levels. We were seeking to avoid toxic

side effects especially as DMSO had already been shown to significantly increase MT index values over untreated controls (Fig. 2-3a). Taxol treatment did not increase the MT index (Fig. 2-3d), perhaps for lack of polymerizable tubulin. However, unexpectedly, taxol treated cells had a significantly higher average hyphal growth rate ($P<0.01$) than the DMSO control (Fig. 2-3d), and a higher proportion of taxol treated cells were growing than DMSO control cells (Fig. 2-3d).

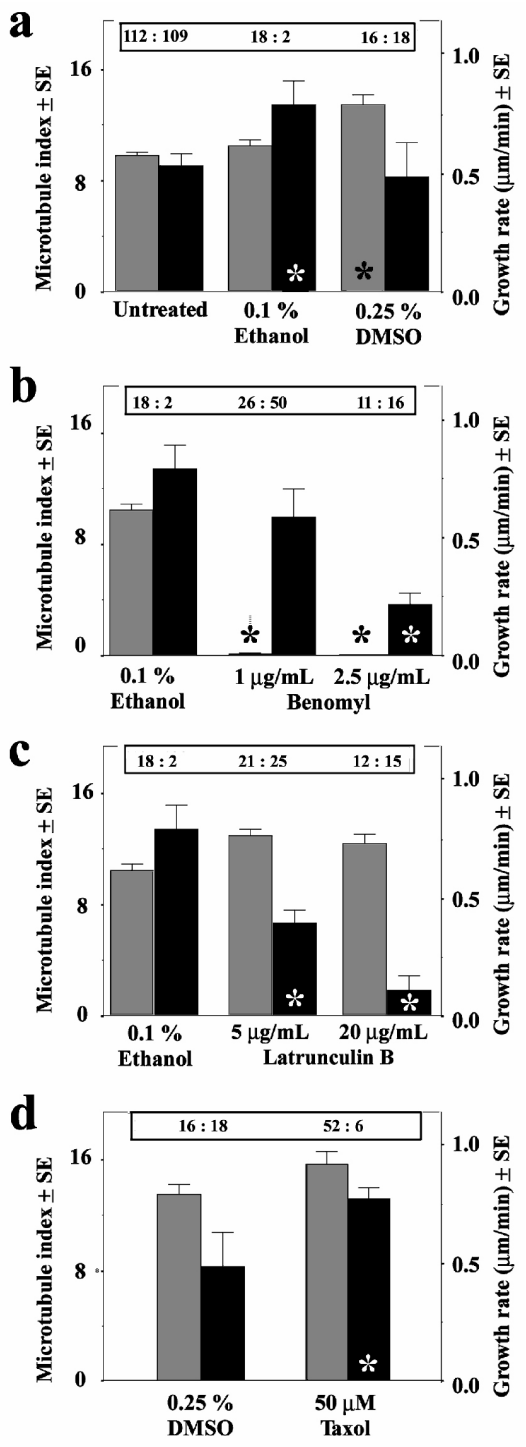

Figure 2-3. Effect of solvents and cytoskeleton-selective drugs on relative microtubule abundance and growth rates of *Aspergillus nidulans* hyphae. Microtubule index is an estimate of relative microtubule abundance. Microtubule index (light bars) and growth rate (dark bars) data are shown for growing hyphae. The boxed numbers indicate the

number of growing and non-growing cells analyzed for each treatment. Observations were made between 30-120 min after treatment application. Calculation of microtubule index and growth rate is described in Methods. Error bars indicate standard error of the mean. Asterisks indicate a significant difference ($P<0.05$) with respect to the corresponding control. (a-d) show results for untreated and solvent treated hyphae, ethanol *vs* benomyl/ethanol treatment, ethanol *vs* latrunculin/ethanol treatment, and DMSO *vs* taxol/DMSO treatment.

(a) Microtubule index and growth rate for untreated, 0.1 % ethanol-treated, and 0.25 % DMSO-treated hyphae. The ethanol concentration is consistent with Kaminskyj (2001) and early experiments in this study (not shown), but is higher than that used for the benomyl and latrunculin B treatment results below. Ethanol treatment significantly increased growth rate but not microtubule abundance; the converse was found for DMSO.

(b) Effect of benomyl dissolved in 0.01 % ethanol. Both concentrations of benomyl depolymerized microtubules within 2 min; growth rate measurements began 30 min after treatment. Growth rates for the 1 μg/mL treated cells were statistically similar to ethanol control cells, but fewer cells in the benomyl treated population were growing. Average growth rate was lower following 2.5 μg/mL benomyl.

(c) Effect of latrunculin B dissolved in 0.02 % ethanol. Latrunculin treatment was associated with a higher microtubule index, but the difference was not statistically significant ($P=0.08$). Latrunculin affected the number of growing cells in the treated population and the growth rate of the growing cells.

(d) Effect of taxol dissolved in 0.25 % DMSO. Taxol significantly increased growth rate but not microtubule index compared to DMSO, and more cells in the taxol-treated population were growing than the control.

2-4.4. Hyphal growth rate variability

Hyphal growth rates vary over short time intervals (López-Franco et al. 1994; Sampson et al. 2003) although the underlying mechanism(s) are not fully understood. In *N. crassa* growth rate variations are temporally correlated with *de novo* generation and fusion of satellite Spitzenkörper (López-Franco et al. 1995) but this phenomenon has not been reported for *A. nidulans.* Having data in hand for large numbers of hyphae that we knew had grown during 60-300 s data collection intervals, we examined growth rate for 15-30 s intervals. Confocal imaging requires fluorescence irradiation, thus energy absorption and the potential for damage. We wished to minimize the impact of irradiation; to do so, we used longer intervals (and hence fewer cycles of irradiation) than previous studies of this type. Results for four to seven hyphae per treatment are shown in Fig. 2-4 to demonstrate the range of growth rate variation without compromising visual clarity. For a larger number of hyphae than we have shown graphically, Fig. 2-4 also reports the number of time intervals in which hyphae did or did not grow.

Growth rates of untreated hyphae varied considerably (Fig. 2-4a), with rate changes up to 1 μm/min within 60 s. As expected from Fig. 2-2, there were substantial differences in average growth rates between untreated hyphae, but almost all intervals had measurable growth (Fig. 2-4a). DMSO treatment (Fig. 2-4b) did not affect the growth rate variation compared to untreated cells, but fewer intervals had measurable growth (Fig. 2-4b). Ethanol treatment (Fig. 2-4d) dramatically increased hyphal growth rate variability, with rate changes exceeding 2 μm/min in 30 s. However compared to untreated cells, ethanol treated hyphae had fewer intervals with measurable growth (Fig. 2-4d).

Benomyl treatment depolymerized cytoplasmic MTs but did not abolish tip growth (Fig. 2-3b). Compared to the ethanol control (Fig. 2-4d) there were fewer intervals with measurable growth following benomyl treatment (Fig. 2-4e). Latrunculin treatment (Fig. 2-4f) suppressed hyphal growth rate variability, consistent with its effect on reducing average hyphal growth rate (Fig. 2-3c), and the proportion of intervals with measurable growth was similar to the ethanol control (Fig. 2-4d).

Hyphal growth rate was not affected by repeated imaging for most of the treatment populations (Fig. 2-4a, b, d-f). Consequently, its effect on taxol treated cells

(Fig. 2-4c) was notable: the average growth rate decreased significantly following imaging. Growth rates for 12 taxol-treated cells including the six shown in Fig. 2-4c were grouped by time from the beginning of observation (0-39.9 s, 40-79.9 s, 80-119.9 s, 120-159.9 s). The average growth rate for 0-39.9 s interval (1.24±0.15 μm/min) was significantly higher than for all subsequent periods (0.78±0.11 μm/min, 0.71±0.10 μm/min, 0.51±0.08 μm/min, respectively) (P=0.001, ANOVA), and there was a trend for the average growth rate to decrease with continued fluorescence imaging. However, consistent with increased growth rate following taxol treatment, almost all intervals had measurable growth. The hyphae shown in Fig. 2-4c were analyzed at similar times after treatment began, about 90 min, so there were minimal inter-hypha differences, again suggesting that growth rate depression was fluorescence imaging related. In addition, it appears that irradiation of taxol-treated hyphae at 488nm (the wavelength absorbed maximally by GFP) correlates with a decrease in hyphal growth rate during imaging, while irradiation at 633nm (a wavelength not absorbed by GFP) does not correlate with a decrease in hyphal growth rate during imaging (Fig. A-2).

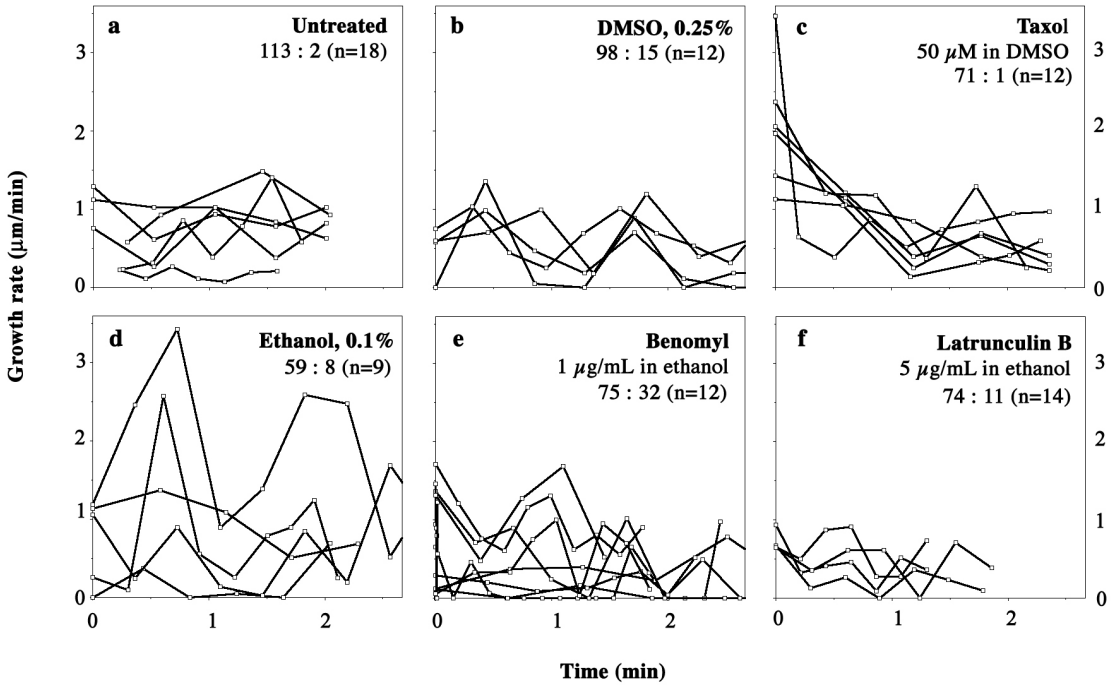

Figure 2-4. Effect of solvents and cytoskeleton-selective drugs on growth rate variability of *Aspergillus nidulans* hyphae. Growth rates are calculated for 15-30 s intervals. All graphs use the same axis scales. Each line represents a different hypha; only a representative subset from each treatment is shown for visual clarity. A tally of growing : non-growing intervals from a larger number of cells is shown for each treatment population. The drug treatments used the same (DMSO) or lower (ethanol) solvent concentrations than the solvent controls. See Figure A-2 for a control for the wavelength of irradiation on the growth rate variability of taxol-treated hyphae.

2-5. Discussion

Cytoplasm is permeated by a meshwork of cytoskeletal filaments and associated proteins. Apart from very small molecules, nothing moves by diffusion through a living cell (Bray 1992) and even diffusion can be constrained by membranes. Consequently, energy must be expended for motility of organelles within the cytoplasm (Bray 1992), and for apical migration of bulk cytoplasm with respect to cortical cytoplasm (Kaminskyj and Heath 1996). Motor proteins associated with MTs and with actin have been characterized in *A. nidulans* (reviewed in Bartnicki-Garcia 2002), but the mechanics underlying wall vesicle motility remain unclear (Bartnicki-Garcia 2002).

As well as MTs, *A. nidulans* hyphal tips contain filamentous actin arrays that have been imaged using electron tomography (Hohmann-Marriott et al. 2006), complementing whole-cell studies using actin immunofluorescence (Harris et al. 1994; Torralba et al. 1998). *A. nidulans* actin is concentrated in the apical 5 μm of growing hyphae; its abundance in more basal regions is much lower. Conversely, *A. nidulans* MTs are more abundant in basal regions than near the apex. Since the metabolic resources of a considerable length of hypha (the hyphal growth unit: Trinci 1973) are needed to support tip growth, it is intuitively attractive to ascribe long-distance transport of hyphal growth materials to MTs, and near apical transport to actin. If this notion is correct, then even if individual hyphal growth rates fluctuated (Lopez-Franco et al. 1995; Sampson and Heath 2005), growth rates for groups of hyphae should correlate with MT abundance.

This is the first study to examine the quantitative relationship between relative MT abundance, expressed as MT index, and hyphal growth rate in large numbers of *A. nidulans* hyphae. Contrary to our initial expectation, there was no correlation between growth rate and MT index for 112 growing, untreated hyphae. Untreated hyphae that failed to grow could not be predicted from their morphology prior to data collection, nor from their MT index. The only correlation we could find between growth rate and MT abundance for untreated hyphae was that, as a group, non-growing hyphae had fewer MTs than growing ones.

2-5.1. Effect of cytoskeleton-selective drugs on relative microtubule abundance and hyphal growth rate

Our early studies on untreated hyphae showed MT index-related differences between growing *vs* non-growing cells. Our subsequent growth rate comparisons were between growing cells (only) from different treatment groups so that our data could not be confounded by treatment-induced changes in proportion of growing cells. We compared groups of hyphae treated with cytoskeleton selective drugs known to be effective in *A. nidulans*; we also considered the effects of low levels of solvents in which the drugs would be dissolved.

Previous work including Kaminskyj (2000) had shown that 0.1 % ethanol or DMSO had a negligible growth effect on *A. nidulans*, but that study considered a longer time period and a different cellular event. Compared to untreated cells, low concentrations of ethanol or DMSO each had significant effects: ethanol increased growth rate but not MT index and the converse was true for DMSO. Thus group MT index and growth rate responses to these solvents did not change in a coordinate manner.

Benomyl at 1 μg/mL rapidly abolished essentially all visible MTs (1 MT in 76 hyphae in the treated population compared to an expected 893 MTs estimated for 76 ethanol control hyphae) but did not significantly reduce the average growth rate. However, 2.5 μg/mL benomyl significantly reduced hyphal growth rate compared to the control and to the 1 μg/mL dose. It seems unlikely that there are invisible but functional MTs given the provenance of LO1022 (Horio and Oakley 2005) whereas secondary drug effects cannot be discounted. Based on our data, we recommend cautious interpretation of published results that employ solvents, and use of the lowest drug concentrations possible.

In cells lacking MTs, wall vesicle transport must use the actin cytoskeleton. Growth at 0.5 μm per min (Fig. 2-3b) of a 3 μm wide hypha (Kaminskyj and Hamer 1998) requires addition of 4.7 μm^2 of cell surface per minute. A wall-forming vesicle ~ 50 nm in diameter (Hohmann-Mariott et al., 2006) has a membrane surface of ~ 65 nm^2. At least 72,000 vesicles this size must fuse at the tip each minute in order to generate sufficient new cell membrane to maintain that growth rate. Generating these vesicles and their contents likely requires much of the resources of the hyphal growth unit. If vesicle transport in *A. nidulans* were MT-based, the relatively few cytoplasmic MTs would have to be heavily coated with vesicles. Hohmann-Marriott et al. (2006)

showed that putative wall forming vesicles were about ~ 50nm from cytoplasmic MTs, whereas dynein is about 25 nm long, suggesting MTs are not the direct scaffold for vesicle transport. Taken together, the actin cytoskeleton appears to be responsible for much of the long distance vesicle transport in benomyl-treated as well as in untreated cells of *A. nidulans.*

MT assembly depends in part on the pool of unpolymerized tubulin. DMSO treatment induced a significant increase in MT index, so cells treated with taxol in DMSO might have had a reduced tubulin pool. Evidence from Ovechkina et al. (2003) suggests mitotic spindle MTs form from the same subunits as interphase cytoplasmic MTs, so there appears to be a limited pool of unpolymerized tubulin in *A. nidulans*.

Actin and MTs have been shown to interact *in vitro* (Pollard et al. 1984) and *in vivo* (Chang et al. 2005; Schuchardt et al. 2005). Our evidence shows these systems interact *in vivo* in *A. nidulans*. The growth rate reduction caused by 2.5 μg/mL benomyl, despite complete MT depolymerization from 1 μg/mL, implies an ancillary effect on actin-based transport. Latrunculin treatments reduced growth rate and caused morphological abnormalities (see also Bachewich and Heath 1998; Sampson and Heath 2005). Notably, MT index values increased following latrunculin treatment, implying compensatory MT polymerization or MT unbundling following weakening of the actin cytoskeleton. The tensegrity model of cytoplasm structure proposed for *Saprolegnia* hyphae (Kaminskyj and Heath 1996), suggests that MTs may have a role in cytoplasm cohesion.

Prolonged treatment with sublethal benomyl concentrations induce multiple apical branch formation in *N. crassa* (Riquelme et al. 1998) and in *A. nidulans* (Kaminskyj, unpublished) so MTs appear to have a role in Spitzenkörper stability. Riquelme et al. (1998) also showed that sublethal cytochalasin A treatment (another actin poison) was substantially similar to the effect of benomyl, except that the apical branches had impaired direction control. This is consistent with our suggestion that MTs and actin have some functional redundancy.

2-5.2. Hyphal growth rate variability

Growth rates in many species vary over periods as short as 1-5 s periods (López-Franco et al. 1994; Sampson et al. 2003) related in part to cytoplasmic ion gradients (Torralba and Heath 2000) and likely there are multiple feedback loops. The erratic growth rate variation we observed for untreated cells is consistent with those reports, and like Sampson et al. (2003) we found that growth rate varied between hyphae as well as over time.

Two treatments had notable effects on growth rate variability. Treatment with 0.1 % ethanol greatly increased growth rate variability, while also increasing average growth rate, perhaps by affecting membrane permeability and ion homeostasis. This argues for caution in interpreting results using strains containing *alcA*-inducible genes grown on ethanol media.

Most notable regarding growth rate variability was the effect of fluorescence imaging on taxol treated cells: the average growth rate in the first 40 s of imaging was significantly faster than for all subsequent intervals, although growth was not halted during the observation period. It is unlikely that growth rate changes were due to drug effects prior to irradiation, so they appear to have been caused by the fluorescence imaging. We minimized cell irradiance in all our experiments, and repeated imaging did not diminish average growth rates following other treatments. The binding of taxol to MTs (Horwitz 1992; Ross and Fygenson 2003) is of considerable interest due to its use in cancer chemotherapy, which is being studied using fluorescent taxol derivatives (Li et al. 2000). Visible light irradiation may thus enhance the efficacy of taxol chemotherapy, given the use of fluorescent taxol derivatives. In addition, the fact that irradiation with a wavelength absorbed my GFP (488nm), but not a longer wavelength not absorbed by GFP (633nm), reduce hyphal growth rate (Fig. A-2) suggest that either only certain wavelength might enhance the efficacy of taxol chemotherapy and/or that a molecule, such as GFP, capable of absorbing the radiation used is required to be in contact with taxol. The use of irradiation to enhance taxol chemotherapy would require that the effect of fluorescence imaging of taxol treated GFP-α-tubulin in *A. nidulans* was shown to be comparable to fluorescent taxol treated cancer cell MTs. Treatment could be achieved by treating tissue with a fluorescent taxol derivative followed by appropriate wavelength visible light irradiation.

2-5.3. What roles do MTs appear to play in hyphal tip growth?

Our results show that MT index and hyphal growth rate are not correlated for individual cells nor for groups of cells following solvent or drug treatments. In particular, 1 μg/mL benomyl depolymerized all cytoplasmic MTs but did not significantly affect growth rate over 30-60 min. Hyphal growth rates were significantly reduced by 2.5 μg/mL benomyl over the same period, suggesting that some short-term fungi toxic effects may be ancillary to MT depolymerization. Benomyl impairs progress through metaphase (Oakley and Morris 1981) and perturbs the Spitzenkörper (Riquelme et al. 1998) but morphology was not affected in the first hour, and we specifically excluded analysis of mitotic cells. Weakening the actin cytoskeleton with latrunculin, which reduced growth rates, was associated with more abundant MTs. Solvent control treatments significantly affected growth rate or MT index, but not both.

There was a correlation between effects on growth rate and on proportion of growing cells. Treatments that increased average growth rate also increased proportion of growing cells (ethanol compared to untreated; taxol compared to DMSO) and *vice versa* (latrunculin compared to ethanol). Also, with the exception of benomyl treated cells, all of which lacked MTs, the average MT index in non-growing cells was similar or lower than in growing cells for all treatments.

Taken together, our results suggest that the most likely roles of MTs are in overall regulation of average tip growth rate, whereas actin likely controls vesicle transport and targeting for tip growth. The MT system can respond to actin-selective agents by limited polymerization but cannot take over actin-specific function, and although many details require clarification tip growth rate and dynamics are influenced by cytoplasmic ion homeostasis.

CHAPTER 3: The distribution and movement of fungal Golgi are related to growth rate and the cytoskeleton in *Aspergillus nidulans* hyphae

3-1. Summary

The distribution of fungal Golgi may be related to polar growth. An *Aspergillus nidulans* strain containing a GFP tagged putative fungal Golgi marker, α-COPI, was utilized. GFP tagged α-COPI co-localized with RFP tagged α-2,6-sialyltransferase (ST), a known Golgi marker, in untreated and brefeldin A (BFA) treated *A. nidulans* hyphae. α-COPI localized to numerous, mobile, structures frequently approximately 0.5-1 μm in diameter, hereafter referred to as fungal Golgi. Fungal Golgi were more abundant at hyphal tips than subapically. Forward (tip directed) velocity of fungal Golgi was positively correlated with hyphal growth rate, while being approximately ten times greater. The actin inhibitor latrunculin B decreased the average forward velocity of fungal Golgi and hyphal growth. The above results suggest that forward fungal Golgi movement is interrelated to hyphal growth rate. The movement of fungal Golgi is likely dependant on both actin and MTs, though actin may be more important.

3-2. Introduction

The process of secretion is essential for polar growth in filamentous fungi (reviewed in Bartnicki-Garcia 2002; Heath 1990a, 1994, 1995). Golgi are involved in processing and sorting materials (reviewed in Farquhar and Palade 1998) prior to secretion (reviewed in Mogelsvang and Howell 2006). Thus, it appears likely that Golgi are involved in polar growth. It is possible that the spatial positioning and movement of fungal Golgi is related to polar growth.

Although Golgi bodies differ morphologically between animals, plants and fungi, the Golgi is functionally similiar between kingdoms. Animal cells contain a single central Golgi apparatus (reviewed in Bentivoglio and Mazzarello 1998; Ladinsky et al. 1999; Palade 1975) whose morphology and dynamics have been shown to depend on the actin cytoskeleton (Egea et al. 2006; Lazaro-Dieguez et al. 2006). MTs are also associated with animal Golgi (Farah et al. 2006; Papoulas et al. 2005). In addition, the position of the Golgi apparatus in animal cells depends on the presence of an intact microtubule (MT) cytoskeleton (Burkhardt 1998). Unlike animal cells, which have one large centrally located Golgi body (Ladinsky et al. 1999), plant cells contain numerous small Golgi bodies (Boevink et al. 1998; daSilva et al. 2004; Saint-Jore-Dupas et al. 2004). Plant Golgi have been shown to be mobile within the cytoplasm (Boevink et al. 1998; reviewed in Hawes and Satiat-Jeunemaître 2005) and to depend on the actin cytoskeleton for mobility (Boevink et al. 1998; Nebenfuhr et al. 1999; Satiat-Jeunemaître et al. 1996). In the hyphae of *Candida albicans*, Golgi have been shown, via immunofluorescent microscopy, to concentrate at the growing hyphal tips (Rida et al. 2006). This association of *C. albicans* Golgi with the apical portion of the hypha during its extension is maintained in a formin-dependant manner (Rida et al. 2006). Formin is an actin-associated protein, functioning as an actin cable nucleator (Evangelista et al. 2002; Pruyne et al. 2002; Sharpless and Harris 2002). Fungal Golgi resemble plant Golgi (Boevink et al. 1998; daSilva et al. 2004; Saint-Jore-Dupas et al. 2004) and *C. albicans* Golgi (Rida et al. 2006) in that they are small and numerous (Akao 2006; Cole et al. 2000; Kaminskyj and Boire 2004). However, fungal and plant Golgi differ in that the plant Golgi consists of distinct, roughly parallel stacks of cisternae with a clear *cis-trans* polarity (reviewed in Saint-Jore-Dupas et al. 2004) whereas the cisternae of fungal Golgi,

except those of *Saccharomyces*, are non-stacked and lack clear *cis-trans* polarity (Beckett et al. 1974; Cole et al. 2000).

The actin and microtubule (MT) cytoskeletons have roles in polarized growth of filamentous fungi (reviewed in Bartnicki-Garcia 2002; Heath 1990a, 1994, 1995; Chapter 2, section 2-4.3., page 27). F-actin arrays are concentrated in areas of active cell extension and cell wall deposition (reviewed in Heath 1990a, 1990b, 1994, 1995) as is the *A. nidulans* actin motor protein *myoA* (McGoldrick et al. 1995). In *A. nidulans,* cytoplasmic actin arrays have demonstrated roles in hyphal extension and morphogenesis (Fidel et al. 1988; Harris et al. 1994; Sampson and Heath 2005; Torralba et al. 1998) as well as septation (Momany and Hamer 1997). In addition, both actin and MTs have documented roles in organelle movement in filamentous fungi. For example, the actin cytoskeleton is involved in mitochondrial movement in *A. nidulans* (Suelmann and Fischer 2000a) and the MT cytoskeleton is involved in nuclear migration in filamentous fungi (Morris et al. 1995; Plamann et al. 1994; Suelmann and Fischer 2000b).

It has not, to our knowledge, been demonstrated that Golgi in filamentous fungi are motile independent of hyphal extension. However, as plant Golgi are mobile (Boevink et al. 1998; reviewed in Hawes and Satiat-Jeunemaître 2005), it is possible that fungal Golgi shared this characteristic. Because of the role of the Golgi in secretion, which in fungal hyphae, is concentrated at the tips (Bartnicki-Garcia and Lippman 1969), we expect *A. nidulans* fungal Golgi to show a tip-high concentration gradient, similar to that found in *Candida albicans* (Rida et al. 2006). The relationship between 1) the longitudinal spatial distribution of fungal Golgi and tip growth, 2) the tip-directed movement of fungal Golgi and tip growth, and 3) the movement of fungal Golgi and the cytoskeleton, all represent novel aspects of fungal cell biology. To our knowledge, this is the first work exploring any of these relationships. Based on the results found in animal and plant cells discussed above, we expect that the movement of fungal Golgi will be observed to be dependent on the actin and/or MT cytoskeleton.

In order to study the relationship between fungal Golgi, polar growth and the cytoskeleton in *A. nidulans* we exploited two genes: *s*uppression *o*f *d*isomy in *c*hromosome *VI* (*sod*^{VI}*C*) (Whittaker et al. 1999) and *hyp*ercellularA (*hypA*) (Kaminskyj and Boire 2004; Kaminskyj and Hamer 1998; Shi et al. 2004). Morphological mutant

alleles have been shown to be useful tools for studying factors that contribute to polar growth (e.g. Gatherar et al. 2004; Harris et al. 1999; Momany et al. 1999).

The *hypA1* morphological mutation allele is a useful tool with which to study hyphal polarity because, in *hypA1* mutant strains, hyphal growth resembles wildtype at 28˚C, but at 42˚C cells exhibit reduced polarity, defects in fungal Golgi, slower growth, and abnormal morphology (Shi et al. 2004). When the growth temperature is changed from 42˚C to 28˚C, *hypA1* mutant cells regain wildtype morphology and polarity. The *Saccharomyces cerevisiae* homolog of *hypA, trs120* encodes a component of the TRAPP II (transport protein particle) complex that has a variety of fungal Golgi-related functions (Cai et al. 2005; Guo et al. 2000; Kim et al. 2006).

A. nidulans s*od*^{VI}*C* encodes a protein similar to the yeast α-COPI (Whittaker et al. 1999), and thus was proposed to localize to vesicles derived from putative fungal Golgi. Using an *A. nidulans* strain containing GFP tagged *sod*^{VI}*C* (α-COPI) in a *hypA1* background, we characterized the distribution and rate of forward-moving (see section 3-3.5, page 46) GFP tagged α-COPI particles in hyphae grown at 28˚C and 42˚C as well as in hyphae treated with drugs targeting the actin and MT cytoskeletons.

3-3. Materials and methods

3-3.1. *Aspergillus nidulans* strains and growth conditions

The *Aspergillus nidulans* strain used for distribution and movement studies was AAB1. Susan Kaminskyj, Univ Saskatchewan, Saskatoon, SK, Canada, gave Sue Assinder the *A. nidulans* strain ASK30. In return, Assinder, Univ Wales, Bangor, Gwynedd UK, gave Kaminskyj the *A. nidulans* strain AAB1 (*hypA1, wA2, pabaA1, veA1*). AAB1 is ASK30 transformed with *alcA*-GFP-*sod*^{VI}*C*. The *A. nidulans* strain used for a wildtype control was A28 (*paba6, veA1*), the mutagenesis parent of the *hypA1* strains (Kaminskyj and Hamer 1998).

In AAB1, GFP is under the control of the *alcA* promoter, which requires alcohol to induce expression of genes under its control (reviewed in Felenbok 1991). The expression of genes under the control of *alcA* is repressed by glucose (reviewed in Felenbok 1991). AAB1 was maintained at 28ºC on complete medium (CM) (Kaminskyj

2001), supplemented with p-aminobenzoic acid, with 1% ethanol as the sole carbon source, or on nutrient broth (Difco), supplemented with paba, with 0.5% threonine as the alcohol inducer of *alcA* controlled expression. Nutrient broth with threonine was used as an *alcA* inducer as a control for impact of ethanol. Ethanol has been shown to alter hyphal growth dynamics when used even at 0.1% in addition to a glucose carbon source (see Chapter 2, Fig. 2-4, section 2-4.4., page 32).

For confocal microscopy, freshly harvested spores were inoculated onto sterile dialysis tubing overlying CM agar (Kaminskyj 2000) or nutrient broth agar, and grown for at least 24 h at 28ºC. The dialysis tubing and overlying hyphae were mounted in a microscope slide chamber (Heath 1988) in ~100 µL of liquid medium, containing solvents and cytoskeleton targeting inhibitors as required, and allowed to recover for 30 min before observation. Mounting induced transient hyphal tip swelling that made a convenient marker for treatment initiation. Observations were terminated after 120 min. Hyphae were treated with the endomembrane targeting inhibitor BFA after mounting in CM and the allowance of a 30 min period of recovery and observation. Subsequently, CM plus BFA was added via rinsing through the slide chamber. Observations began immediately following addition of BFA and terminated after 50 min. The controlled and reproducible nature of the slide chamber increase the likelihood of the growth observed being a normal, intrinsic feature of the hyphae of *A. nidulans.*

3-3.2. Inhibitors

Benomyl, paclitaxel (trade name, Taxol®), and anhydrous dimethyl sulphoxide (DMSO) were obtained from Sigma (www.sigmaaldrich.ca). Latrunculin B (hereafter, latrunculin) was obtained from Molecular Probes (probes.invitrogen.com). All other chemicals were obtained from VWR (www.vwrcanlab.ca). Inhibitors were diluted from stock solutions with room temperature liquid CM immediately before use.

Benomyl was stored at 4 °C as a 10 mg/mL stock in 100 % ethanol, and used at 1 µg/mL in 1 % ethanol. Latrunculin was stored as a 25 mg/mL stock in 100 % ethanol at -20 ºC, and used at 5 µg/mL in 1 % ethanol. Taxol was stored at -20 ºC as a 2 mM stock in 100 % DMSO and used at 50 µM in 0.25 % DMSO plus 1 % ethanol. DMSO was purchased as 1 mL ampoules of dry solvent, and the stock was stored over desiccant and

used at 0.25% DMSO plus 1 % ethanol. BFA was stored at –20°C as a 5mg/mL stock in 100% methanol, and used at 10 µg/ml in 0.5% methanol plus 1% ethanol. The inhibitor concentrations were similar to those used in the literature (benomyl and latrunculin) and/or were the lowest for which a response was detected (taxol). Threonine was stored at room temperature as a powder, and added to cool, autoclaved media to a final concentration of 0.5 %. Ethanol was stored at room temperature as a 100 % stock, and added to cool, autoclaved media to a final concentration of 1 %.

3-3.3. Confocal microscopy

Aspergillus nidulans hyphae were imaged with a Zeiss META 510 laser scanning confocal microscope (www.zeiss.com) with a Plan Apochromat 63x, N.A. 1.4 multi-immersion objective equipped with differential interference contrast (DIC) optics. GFP-*sod*^{VI}*C* fluorescence imaging used 488 nm excitation Argon laser with emission controlled by a BP505-530 filter, an excitation intensity of 5 - 10 %, and a laser current of 5.9 amps. ST-RFP fluorescence imaging used 543 nm excitation HeNe1 laser with emission controlled by LP585 filter and an excitation intensity of 100%. Eight or 16 scans per pixel at 0.6-2.5 µs/pixel were used to improve signal to noise ratio. Optical sections were 1.2 µm thick, and chosen to be near-median focal level as judged by cell profile. Observations were made based on single optical sections.

Hyphae were chosen for analysis if they were located at the colony margin, had an even profile, a smoothly tapered tip, and had grown out from the characteristic mounting-induced morphology, that is, a swollen tip or an abrupt change in growth direction. Hyphae that had not responded in this way to mounting were assumed to be non-growing, and were not selected for analysis. However, whether a particular hypha was actually growing, and at what rate, was not determined until after the data were collected. For each tip for which GFP tagged α-COPI movement and growth rate data was collected, 5-20 images were collected over 60-300 s.

3-3.4. α-2,6-sialyltransferase (ST)-RFP

The mammalian enzyme α-2,6-sialyltransferase (ST) contains a transmembrane domain important in Golgi retention (Munro 1991). ST has been shown to localize to the

animal (Munro 1991), plant (Wee et al. 1998) and *Saccharomyces cerevisiae* (Schwientek et al. 1995) Golgi. The Brandizzi group, University of Saskatchewan, Saskatoon, SK, Canada and the Hawes' group, Research School of Biological & Molecular Sciences, Oxford Brookes University, Oxford, UK kindly provided an ST-monomeric red fluorescent protein (mRFP, hereafter RFP) plasmid.

The ST-RFP is under the control of the cauliflower mosaic virus 35S promoter. This promoter has been shown to induce expression in plants (Jefferson et al. 1987; Odell et al. 1985), yeast (Hirt et al 1990) and filamentous fungi including *Uromyces* (Li et al. 1993), *Ganoderma lucidum* and *Pleurotus citrinopileatus* (Sun et al. 2002) and *Pleurotus ostreatus* (Xu et al. 2004).

In preparation for transformation with ST-RFP, AAB1 was crossed with ASK376 (*pyrG89, yA2, pabaA1, veA1*). An *alcA*-GFP-*sod*^{VI}*C, pyrG89, yA2* progeny was selected and assigned the name AMH1. Transformation of AMH1 used 4 µg of ST-RFP DNA plus 1 µg of the ARp1 DNA (Gems et al. 1991) that contains *Neurospora crassa pyr4*$^{+}$ as a selectable marker (Shi et al. 2004). The transformation followed a protocol adapted from Osmani et al. (1987) described in Shi et al. (2004). After transformation, aliquots of protoplast suspension were mixed with CM (Kaminskyj 2000) containing 0.6% agar and 1 M sucrose but lacking exogenous pyrimidine and plated over the same medium containing 1.5% agar. Protoplasts were incubated at 28 °C for 72 h before testing for RFP and GFP fluorescence. The resultant *A. nidulans* strain (*alcA*-GFP-*sod*^{VI}*C,* ST-RFP*, yA2*) was assigned the name AMH2.

3-3.5. Protein extraction, SDS-PAGE and western blotting for 35S CaMV promoter induced α-2,6-sialyltransferase (ST)-RFP expression

A. nidulans strains A28 (*paba6, veA1*; negative control for GFP and RFP), LO1022 (GFP-α-tubulin; *pabaA1; wA2; cnxE16, sC12; veA1*; positive control for GFP), and AMH2 (ST-RFP; fluorescence visible using confocal microscopy, described in section 3-3.3., page 45) were grown in 50 mL CM shaking at 200 rpm at 28 °C for 48 h. A protease inhibitor cocktail containing 4**-** (2**-**aminoethyl)benzenesulfonyl fluoride (AEBSF), pepstatin A, E**-**64, and 1,10**-**phenanthroline (Sigma) was added to the growth media (1:500 dilution) and incubated for ~ 2 min at room temperature with gentle

shaking. The growth media was filtered off using a funnel made from a sterile paper towel. Protein was extracted by gently scooping ~ 1 mL of mycelium into a mortar pre-chilled with liquid nitrogen, pouring ~ 5 mL of liquid nitrogen onto the mycelium, and grinding the frozen mycelium with a pre-chilled pestle. Additional liquid nitrogen was added as required to maintain a low grinding temperature. With a pre-chilled spatula, ~ 500 µL of the ground mycelium was placed directly into 100 °C denaturing sample buffer and vortexed immediately.

In preparation for western blot analysis, equivalent amounts of protein extract (20 µL) were separated on a 10% denaturing SDS–PAGE gel for 1 h at 200 V. The protein was then electrophoretically transferred to a nitrocellulose membrane, using a buffer consisting of 25 mM Tris, 192 mM glycine, and 20 % methanol, at 100 V for 1 h. Total protein was visualized via ponceau S staining. The membranes were subsequently incubated for 1 h at room temperature in MPBS (0.137 M NaCl, 2.7 mM KCl, 8.0 mM Na_2HPO_4, 1.8 mM KH_2PO_4, and 4% skimmed milk powder). To detect GFP-α-tubulin expression in LO1022 and ST-RFP expression in AMH2, anti-GFP polyclonal antibody (Santa Cruz Biotechnology Inc.) was used at a dilution of 1:1000 in MPBS (2% skim milk). Santa Cruz Biotechnology Inc. expects the anti-GFP use to detect both GFP and RFP (Santa Cruz Biotechnology Inc. Technical Service Representative, *personal communication*). Anti-GFP was incubated with the membrane for 2 h, shaking, at room temperature. The membrane was washed 3×5 min with PBST. Subsequently, goat-anti-rabbit-HRP conjugated antibody (Bio-Rad Laboratories) was used as the secondary antibody at a 1:5,000 dilution in MPBS (2% skim milk) and was incubated with the membrane for 1 h, shaking, at room temperature. The membrane was washed 3×5 min with PBST, followed by detection using the ECL chemiluminescent system (Amersham GE Healthcare). Chemiluminescence was detected using X-ray film (40 min exposure).

3-3.6. Analysis of *sod^{VI}C*-GFP particle movement and distribution

Sod^{VI}C-GFP particle movement was considered forward (tip directed) if the net movement between subsequent frames brought the *sod^{VI}C*-GFP particle in question closer to the tip. Because *sod^{VI}C*-GFP particle movement was roughly ten times greater than

hyphal growth rate, the movement of the hyphal tip was easily taken into account in the calculation of *sod*^{VI}*C*-GFP particle movement. In order to be considered forward, the net tip-directed movement was required to be at a ≤ 45 ° relative to an imaginary line drawn from the hyphal tip to the *sod*^{VI}*C*-GFP particle in question (Fig. 3-1). Only the movement and/or distribution of *sod*^{VI}*C*-GFP particles that could be identified, by means of intensity and/or size, were measured.

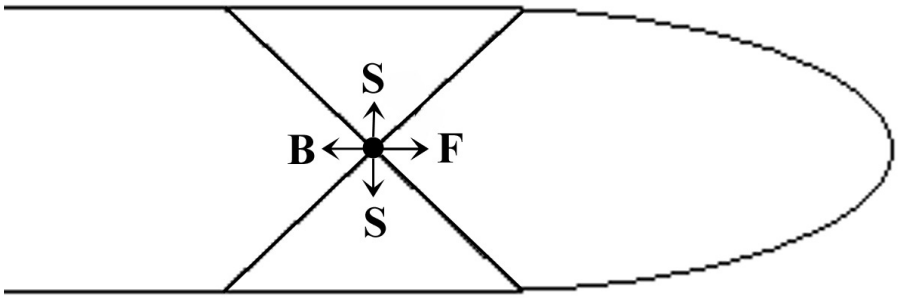

Figure 3-1. Definition of *sod*^{VI}*C*-GFP particle movement as forward, backwards or sideways. *Sod*^{VI}*C*-GFP particle movement was considered forward if the *sod*^{VI}*C*-GFP particle being observed moved toward the hyphal tip, or within a 45˚ angle of this trajectory. *sod*^{VI}*C*-GFP particle movement was considered backwards if the *sod*^{VI}*C*-GFP particle being observed moved away from the tip or within a 45˚ angle of this trajectory. *sod*^{VI}*C*-GFP particle movement was considered sideways if the *sod*^{VI}*C*-GFP particle being observed moved at a 90˚ angle to the tip (i.e. towards the side of the hypha) or within a 45˚ angle of this trajectory.

3-3.7. Statistical and graphical analysis

Data are expressed as the mean ± standard error of the mean. Statistical analyses used the 2000 version of Microsoft Excel with data analysis add-ins, which generates probability values. Statistical comparisons between treatments used one-way, single factor ANOVA, and post-*hoc* comparisons used Fisher PLSD. Numerical data are presented using the 2000 version of Microsoft Excel. Images are presented using Adobe Photoshop 7.0 with minor contrast adjustment.

Comparisons were made only between groups with similar variances. Data for α-COPI-GFP particle movement was collected in groups of 10-20 α-COPI-GFP particles hyphae per treatment, followed by α-COPI particle movement from 10-20 α-COPI-GFP particles from another treatment. Hyphal growth rates were collected after α-COPI-GFP particle movement rates had already been recorded. Individual α-COPI-GFP particles were selected arbitrarily from the brighter particles visiable within a given hypha. Individual hyphae were selected arbitrarily from a field of view containing numerous apparently growing (ie hyphae with a tapered tip profile).

3-4. Results

3-4.1. Sub-cellular localization of α-2,6-sialyltransferase (ST)-RFP and *sod^{VI}C*-GFP particles

Both ST-RFP and *sod^{VI}C*-GFP particles resembled numerous oval or horse-shoe shaped or dot-like, structures, roughly 0.5-1 μm, in diameter, found in each *Aspergillus nidulans* hypha (Figs. 3-2a and e and b and f, respectively). The shape described above is consistent with that shown of *A. nidulans* fungal Golgi in transmission electron microscopy such as those in Figure 2c of Kaminskyj and Boire (2004). When ST-RFP and *sod^{VI}C*-GFP were visualized in the same cell, the two patterns co-localized (Fig. 3-2c and g) in *A. nidulans* hyphae (shown in DIC in Fig. 3-2d and h). Negative controls for ST-RFP and An *sod^{VI}C*-GFP fluorescence are shown in Figure 3-2i-t.

Sod^{VI}C-GFP particles were mobile, independent of hyphal extension (Figs. 3-5, 3-6g). *Sod^{VI}C*-GFP particles were observed to move forward (tip directed), backwards (away from the tip) and sideways. Distinctive shapes and intensity profiles permitted the

identification of individual *sod^{VI}C*-GFP particles between frames, taken at 7 to 25 s intervals, in a time series.

The Sod^{VI}C protein has 71 % sequence similiarity to the α-COPI protein from yeast *Saccharomyces cerevisiae* (Gerich et al. 1995; Letourneur et al. 1994), as well as significant sequence similiarity to the human (Chow and Quek 1996) and bovine (Faulstich et al. 1996; Whittaker et al. 1999) α-COPI protein. Consistent with the relatively close phylogenetic relationship between the ascomycetes *S. cerevisiae* and *A. nidulans*, the *A. nidulans* Sod^{VI}C protein is closer in sequence to the *S. cerevisiae* homolog than to the human or bovine α-COPI protein (Whittaker et al. 1999). The *A. nidulans* Sod^{VI}C protein has 71 % similarity to the *S. cerevisiae* homolog (Whittaker et al. 1999). Because of the similarity between *A. nidulans* Sod^{VI}C protein and *S. cerevisiae* α-COPI, *sod^{VI}C* will hereafter be referred to as α-COPI. In *S. cerevisiae,* α-COPI has been shown to function in a very early Golgi compartment (Boehm et al. 1997), suggesting that α-COPI may also function in the Golgi, or be a reasonable proxy for Golgi localization. Because of the findings of Boehm et al. (1997) and Whittaker et al. (1999), the consistency of the appearance of α-COPI-GFP particles (Fig. 3-2b, f) with that expected for fungal Golgi (Beckett et al. 1974; Kaminskyj and Boire 2004) and the co-localization of α-COPI-GFP and ST-RFP (Fig. 3-2c and g) we expected that the morphology of α-COPI-GFP and ST-RFP particles would respond to the Golgi-targeting inhibitor BFA (Sciaky et al. 1997) in a similar manner.

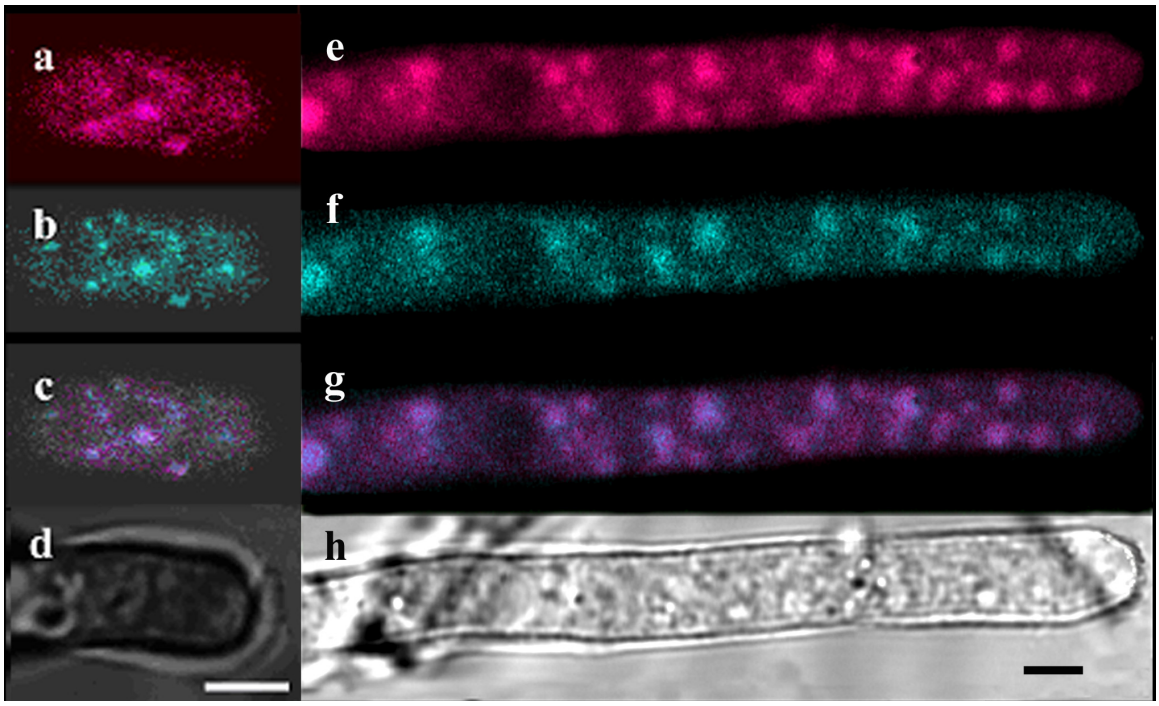

Figure 3-2. Co-localization of α-2,6-sialyltransferase (ST)-RFP and α-COPI-GFP. When visualized using confocal epifluorescence microscopy of single near-median sections, the Golgi marker, ST-RFP (magenta), co-localizes with α-COPI-GFP (cyan). ST is a mammalian enzyme that localizes to Golgi via a transmembrane domain (Munro 1991). (a-h) show *Aspergillus nidulans* strain AMH2 expressing both ST-RFP and α-COPI-GFP. (e) ST, (b and f) α-COPI, (c and g) co-localization and (d and h) transmitted light.

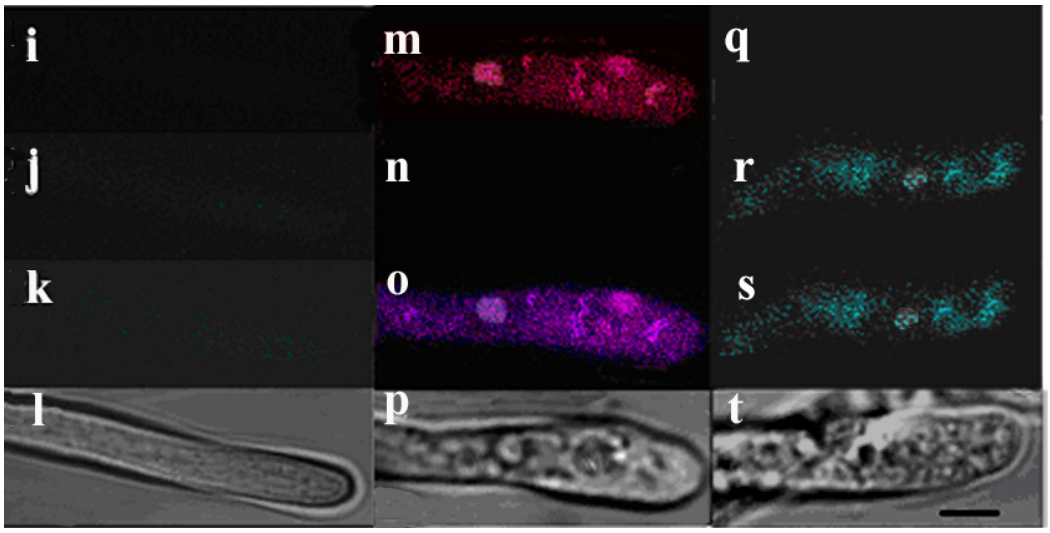

(i-l) show a wildtype *A. nidulans* (strain A28) hypha not transformed with α-COPI-GFP or ST-RFP. m-p) show *A. nidulans* strain AMH2 grown in glucose and hence expressing ST-RFP, but not α-COPI-GFP. (q-t) show *A. nidulans* strain AMH1 (not transformed with ST-RFP). (i, m and q) were imaged using microscope settings for RFP detection. (j, n and r) were imaged using microscope settings for GFP detection. (k, o and s) were imaged using microscope settings for detection of both the RFP and GFP signal. (l, p and t) show DIC images of the hyphae shown above. See Figure 3-3 for confirmation, by western blot, of 35S CaMV promoter-driven expression of ST-RFP in *A. nidulans.* Bar = 2 μm

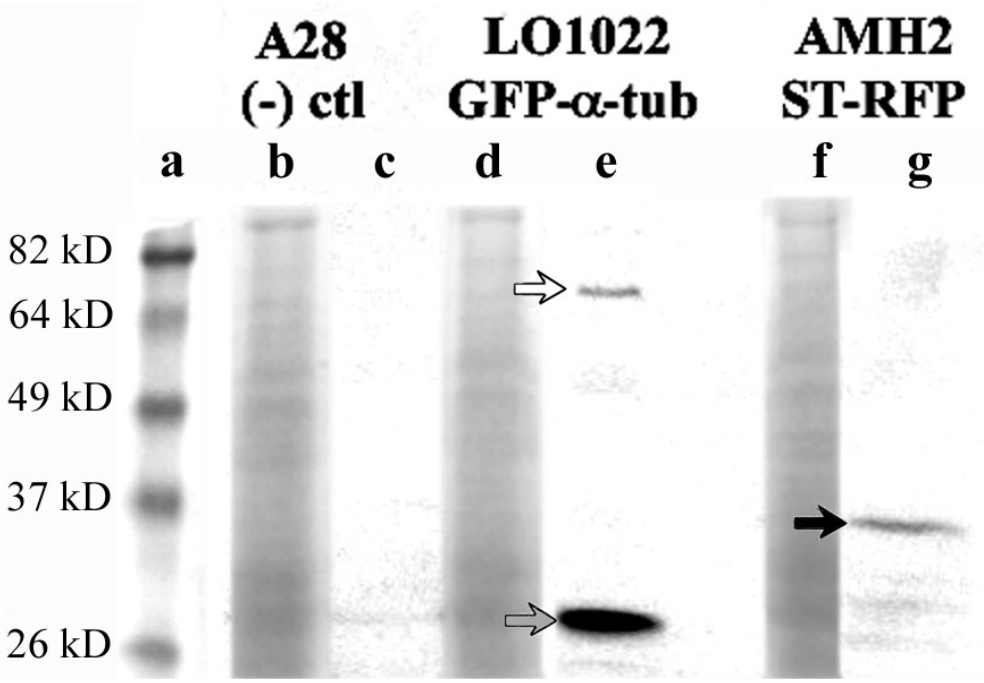

Figure 3-3. Western blot for expression of α-2,6-sialyltransferase (ST)-RFP in *Aspergillus nidulans* under the control of the 35S CaMV promoter. The primary antibody, anti-GFP (Santa Cruz Biotechnology Inc) was expected to bind both GFP and RFP. (a) shows the protein ladder with molecular weights of bands shown at left. (b and c) show protein extracted from A28, an *A. nidulans* strain not expressing GFP or RFP. (d and (e) show protein extracted from LO1022, an *A. nidulans* strain expressing GFP-α-tubulin. (f and g) show protein extracted from AMH2 grown with glucose so as to express ST-RFP under the control of the 35S CaMV promoter, but not α-COPI-GFP. (b, d and f) shown total protein stained with Ponceau S. (e) I interpret the band at approximately 77 kD (white arrow) to represent GFP-α-tubulin and the band at approximately 27 kD (grey arrow) to represent free GFP. (g) I interpret the band at approximately 35 kD (black arrow) to represent ST-RFP.

3-4.2. Brefeldin A (BFA) alters α-2,6-sialyltransferase (ST)-RFP and α-COPI-GFP particle morphology in *Aspergillus nidulans* hyphae

The endomembrane-targeting drug BFA has been shown to alter the morphology of fungal Golgi (Sciaky et al. 1997). Hence, we expected that BFA treatment would alter ST-RFP particle distribution. If α-COPI-GFP can be used as a proxy for fungal Golgi, we expected that BFA would alter α-COPI-GFP particle distribution in parallel ways. We found that BFA altered the distribution of both ST-RFP (Fig. 3-4a, d, g and j) and α-COPI-GFP particles (Fig. 3-4b, e, h and k). Within 10 min of BFA treatment, ST-RFP and α-COPI-GFP particles began to appear larger and more diffuse than they did prior to treatment (Fig. 3-4d and e). 25 min after treatment ST-RFP and α-COPI-GFP particles were still more diffuse and less distinct (Fig. 3-4 g and h). 40 min after treatment ST-RFP and α-COPI-GFP particles were extremely diffuse and almost indiscernible (Fig. 3-4j and k). Under all BFA treatments, ST-RFP and α-COPI-GFP particles co-localized (Fig. 3-4c, f, i and l).

Based on the sequence similiarity of α-COPI-GFP with *Saccharomyces cerevisiae* α-COPI (Whittaker et al. 1999), the co-localization of ST-RFP and α-COPI-GFP, in untreated and BFA treated cells, the similar response of ST-RFP and α-COPI-GFP to BFA, and the consistency of the appearance of α-COPI-GFP with that expected for fungal Golgi (Akao et al. 2006; Cole et al. 2000; Kaminskyj and Boire 2004), we propose that α-COPI-GFP can be used as a proxy for fungal Golgi. For this reason, α-COPI-GFP particles will hereafter be referred to as fungal Golgi.

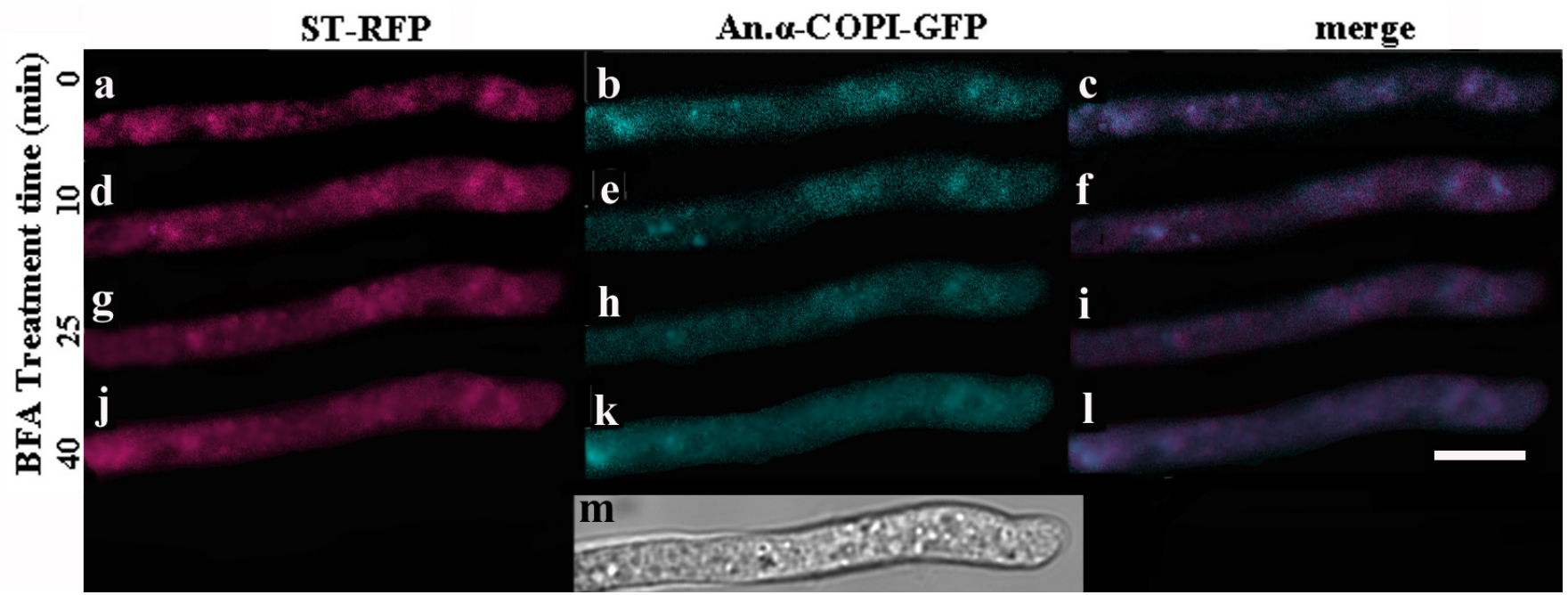

Figure 3-4. Brefeldin A (BFA) alters α-2,6-sialyltransferase (ST)-RFP and α-COPI-GFP particle morphology in *Aspergillus nidulans* hyphae. (a-c) The Golgi marker ST, tagged with RFP, (magenta) and the putative fungal Golgi marker α-COPI, tagged with GFP, (cyan) appeared as numerous, small, relatively distinct, oval or horse-shoe shaped structures before BFA treatment. (d-f) ST-RFP and α-COPI-GFP particles appeared somewhat larger, more diffuse and less numerous 10 min post treatment with BFA. (g-i) ST-RFP and α-COPI-GFP particles appeared still more diffuse, elongated and less numerous 25 min post treatment with BFA. (j-l) ST-RFP and α-COPI-GFP particles appeared very diffuse and almost indiscernible 40 min post treatment with BFA. Under all conditions shown, ST-RFP and α-COPI-GFP co-localize. (a, d, g and j) show ST-RFP. b, e, h, and k show α-COPI-GFP. (c, f, i and l) show co-localization of ST-RFP and α-COPI-GFP. (m) shows a DIC image of the same hypha. Bar = 5 μm.

3-4.3. Distribution of fungal Golgi

Golgi play a central role in secretion (e.g. reviewed in Farquhar and Palade 1998). Secretion is needed at growing hyphal tips (reviewed in Bartnicki-Garcia 2002; Bartnicki-Garcia and Lippman 1977). This tip-targeted secretion combined with the tip-high Golgi distribution gradient found in the hyphae of *Candida albicans* (Rida et al. 2006) suggest that fungal Golgi might also display a tip-high gradient in *A. nidulans* hyphae. Fungal Golgi were more abundant in the apical 25μm of *hypA1 A. nidulans* hyphae grown at 28 °C (which generally exceed 100 μm in length) than at 30, 35 or 40 μm from the tip ($P < 0.01$; Fig. 3-5). Fungal Golgi were more abundant in the apical 5 μm of *hypA1 A. nidulans* hyphae (which are generally approximately 15 μm in length) grown at 42°C than at 10 or 15 μm from the tip ($P < 0.01$; Fig. 3-5). This trend was also observed in hyphae treated with cytoskeleton-targeting inhibitors and the DMSO solvent control (data not shown).

3-4.4. Average forward velocity fungal Golgi at 42°C and 28°C

Fungal Golgi were observed to move forward (tipward), backward (away from the tip) and sideways in all hyphae observed (see Fig. 3-1 for definition of forward, backward and sideways movement). Forward velocity of fungal Golgi was faster than backwards or sideways under all conditions observed *A. nidulans* hyphae. In addition, the forward (but not backward of sideways) velocity of fungal Golgi correlated with hyphal polarity as determined by restrictive or permissive growth temperature for the *hypA1* mutant allele (Fig. A-3). There was no significant relationship between hyphal growth rate or cytoskeletal inhibitor treatment and backwards or sideways velocity of fungal Golgi movement; in contrast, a significant relationship was found between hyphal growth rate or cytoskeletal inhibitor treatment and forward velocity of fungal Golgi (discussed later, section 3-4.4., pages 55 and 57; section 3-4.5., pages 58). Furthermore, more fungal Golgi moved forward, than backward or sideways, although sideways movement has twice the angular proportion of either forward or backward movement (Fig. 3-5). We chose to show only data pertaining to the forward velocity of fungal Golgi in order to emphasize significant trends while reducing visual clutter.

As fungal Golgi were found to be quantitatively more abundant at the tips of *hypA1* hyphae grown at both 28ºC and 42ºC (Fig. 3-5), we investigated whether there was a relationship between the average forward velocity of fungal Golgi and average hyphal growth rate at 28ºC and 42ºC. Based on the work of Kaminskyj and Hamer (1998) and Kaminskyj and Boire (2004), it was expected that *hypA1* hyphae would grow more slowly at 42ºC than at 28ºC. *HypA1 Aspergillus nidulans* hyphae grown at 42ºC for approximately 14 h before being shifted to 28 ºC show increased polarity within 1 h and even greater polarity after 2 h at 28ºC (Kaminskyj and Boire 2004; Kaminskyj and Hamer 1998; Shi et al. 2004). The average forward velocity of fungal Golgi was significantly greater in *hypA1 A. nidulans* grown at 28ºC for 1 and 2 h after being grown at 42ºC for approximately 14 h than in hyphae grown at 42ºC for approximately 14 h without being shifted to 28 ºC (all $P < 0.001$) (Fig. 3-6a). The average forward velocity of fungal Golgi in *hypA1 A. nidulans* hyphae grown at 28ºC differed significantly from that of *hypA1 A. nidulans* hyphae grown at 42ºC ($P < 0.001$) or grown at 42ºC for approximately 14 h before being grown at 28ºC for 1 h ($P< 0.001$) or 2 h ($P = 0.01$) (Fig. 3-6a). The growth rates of the same hyphae discussed above were measured; hyphae grown at 42 ºC grew the most slowly ($P < 0.01$; Fig. 3-6b). Hyphal growth rate increased as time after growth temperature change from 42 ºC to 28 ºC increased ($P < 0.01$; Fig. 3-6b). Hyphal growth rate was greatest in the hyphae grown at 28ºC without pre-incubation at 28ºC ($P < 0.01$; Fig. 3-6b).

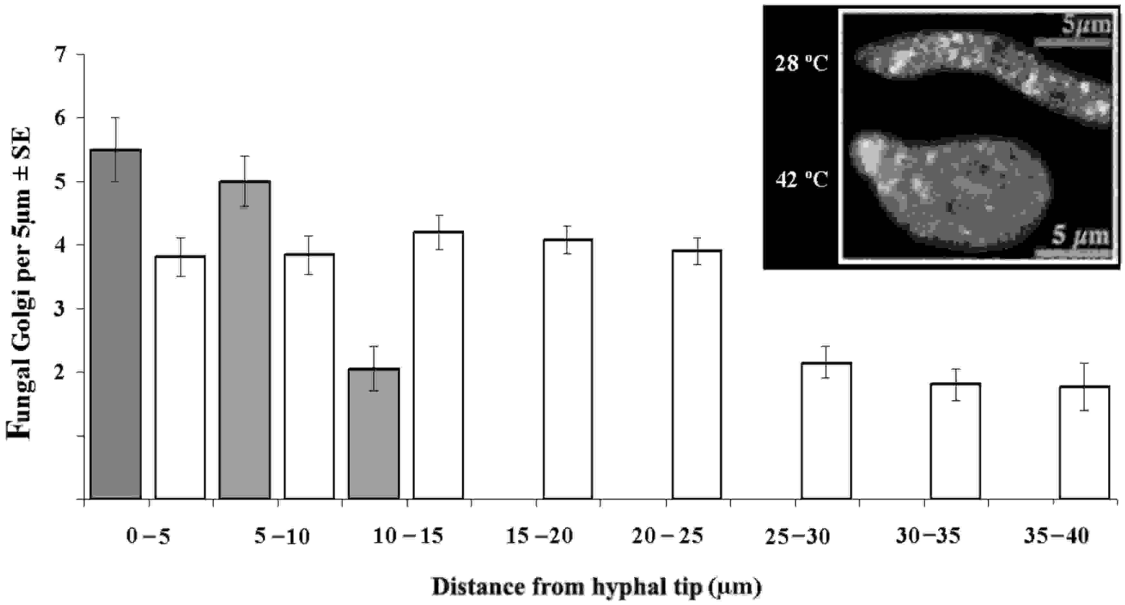

Figure 3-5. Fungal Golgi are more abundant in the apical region of *Aspergillus nidulans* hyphae**.** In *hypA1 A. nidulans* hyphae grown at 42˚C and 28˚C, fungal Golgi were significantly more abundant at the tip. In hyphae grown at 42˚C the apical 10 µm was considered the tip. In hyphae grown at 28˚C the apical 25 µm was considered the tip. Fungal Golgi distribution was observed in 15 *hypA1 A. nidulans* hyphae grown at 42˚C and 22 *hypA1 A. nidulans* hyphae grown at 28˚C. The inset image shows the relative morphology of *A. nidulans* hyphae expressing GFP tagged α-COPI grown at 28˚C and 42˚C. Grey bars = 42˚C; White bars = 28˚C.

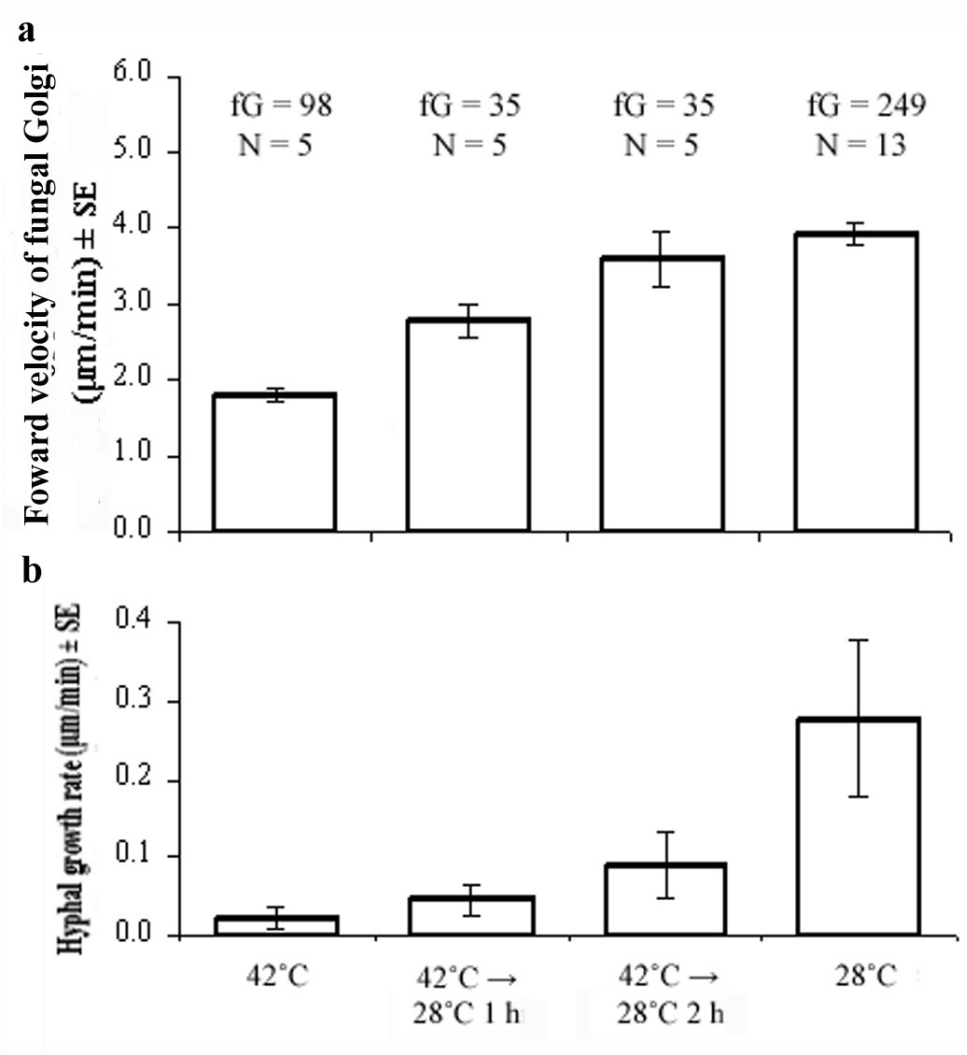

Figure 3-6. Average forward velocity of fungal Golgi and hyphal growth rate increase significantly as *hypA1 Aspergillus nidulans* hyphae are downshifted from 42ºC to 28ºC. For each growth condition, 42ºC, 42ºC → 28ºC 1 h, 42ºC → 28ºC 2 h and 28ºC, data on the forward velocity of fungal Golgi a) and hyphal growth rate b) were collected in the same cells. All *A. nidulans* hyphae were grown on complete medium containing ethanol as a sole carbon source. The average forward velocity of fungal Golgi was slowest in hyphae grown at 42ºC, significantly greater in 42ºC → 28ºC 1 h hyphae, significantly greater again in 42ºC → 28ºC 2 h hyphae and greatest in hyphae grown at 28ºC (all $P < 0.001$). Statistical comparisons between treatments used one-way, single factor ANOVA. fG = number of fungal Golgi; N = number of hyphae.

3-4.5. The relationship between the forward velocity of fungal Golgi and *Aspergillus nidulans* hyphal growth rates

We found that forward velocity of fungal Golgi was greater in more rapidly growing hyphae, grown 28ºC, then in slower growing hyphae grown at 42ºC or at 42ºC and subsequently transferred to 28ºC (Fig. 3-6). We explored the relationship between the forward velocity of fungal Golgi and hyphal growth rates in hyphal grown only at 28ºC. We expected that a positive correlation might be found. A positive correlation was observed between the rate of fungal Golgi movement and the growth rate of *A. nidulans* hyphae when the hyphae were grown in either threonine (Fig. 3-7a) or ethanol (Fig. 3-7b). A positive correlation was also observed between the rate of forward-moving fungal Golgi and hyphal growth rate when the hyphae were treated with benomyl (Fig. 3-7d), DMSO solvent control (Fig. 3-7e) or taxol (Fig. 3-7f). In contrast, no correlation was observed between the forward velocity of fungal Golgi and hyphal growth rate when the hyphae were treated with latrunculin (Fig. 3-7c). While 42% of fungal Golgi observed were moving forward in latrunculin treated hyphae, albeit at a reduced average rate relative to other growth conditions (Fig. 3-7g), none of the latrunculin treated hyphae observed were growing.

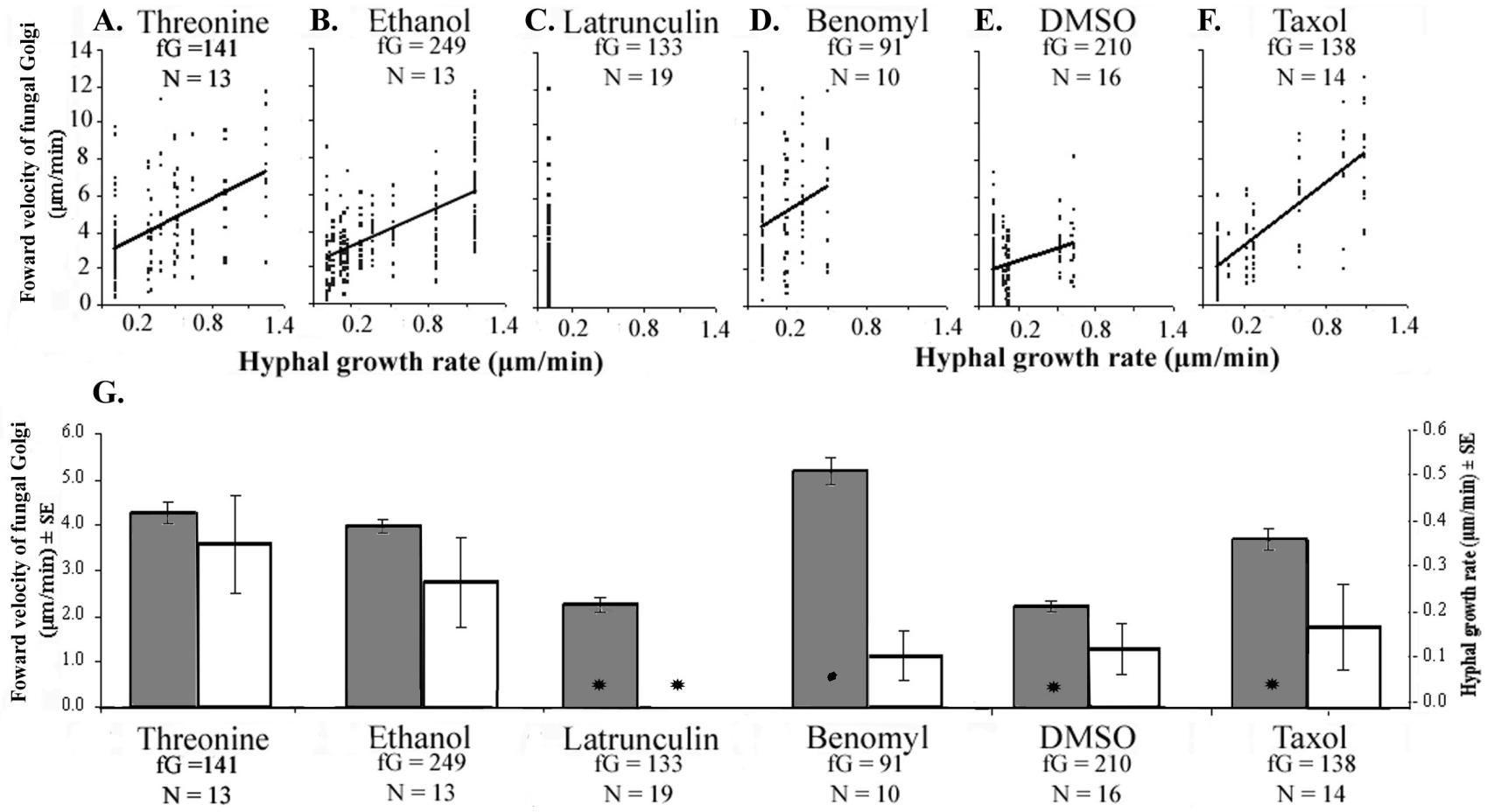

Figure 3-7. Correlation between forward fungal Golgi movement and growth rates of *Aspergillus nidulans* hyphae and impact of cytoskeletal inhibitors. a-f) all use the same x and y-axis to show the correlation between the forward velocity of fungal Golgi movement and hyphal growth rate for each treatment. In same cells, g) shows the average forward velocity of fungal Golgi and

hyphal growth rate. There was a positive correlation between the rate of forward-moving fungal Golgi and hyphal growth rate for cells grown with a) nutrient broth threonine, b) CM ethanol, d) benomyl, e) DMSO solvent control and f) DMSO plus taxol. There was no correlation between the forward velocity of fungal Golgi and hyphal growth rate for cells grown with c) CM ethanol latrunculin.

g) White bars show average hyphal growth rate and grey bars show average forward velocity of fungal Golgi in the same cells. Error bars show standard error of the mean. *A. nidulans* hyphae grown on CM ethanol (13 hyphae observed) did not significantly differ in either the forward velocity of fungal Golgi or hyphal growth rate as compared to a control grown on nutrient broth threonine (13 hyphae observed) ($P > 0.1$). Out of the 13 hyphae grown on CM ethanol, only 3 did not grow during the period of observation. Out of the 13 hyphae grown on nutrient broth threonine, 5 did not grow during the period of observation. All inhibitor and solvent controls were grown in CM ethanol. Latrunculin, benomyl and DMSO reduced the average rate of forward-moving fungal Golgi with respect to the CM ethanol control ($P < 0.001$, $P = 0.01$, $P < 0.001$). Taxol plus DMSO increased the average rate of forward-moving fungal Golgi with respect to the DMSO solvent control ($P < 0.01$). Latrunculin reduced hyphal growth rate as compared to the CM ethanol control ($P < 0.01$) while benomyl, DMSO and taxol plus DMSO did not ($P > 0.1$). Statistical comparisons between treatments used one-way, single factor ANOVA. Asterisks indicate a significant difference ($P < 0.05$) with respect to the corresponding control. fG = number of fungal Golgi; N = number of hyphae.

3-4.6. Impact of cytoskeleton-targeting drugs on forward velocity of fungal Golgi and hyphal growth rate

Based on animal Golgi, which appear to depend on both the actin and MT cytoskeleton for movement and organization (Farah et al. 2006; Lazaro-Dieguez et al. 2006; Papoulas et al. 2005), and plant Golgi, which appear to depend on actin and not MTs for motility (Boevink et al. 1998; Satiat-Jeunemaître et al. 1996), we hypothesized that fungal Golgi would depend on either the actin and MT or only the actin cytoskeleton for motility. To test this idea, *A. nidulans* hyphae were treated with the cytoskeleton-targeting inhibitors benomyl, latrunculin, and taxol and the solvent control DMSO. Benomyl and latrunculin are both well-characterized and known to have an impact on hyphal tip growth in *A. nidulans* (Chapter 2, Fig. 2-3; Horio and Oakley 2005; Sampson and Heath 2005) by targeting MTs and F-actin, respectively. Taxol has been shown to induce polymerization of *A. nidulans* MTs *in vitro* (Yoon and Oakley 1995) but to our knowledge had not been studied *in vivo* in *A. nidulans* prior to our results in Chapter 2. As controls, *A. nidulans* hyphae were grown, and the forward velocity of fungal Golgi measured, without inhibitor treatment. These inhibitor-free hyphae were grown in CM with ethanol as the sole carbon source (Fig. 3-7b and g) and in nutrient broth with threonine as an alterative *alcA* inducer (Fig. 3-7a and g). *A. nidulans* hyphae grown on CM ethanol did not significantly differ in either the forward velocity of fungal Golgi or hyphal growth rate as compared to hyphae grown on nutrient broth threonine ($P < 0.001$). The impact of cytoskeletal inhibitors and solvents controls on the forward velocity of fungal Golgi and hyphal growth rate was observed in the same cells. Latrunculin and DMSO reduced the average forward velocity of fungal Golgi with respect to the ethanol control (each $P < 0.001$; Fig. 3-7g) while benomyl did to a lesser extent ($P > 0.1$; Fig. 3-7g). Taxol plus DMSO increased the average forward velocity of fungal Golgi with respect to the DMSO solvent control ($P < 0.01$; Fig. 3-7g). Latrunculin significantly reduced hyphal growth rate as compared to the ethanol control ($P < 0.01$) while benomyl, DMSO and taxol plus DMSO did not (all $P > 0.1$; Fig. 3-7g).

3-5. Discussion

The Golgi complex is involved in the secretory pathway in eukaryotic cells. Proteins and carbohydrates destined for secretion pass through the Golgi as they move towards the plasma membrane (reviewed in Farquhar and Palade 1981, 1998 and Mogelsvang and Howell 2006), or, in fungi, primarily the growing hyphal tip (reviewed in Bartnicki-Garcia 2002; Bartnicki-Garcia and Lippman 1977). Because of the contribution of Golgi to secretion (reviewed in Farquhar and Palade 1981, 1998 and Mogelsvang and Howell 2006), and the role of secretion in polar growth (reviewed in Bartnicki-Garcia 2002), it seems reasonable that the distribution and/or movement of fungal Golgi might be related to polar growth. We set out to investigate 1) fungal Golgi distribution relative to the hyphal tip and polarity, 2) the movement of fungal Golgi, independent of tip extension, and polar growth and 3) the movement of fungal Golgi and the actin and MT cytoskeleton, using *A. nidulans* as a model system.

3-5.1. α-COPI localizes to fungal Golgi

Because ST-RFP and α-COPI-GFP co-localize in *Aspergillus nidulans* hyphae (Fig. 3-2) we hypothesize that α-COPI-GFP is associated with COPI coated fungal Golgi-derived vesicles and can thus be used as a proxy for fungal Golgi. ST is a mammalian enzyme that contains a transmembrane domain important in Golgi retention (Munro 1991). ST has been shown to localize to the animal (Munro 1991), plant (Wee et al 1998) and *Saccharomyces cerevisiae* (Schwientek et al. 1995) Golgi. Given that, in the yeast *S. cerevisiae,* α-COPI has been shown to function in a very early Golgi compartment (Boehm et al. 1997) it is not unexpected that the α-COPI homolog, α-COPI, should appear to be a reasonable proxy for fungal Golgi in *A. nidulans*. Slight differences in shape or intensity of ST-RFP and α-COPI-GFP localization could be attributed to the fact that ST is associated with the Golgi via a transmembrane domain (Munro 1991) while α-COPI (Chow and Quek 1996; Faulstich et al. 1996; Gerich et al. 1995; Letourneur et al. 1994; Whittaker et al. 1999) functions as a vesicle coatomer (Rothman 1996), implying that α-COPI is likely to associate peripherally with Golgi membranes.

The cauliflower mosaic virus 35S promoter has been shown to induce expression in plants (Jefferson et al. 1987; Odell et al. 1985), the yeast *Saccharomyces*

(Hirt et al 1990) and filamentous fungi including *Uromyces* (Li et al. 1993), *Ganoderma lucidum* and *Pleurotus citrinopileatus* (Sun et al. 2002) and *Pleurotus ostreatus* (Xu et al. 2004). As *Saccharomyces* is an ascomycete, and *Uromyces*, *Ganoderma* and *Pleurotus* are filamentous fungi, and hence related to *A. nidulans*, it was not unexpected that the cauliflower mosaic virus 35S promoter also induced expressed in *A. nidulans* (see western blot for ST-RFP protein expression, Fig. 3-3). Therefore, ST-RFP, under the control the cauliflower mosaic virus 35S promoter can be used as a marker for Golgi in *A. nidulans.*

Treatment of *A. nidulans* hyphae with BFA results in both ST-RFP and α-COPI-GFP particles increasing in diameter and becoming more diffuse (Fig 3-4). The impact of BFA on α-COPI-GFP particle morphology is consistent with α-COPI-GFP being a reasonable proxy for fungal Golgi. For example, treatment with BFA leads to the disassembly of the Golgi apparatus in animal (e.g. Fujiwara et al. 1988) or plant cells (e.g. Ritzenthaler et al. 2002). Similar BFA-induced effects have been observed on Golgi morphology in *Aspergillus niger* (Khalaj et al. 2001), *Schizophyllum commune* (Rupeš et al. 1995) and *Pisolithus tinctorius* (Cole et al. 2000). These effects include increased size of the fungal Golgi (Cole et al. 2000; Rupeš et al. 1995) and Golgi disassembly (Khalaj et al. 2001). The impact of BFA treatment on ST-RFP and α-COPI-GFP particle morphology is consistent with Cole et al. (2000) and Rupeš et al. (1995) in that ST-RFP and α-COPI-GFP particles appear larger hyphae treated with BFA for 10 to 40 min (Fig. 3-4). The impact of BFA treatment on ST-RFP and α-COPI-GFP particles can also be interpreted as being consistent with Khalaj et al. (2001) in that ST-RFP and α-COPI-GFP particles appear more diffuse post-BFA treatment than prior to treatment (Fig. 3-4); the diffuse appearance of ST-RFP and α-COPI-GFP particles could indicate at least some degree of disassembly. Notably, interpretation of the impact of BFA on α-COPI-GFP particle morphology is complicated by the fact that one of the first effects of BFA is the release of COPI coat proteins from the Golgi complex (Donaldson et al. 1992; Helms and Rothman 1992). Thus, the fact that ST-RFP and α-COPI-GFP particles show a coordinated response to BFA treatment, appearing more diffuse and less punctate, strongly supports our interpretation of α-COPI-GFP as a proxy for fungal Golgi prior to

BFA treatment. Even if the impact of BFA on α-COPI-GFP morphology does not demonstrate their equivalence to fungal Golgi, it does not argue against this hypothesis.

α-COPI-GFP particles appeared as numerous oval or horseshoe shaped structures in each hypha (Figs. 3-2b and f; 3-3b; and 3-4 inset). This shape is consistent with that shown in Figure 2c of Kaminskyj and Boire (2004). In the filamentous basidiomycete *Pisolithus tinctorius*, many small fungal Golgi have been observed per hypha, each made up of two to four oval membranous compartments, which together outline a roughly circular region (Cole et al. 2000). Consistent with and the observations of Kaminskyj and Boire (2004) and Cole et al. (2000), α-COPI-GFP particles in *A. nidulans* (Figs. 3-2b and f; 3-3b; and 3-4 inset), in *Aspergillus oryzae* the putative fungal Golgi marker, FmanIBp:GFP, was observed with fluorescent microscopy as dot-like structures distributed through the hyphal cytoplasm (Akao et al. 2006). Thus, the appearance of GFP tagged α-COPI in living *A. nidulans* hyphae is consistent with that expected for fungal Golgi (Akao et al. 2006; Beckett et al. 1974; Cole et al. 2000; Kaminskyj and Boire 2004).

3-5.2. Role of fungal Golgi in hyphal growth

There are four lines of evidence to suggest that fungal Golgi could contribute to polar growth in *Aspergillus nidulans.* 1) fungal Golgi are observed to have a tip localized distribution (Fig. 3-5). 2) Forward velocity of fungal Golgi was more rapid in more highly polarized *hypA1 A. nidulans* hyphae (i.e. hyphae grown at the permissive temperature; Kaminskyj and Boire 2004; Kaminskyj and Hamer 1998) (Fig. 3-6). 3) A positive correlation was observed between the forward velocity of fungal Golgi movement and hyphal growth rate (Fig. 3-7a-f). 4) Inhibition of the actin cytoskeleton reduced hyphal growth rate to zero and led to a significant decrease in the average forward velocity of fungal Golgi (Fig. 3-7g). The elimination of hyphal growth in latrunculin treated hyphae (Fig. 3-7g) differs from results of chapter 2 (Figs. 2-3c, page 30 and 2-4f, page 34). This discrepancy will be discussed below (page 71).

In fungal hyphae growth occurs at the tips or at branch sites. It seems reasonable that fungal organelles involved in polar growth would be more abundant near the tip than subapically. Consistent with this idea, vesicles in *Neurospora crassa,*

presumed to be destined for fusion at the growing tip, and thus involved in polar growth, are found with dramatically higher density near the tip (Collinge and Trinci 1974; Silverman-Gavrila and Lew 2003). The Spitzenkörper is positioned immediately behind the growing tip (reviewed in Bartnicki-García 2002; Harris 2006). Displacement of the Spitzenkörper can alter the direction of hyphal growth (reviewed in Bartnicki-García 2002; Bracker et al. 1997; Riquelme et al. 2000). In addition, SNAREs (soluble NSF attachment receptors that mediate fusion of cellular transport vesicles) involved in exocytosis (Gupta and Heath 2000; Weinberger et al. 2005) and ER to Golgi transport (Weinberger et al. 2005) have been observed to be concentrated in the apical domain of growing fungal hyphae (Gupta and Heath 2000). In contrast to fungal Golgi of *A. nidulans,* which were most abundant in the apical 25 μm, Golgi in rapid freeze fixed specimens of the oomycete *Saprolegnia ferax* were absent from the apical 5 μm, and roughly evenly disrupted subapically (Heath and Kaminskyj 1989). Potentially, the differences in Golgi distribution between *A. nidulans* and *S. ferax* can be explained by 1) taxonomic differences, 2) the larger size of *S. ferax* cells, meaning that the apical 5 μm is a smaller portion of the cell size, 3) differences between living and fixed cells or 4) the smaller number of *S. ferax* cells (N = 3; Heath and Kaminskyj 1989) observed compared to *A. nidulans* cells (N = 22). The greater abundance of fungal Golgi in the apical region of both *hypA1 A. nidulans* hyphae grown at both 28˚C and 42˚C (Fig. 3-5), suggests that fungal Golgi could be involved in polar growth. The contribution of fungal Golgi to polar growth probably, based on Golgi functions (reviewed in Farquhar and Palade 1998), involves the processing and sorting of material to be packaged into vesicles destined to fuse with the hyphal tip.

Although motility of fungal Golgi has not, to our knowledge, been previously demonstrated, plant Golgi have been shown to be mobile (Boevink et al. 1998; reviewed in Hawes and Satiat-Jeunemaître 2005). Since both plant and fungal Golgi are small with respect to animal Golgi and found in multiple copies per cell (Boevink et al. 1998; Cole et al. 2000; daSilva et al. 2004; Saint-Jore-Dupas et al. 2004), it is not unexpected that fungal Golgi were also observed to be mobile independent of hyphal growth (Figs. 3-5 and 3-6).

Based on observations made at 28°C and 42°C in *hypA1 A. nidulans* hyphae, it appears that forward movement of fungal Golgi is related to hyphal polarity (Fig. 3-6). *A. nidulans* strains containing the *hypA1* mutant allele are a useful tool for exploring polarity because *hypA1* has been shown to decrease hyphal polarity at 42°C while permitting wildtype polarity at 28°C (Kaminskyj and Boire 2004; Kaminskyj and Hamer 1998; Shi et al. 2004). When *hypA1 A. nidulans* hyphae are transferred from restrictive temperature (42°C) to the permissive temperature (28°C), the average forward velocity of fungal Golgi increased significantly while polarity and growth rate increased in the same cells (Fig. 3-6). A precedent for the validity of using temperature sensitive morphological mutants to study factors potentially contributing to polarity has been shown (Gatherar et al. 2004; Harris et al. 1994, 1999; Momany et al. 1999). For example, Gatherar et al. (2004) used the *hbrB* temperature sensitive hyperbranching *A. nidulans* mutant involved in vacuolar import, *hbrB3*, to investigate hyphal polarity. Gatherar et al. (2004) found that the *hbrB3* mutant influences polarity through osmoregulation and cell wall biogenesis. Harris et al. (1999) used temperature sensitive *pod* (*po*larity *d*efective) morphogenesis mutants to show that polarity establishment is dependant on the actin cytoskeleton. Momany et al. (1999) used temperature sensitive *swo* (*swo*llen cell) morphogenesis mutants to suggest that polarity establishment and polarity maintenance are genetically separate events and that a persistent signal is required for apical extension in *A. nidulans*.

The positive correlation between the average forward velocity of fungal Golgi and hyphal growth rate (Fig. 3-7a-f) suggests that forward moving fungal Golgi could contribute to polarity. Forward moving fungal Golgi could act as components of the machinery presumably needed to transport material to the tip. This correlation between the forward velocity of fungal Golgi and hyphal growth is found in cells grown in nutrient broth with threonine, cells grown on CM with ethanol as the carbon source and cells grown on CM treated with MT inhibitors or solvent controls (Fig. 3-7a-f). The fact a positive correlation between the forward velocity of fungal Golgi and hyphal growth rate persists even in the presence of cytoskeleton-targeting drugs and under different nutritional conditions, could indicate that the relationship between polar growth and tipward fungal Golgi movement is fundamental to hyphal growth in *A. nidulans,* rather

than being dependant on certain growth conditions. Deviations away from linear correlation between forward velocity of fungal Golgi and hyphal growth rate may be explained by the fact that growth rates of the hyphae were variable, rather than constant, between tip position measurements (see Chapter 2, section 2-5.2., page 37 for a discussion of growth rate variability in *A. nidulans* hyphae). Despite deviations, a positive correlation between forward velocity of fungal Golgi and hyphal growth rate is still observed.

The elimination of hyphal growth in latrunculin treated hyphae (Fig. 3-7g) differs from results of chapter 2 (Figs. 2-3c, page 30 and 2-4f, page 34). This discrepancy can potentially be explained by 1) differences in the growth conditions used between chapters 2 and 3, 2) differences in sample size and 3) differences in data presentation. First, in chapter 2, the hyphae were grown in CM glucose with 0.1% ethanol, while, in this chapter, the hyphae were grown in CM with 1% ethanol without glucose. The impact of ethanol is discussed further in section 3-5.3., page 69. Second, in Figure 2-3c, 46 hyphae were observed, while, in Figure 3-6g, only 19 hyphae were observed. Third, in Figures 2-3 and 2-4 only data from growing hyphae is presented. Of the 46 hyphae observed, 25 were non-growing. Figure 2-3c shows the average growth rate of the 21 growing latrunculin treated hyphae. Figure 2-4c shows a random selection of 4 of these 21 growing hyphae.

The fact that latrunculin treatment both eliminated observable hyphal growth and significantly reduced the average forward velocity of fungal Golgi (Fig. 3-7g), suggests that forward-moving fungal Golgi are important in polar growth. However, the fact that forward fungal Golgi movement continues in the absence of any growth could imply that forward fungal Golgi movement and hyphal growth are partly independent. Figures 3-6a-f also show non-growing hyphae in which some forward fungal Golgi movement was observed. Potentially, non-growing hyphae have a 'residual' degree of fungal Golgi movement in all directions. The rate of fungal Golgi forward movement increases above this 'residual' level with increasing hyphal growth rate and/or polarity.

3-5.3. Relationship between the distribution and movement of fungal Golgi and the cytoskeleton

It seems intuitive that the motors transporting organelles (Bray 1992; reviewed in Heath 1994) would require cytoskeletal tracks. As both actin and MTs form long polymers *in vivo* (reviewed in Heath 1994) it is reasonable to hypothesize that one or both of these cytoskeletal components could be involved in the long-range transport of fungal Golgi in fungal hyphae.

The actin cytoskeleton has been shown to be essential for polar growth in *A. nidulans* (e.g. Fidel et al. 1988; Harris et al. 1994; Kaminskyj 2000; Sampson and Heath 2005; Chapter 2, section 2-4.3., page 27; section 3-4.5., page 58), *Neurospora crassa* (e.g. Virag and Griffiths 2004), and oomycetes such as *Saprolegnia ferax* (Bachewich and Heath 1997; Gupta and Heath 1997; Heath et al. 2000). Consistent with the above, depolymerization of F-actin with latrunculin leads to elimination of observable hyphal growth and significantly reduced the average forward velocity of fungal Golgi (Fig. 3-7g), suggesting that fungal Golgi movement is dependant, at least in part, on the actin cytoskeleton.

Treatment of *A. nidulans* hyphae with 1 μg/mL benomyl reduces hyphal growth rate, though not to a statistically significant degree, but does not reduce the average forward velocity of fungal Golgi (Fig. 3-7g). This suggests that intact MTs are not essential for motility of fungal Golgi in *A. nidulans*. There are three pieces of evidence that MTs did, as expected, depolymerize as a result of 1 μg/mL benomyl treatment. 1) Treatment with 1 μg/mL benomyl eliminated all observation cytoplasmic MTs (data from α-tubulin-GFP *A. nidulans* strain; Chapter 2). 2) Overnight treatment with 1 μg/mL benomyl resulted in morphological changes in *A. nidulans* (Fig. A-4) consistent with that expected from higher levels of benomyl treatment (Kaminskyj, unpublished results; Riquelme et al. 2003; see Riquelme et al. 1998 for *N. crassa* data). 3) Treatment with 1 μg/mL benomyl for more than 2 h led to virtually all hyphae being arrested at metaphase (data from α-tubulin-GFP *A. nidulans* strain; Chapter 2, section 2-4.3., page 27), consistent with the elimination of polymerized cytoplasmic MTs (Ovechkina et al. 2003). Data from section 3-4.5., page 61, suggest that, in the absence of MTs, at least in the first 2 h, the function(s) of MTs in movement of fungal Golgi can be performed by actin, while those of actin cannot be performed by MTs.

The fact that taxol plus DMSO significantly increases the average forward velocity of fungal Golgi over that found in hyphae treated with the DMSO solvent control (Fig. 3-7g) suggests that MTs may play some role in fungal Golgi movement. The presence of additional polymerized MTs, found in taxol treated *A. nidulans* hyphae (e.g. Chapter 2, section 2-4.3., page 27), could facilitate an increase in forward fungal Golgi movement by providing additional tracks if MTs are involved in fungal Golgi movement.

Fungal Golgi were more abundant at *A. nidulans* hyphal tips (Fig. 3-5), while MTs are less abundant at the tip (Chapter 2, section 2-4.2., page 25), suggesting that the positioning of fungal Golgi may be more dependent on actin than MTs. This hypothesis is supported by the fact that actin is abundant at the tips of fungal hyphae (Bartnicki-Garcia 2002; Heath 1994; Heath et al. 2003; Torralba et al. 1998). Consistently, Rida et al. (2006) showed that the actin-nucleating protein formin (Evangelista et al. 2002; Pruyne et al. 2002; Sharpless and Harris 2002), rather than MTs, is required for Golgi distribution in *Candida albicans* hyphae.

When MTs or actin arrays are disrupted or altered (for example by treatment with latrunculin, benomyl, DMSO and taxol) and forward fungal Golgi movement continued, albeit at a decreased or increased rate (Fig. 3-7g), for a period of time. Interpreting results obtained from drug treatments is complicated by the fact that all chemicals have secondary effects. Potentially the continued motility of fungal Golgi could be based on 1) other, non-disrupted, cytoskeletal components (i.e. actin if MTs are disrupted or MTs if actin is disrupted) and/or 2) cytoplasmic flow towards the growing tip, which could continue from the undisrupted cytoskeletal components. In growing hyphae, the apical cytoplasm is presumably migrating forward as the tip extends in order to fill in the nascent hyphal tip. Potentially this forward movement of the cytoplasm could have contributed to the higher forward velocity of fungal Golgi as compared to backwards or sideways velocity as well as movement in the presence of cytoskeletal disruption. The migration of hyphal cytoplasm is likely almost wholly dependent on the actin cytoskeleton (Bray 1992; reviewed in Heath 1994; Kaminskyj and Heath 1995, 1996), potentially explaining why latrunculin-induced actin depolymerization reduced the average forward velocity of fungal Golgi to a greater degree than did benomyl-induced MT depolymerization (Fig. 3-7g).

3-5.3. Impact of ethanol

Ethanol can be used to induce expression of genes under the control of *alcA* promoter (Fernández-Ábalos 1998; Nikolaev et al. 2002; Romero et al. 2003), but the results presented in Chapter 2 (section 2-4.4., page 32) suggest that the impacts of ethanol on hyphal growth are not unimportant. Low concentrations of ethanol altered hyphal growth rate dynamics, leading to increased variability (Fig. 2-4), potentially by altering membrane permeability, thus affecting homeostasis of ions such as Ca^{2+} (Torralba and Heath 2000). In *Neurospora crassa*, dissipation of the tip-high Ca^{2+} gradient has been shown to inhibit tip growth (Silverman-Gavrila and Lew 2000). Silverman-Gavrila and Lew (2001) show that alteration of the tip-high Ca^{2+} gradient corresponds to alterations in the actin cytoskeleton. As discussed above, the migration of hyphal cytoplasm is likely almost wholly dependent on the actin cytoskeleton (Bray 1992; reviewed in Heath 1994; Kaminskyj and Heath 1995, 1996). Also, only a slight tip-high Ca^{2+} gradient is required in *N. crassa* for tip growth (Silverman-Gavrila and Lew 2003), implying that a small change in Ca^{2+} gradient could alter growth. Altered tip growth, cytoplasmic migration and/or actin cytoskeleton all represent significant changes in hyphal biology.

The experiments in this chapter differ significantly from those in Chapter 2 where 0.1% ethanol was added to CM, in addition to glucose, as a carbon source, while, in this work, 1% ethanol in CM is the sole carbon source. Cells grown on threonine in nutrient broth did not different significantly from the ethanol in CM in terms of either average forward velocity of fungal Golgi or hyphal growth rate (Fig. 3-7g).

CHAPTER 4: Discussion

Hyphae of filamentous fungi elongate at the tips by polar growth. In this thesis, I set out to evaluate the contributions of the microtubule (MT) cytoskeleton and the spatial distribution and movement of fungal Golgi to polar growth in the ascomycete *Aspergillus nidulans*.

4-1. The cytoskeleton and tip growth

The cytoskeleton, two major components of which are actin and MTs, is a cellular 'scaffolding' contained within the cytoplasm. The cytoskeleton has many functions as part of the structural framework of eukaryotic cells including assisting in the maintenance of cell shape and distribution of genetic material during cell division. I chose to focus on the roles of MTs in *Aspergillus nidulans* hyphae because 1) the role of MTs are less clearly understood than those of actin (see Chapter 2, section 2-1., page 18) and 2) a GFP tagged MT *A. nidulans* strain was available, facilitating study of MTs *in vivo*.

The study of all possible contributions of MTs to polar growth is a complex topic. Because of this, I set out to explore the role of MTs in tip growth by setting four specific goals. 1) To observe and characterize the appearance and organization of cytoplasmic MT populations in living *A. nidulans* hyphae. 2) To examine the relationship between hyphal growth rate and relative MT abundance in untreated *A. nidulans* hyphae. 3) To examine the effects of inhibitors and the solvents in which the inhibitors were dissolved on relative MT abundance and hyphal growth rate in *A. nidulans*. 4) To assess the effects of cytoskeletal inhibitors and solvent controls on hyphal growth rate variability in *A. nidulans*. I will relate my findings to data presented in the literature on other hyphal organisms. In so doing I hope to put into context my findings on the contribution(s) of MTs to hyphal growth in *A. nidulans*.

4-1.1. MT organization

MTs in living untreated *Aspergillus nidulans* hyphae are long and flexuous, and run parallel to the long axis of the cell (Fig. 2-1a). This arrangement suggests that MTs could act as tracks on which material needed for polar growth could be transported. This

section will examine data on the organization of MTs in other hyphal organisms beyond *A. nidulans.* Subsequent sections will relate MT organization to the role(s) MTs have in polar growth in these organisms. This may provide a more complete understanding of the role(s) of MTs in hyphal growth than could be obtained from looking exclusively at data obtained from *A. nidulans*. The number and arrangement of cytoplasmic MTs varies significantly among filamentous ascomycetes. For example, in *A. nidulans*, MTs are relatively few in number and are predominantly in the central, as opposed to the peripheral, cytoplasm (Meyer et al. 1987; Ovechkina et al. 2003; Sampson and Heath 2005). In *N. crassa* hyphae MTs are relatively numerous and are found in the both central and peripheral cytoplasm (Freitag et al. 2004; Mouriño-Pérez et al. 2006). *A. nidulans* MTs are mostly parallel to the hyphal axis (Meyer et al. 1987; Ovechkina et al. 2003; Sampson and Heath 2005), whereas *N. crassa* MTs are mostly parallel to the axis near the hyphal tip but more randomly oriented in basal compartments (Freitag et al. 2004).

Basidiomycete MT organization appears to more closely to resemble that of *A. nidulans* MTs. In hyphae of the basidiomycete *Pleurotus ostreatus,* cytoplasmic MTs are observed to be long filaments oriented longitudinally within hyphae (Kaminskyj et al. 1989; Torralba et al. 2004). This longitudinal orientation resembles that of *A. nidulans* MTs (Fig 2-1). The organization of *P. ostreatus* MTs also resembles *A. nidulans* MTs in that they circumvent the vicinity of the nucleus (Fig. 2-1; Torralba et al. 2004). The MTs in hyphae of the basidiomycetes *Ustilago maydis* and *Schizophyllum commune* resemble those of *A. nidulans* in that they are also long and flexuous and run parallel to the long axis of the hyphae (Fuchs et al. 2005; Raudaskoski et al. 1991; 1994; Rupeš et al. 1995). Also, like *A. nidulans* MTs, *S. commune* MTs appear to circumvent nuclei and extend into the apical zone, without converging or noticeably increasing in abundance as they do so (Raudaskoski et al. 1991).

When MTs of oomycete hyphae are considered, still greater diversity of MT organization can be observed than is observed among ascomycetes. For example, in hyphae of the oomycete *Phytophthora infestans*, MTs are found in bundles, observed via immunofluorescence, extending from the nucleus-associated centers towards and away from the tip (Temperli et al. 1990; Uchida et al. 2005). In addition, *Saprolegnia ferax*

and *P. infestans* MT density is highest near the nucleus (Kaminskyj and Heath 1994; Temperli et al. 1990; Uchida et al. 2005). This contrasts with MTs in *A. nidulans,* which appear to be less numerous in the vicinity of the nuclei and to circumvent the perinuclear regions (Fig. 2-1). These nucleus-circumventing MTs are likely nucleated by nucleus-associated organelles (reviewed in Aist and Berns 1981; Heath 1981; Heath and Kaminskyj 1989; Kaminskyj et al. 1989). The nucleation of *A. nidulans* MTs by nucleus associated organelles could explain the lower abundance of MTs in the apical 5 µm; *A. nidulans* nuclei are not generally found in the apical 5 µm (e.g. Fig. 2-1a, b, d, and f where nuclei are interpreted as lying in the roughly oval regions from which MTs are largely absent). However, *A. nidulans* and the oomycetes *S. ferax* and *P. infestans* MTs do resemble each other in that all three organisms possess longitudinally oriented MTs (Fig. 2-1; Kaminskyj and Heath 1994; Temperli et al. 1990; Uchida et al. 2005). In addition, the number of MTs in *A. nidulans, S. ferax* and *P. infestans* decrease towards the tip; a few *A. nidulans* MTs reach the extreme apex (Chapter 2, section 2-4.1., page 23; Heath and Kaminskyj 1989; Kaminskyj and Heath 1994; Temperli et al. 1990). Temperli et al. (1990) interpreted immunofluorescent observations made in *P. infestans* as MTs reaching lengths of up to 20 µm and occurring in bundles of up to 10 MTs. These bundles are much larger than those observed by freeze-substitution cross-section serial reconstruction TEM analysis of an *A. nidulans* hypha, which revealed that about half of the cytoplasmic MTs were in bundles of two or three (R. Roberson, *personal communication*). The observations of Roberson (*personal communication*) are roughly consistent with those made the ascomycete fission yeast *Schizosaccharomyces pombe*; *S. pombe* MTs were observed, by electron tomography, to form bundles typically consisting of 4 MTs (Höög et al. 2007). However, the method of observation should be taken into account in interpreting the apparent differences between the sizes of bundles of MTs in *A. nidulans* and *P. infestans.* The resolution of immunofluorescence (the method used by Tempereli et al. (1990)) is much less than that of TEM. Because immunofluorescence cannot resolve individual MTs (discussed in Chapter 2, section 2-3.3., page 22), the numbers of MTs in bundles in *P. infestans* may be inaccurately estimated. MTs have also been observed to converge at the tips of hyphae in the oomycete *P. infestans* (Uchida et al. 2005) and the ascomycete *N. crassa* (Freitag et al. 2004; Mouriño-Pérez et al.

2006). This has not been observed in *A. nidulans*. In the true hyphae of *Candida albicans*, which have Spitzenkörpers (Crampin et al. 2005), MTs are long, flexuous and run parallel to the long axis of the cell (Crampin et al. 2005) as do MTs in *A. nidulans*. In the Chytridiomycete *Allomyces macrogynus* MTs are also long, flexuous, and parallel to the long axis of the hyphae (Bartnicki-Garcia 2002; McDaniel and Roberson 1998, 2000). A large number of *A. macrogynus* MTs also extend to the apex and co-localize with the Spitzenkörper (Bartnicki-Garcia 2002; McDaniel and Roberson 1998, 2000). This MT arrangement contrasts with *A. nidulans* MTs, which are less numerous in the apical 5 µm than 5-20 µm from that the tip (Chapter 2, section 2-4.2., page 25) and do not appear to converge on the apical 1 µm in the way *A. macrogynus* MTs do. Generally, MTs in hyphae are long, flexuous and run parallel to the long axis of the hyphae taxonomically diverse hyphae, potentially suggesting a function as tracks. As there is abundant evidence that MTs are required for nuclear migration in filamentous fungi (Heath 1994, 1995; Morris and Enos 1992; Morris et al. 1995; Plamann et al. 1994; Suelmann and Fischer 2000b), MT tracks may be largely involved in longitudinal nuclear migration and/or the maintenance of hyphal growth direction (see section 4-1.2.2., page 80; Fig. A-4), rather than the longitudinal movement of materials, such as vesicles and/or organelles, needed for polar growth. The differences in MT organization between hyphal organisms could conceivably result in different roles for MTs in polar growth. Alternatively, if MTs play a relatively minor role in hyphal growth, the differences in MT organization between hyphal organisms may be largely irrelevant.

4-1.2. MTs and hyphal growth rate

The arrangement of *Aspergillus nidulans* MTs (Fig. 2-1a) suggests that MTs could act as tracks on which materials, such as vesicles and/or organelles, needed for polar growth could be transported. If MTs function as tracks it would be reasonable to expect a correlation between the relative abundance of MTs and hyphal growth rate. In addition, inhibitor-induced MT depolymerization would equate to a decrease or elimination of these tracks. A reduction in number of intact tracks could lead to a reduction in hyphal growth rate.

The relationship between the relative abundance of MTs and hyphal growth rate was investigated in *A. nidulans.* No correlation between relative MT abundance and hyphal growth rate was observed (Fig. 2-2), although non-growing hyphal had a lower relative MT abundance than did growing hyphae. In addition, 1 μg/mL benomyl induced depolymerization of all visible MTs without a significant decrease in hyphal growth rate (Fig. 2-2). However, 2.5 μg/mL benomyl significantly reduced hyphal growth rate (Fig. 2-2), suggesting secondary cytotoxic effects of the high benomyl concentration in *A. nidulans*. In light of the above findings, the role of MTs in growth of filamentous fungi requires clarification. As the role of MTs in *A. nidulans* is not fully understood, I will discuss the contributions of MTs to polar growth in other hyphal organisms in order to build up a more complete picture of the roles of MTs in hyphal growth.

MTs are reported to be important for hyphal growth in various filamentous fungi and other hyphal organisms, including *A. nidulans* (Horio and Oakley 2005; Konzack et al. 2005; Ovechkina et al. 2003; Sampson and Heath 2005), *Neurospora crassa* (Mouriño-Pérez et al. 2006, Riquelme et al. 2002; That et al. 1988), *Ustilago maydis* (Fuchs et al. 2005; Schuchart et al. 2005; Steinberg et al. 2001), *Fusarium acuminatum* (Howard and Aist 1977), and *Candida albicans* (Akashi et al. 1994). This can be interpreted as being consistent with the proposal that MTs are responsible for the long-distance transport of post-Golgi secretory vesicles to the Spitzenkörper (a model suggested by Plamann et al. (1994)), whereas actin filaments control short-range vesicle transport from the Spitzenkörper to the plasma membrane (Crampin et al. 2005). However, the fact that some *A. nidulans* hyphae continue to grow relatively rapidly in the absence of MTs, as a result of 1 μg/mL benomyl treatment (Fig. 2-3), does not support the above proposal. Growth in the absence of MTs has also been observed in a variety of other hyphal organisms. The continuation of apical growth for several hours in the basidiomycete *Schizophyllum commune* without cytoplasmic microtubules has been observed and interpreted to mean that microtubules are not the major elements in hyphal growth (Raudasksoski et al. 1994). Similarly, in *C. albicans*, nocodazole-induced MT depolymerization did not arrest hyphal growth (Yokoyama et al. 1990). In contrast, Akashi et al. (1994) found that benomyl-induced MT depolymerization reduced the apical growth of *C. albicans* hyphae. Furthermore, in the oomycetes *Phytophthora infestans*

and *Saprolegnia ferax*, nocodazole induced MT depolymerization while permitting 79 % (Temperli et al. 1991) and 50 % (Heath et al. 2002) of the control growth rate, respectively. Clearly there is conflicting evidence as to whether MT depolymerization correlates with a reduction in hyphal growth rate. This is especially notable in organisms such as *A. nidulans* in which MT depolymerization has been shown not to reduce growth rate (Chapter 2, section 2-4.3., page 27) despite the opposite finding in the literature (Horio and Oakley 2005; Konzack et al. 2005; Ovechkina et al. 2003; Sampson and Heath 2005). Similarly, Yokoyama et al. (1990) found that MT depolymerization did not inhibit hyphal growth in *C. albicans* while Akashi et al. (1994) found that MT depolymerization did inhibit hyphal growth. In light of these contradictory findings, I propose that either 1) MT depolymerization inhibits hyphal growth in some organisms, but not in others, and/or 2) MT depolymerization does not inhibit hyphal growth, but can sometimes appear to do so because of secondary cytoxic effects of the drug(s) used. Under the first model, different roles for MTs in different hyphal organisms are implied. Clearly the first model does not apply to *A. nidulans* because contradictory findings exist in the same organism. However, the second model could apply to *A. nidulans*, implying that the reductions in hyphal growth rate observed by Horio and Oakley (2005) and Sampson and Heath (2005) were due to cytotoxic effects of benomyl and MBC rather than to a lack of MTs. Consistent with this second model, the concentration of benomyl used by Horio and Oakley (2005) was equivalent to the higher benomyl concentration used in Chapter 2 (2.5 µg/mL). In Chapter 2, I also observed this benomyl concentration to reduce hyphal growth rate in *A. nidulans* (Fig. 2-3). However, I observed that 1 µg/mL benomyl depolymerized all cytoplasmic MTs without significantly reducing hyphal growth rate (Fig. 2-3). Under the second model, it is implied that the reductions in the rate of hyphal growth observed in *N. crassa* (Mouriño-Pérez et al. 2006, Riquelme et al. 2002; That et al. 1988), *U. maydis* (Fuchs et al. 2005; Schuchart et al. 2005; Steinberg et al. 2001) and *F. acuminatum* (Howard and Aist 1977) were due to cytotoxic secondary effects of the inhibitors used rather than to a lack of MTs. However, it is also possible that polymerized MTs are not essential for tip growth in some hyphal organisms, such as *A. nidulans, C. albicans* (Yokoyama et al. 1990), *P. infestans* (Temperli et al. 1991) and *S. commune* (Raudasksoski et al. 1994), but are required for tip growth in *N.*

crassa (Mouriño-Pérez et al. 2006, Riquelme et al. 2002; That et al. 1988) and *U. maydis* (Fuchs et al. 2005; Schuchart et al. 2005; Steinberg et al. 2001). This might be shown to be the case if inhibitor concentrations minimally sufficient to induce MT depolymerization were shown to inhibit tip growth in *N. crassa* and *U. maydis*, but inhibitor concentrations insufficient to induce MT depolymerization were shown not to inhibit tip growth. Polymerized MTs are non-essential for the maintenance of hyphal growth in many, if not all, hyphal organisms, but do likely play some role in polarity.

4-1.2.1. MTs and germination

Germination, which involves polarity establishment, is a prerequisite to hyphal growth. As polarity initiation and polarity maintenance have been shown to be separate processes (Momany et al. 1999), an examination of the observations recorded in the literature on the roles of MTs in hyphal germination may clarify the roles of MTs in polarity. *C. albicans* can transition from yeast to hyphal growth; this transition, the initiation of hyphal growth, can be interpreted as being similar to germination. Akashi et al. (1994) found that MT depolymerization inhibited hyphal growth initiation in *C. albicans*. This suggests that MTs may be needed for establishment of hyphal growth in this species. However, the observations in *N. crassa* and *A. nidulans* contrast with those made in *C. albicans*. *A. nidulans* conidia have been observed to germinate in the presence of the MT-depolymerizing agent benomyl (Oakley and Morris 1980). Consistent with this, the rate of *N. crassa* conidia germination was not altered by MT depolymerization (That et al. 1988). In addition, *N. crassa* conidia exposed to benomyl for 5 h formed multiple germ tubes (That et al. 1988). This altered germination pattern may be linked to or share common mechanisms with MT-depolymerization-induced hyphal branching, such as Spitzenkörper destabilization.

4-1.2.2. MT depolymerization induces hyphal branching

It is possible that MTs are not essential for continued hyphal growth or for germination, but are involved in the maintenance of appropriate directionality of the hyphae. If MTs are needed to maintain directional growth, it would be expected that, in the absence of polymerized MTs, hyphae would branch more frequently than in control

hyphae. Overnight treatment of *A. nidulans* hyphae with 1 μg/mL benomyl induces apical branching (Fig. A-4), although long-term secondary cytoxic effects are likely under these conditions. Consistent with the above, in *S. commune,* nocodazole-induced MT depolymerization coincides with apical branch formation in the apical cells (Raudasksoski et al. 1991; 1994; Rupeš et al. 1995). Potentially, branching could correlate with MT depolymerization because of a shift in the position of apical vesicles and/or Spitzenkörper. Spitzenkörper are associated with MTs in at least some hyphae. For example, the MTs of *Allomyces macrogynus* converge on the tip; this convergence co-localizes with the Spitzenkörper (Bartnicki-Garcia 2002; McDaniel and Roberson 1998, 2000). In *A. nidulans,* the Spitzenkörper also appears, based on Spitzenkörper-related defects observed in MT dynein mutants, to be at least partially dependent on the MTs (Inoue et al. 1998). A shift of the spatial distribution of apical vesicles from the center to the side of the tip has been observed in freeze-substitution TEM in some nocodazole-treated *S. commune* hyphae (Rupeš et al. 1995). In *F. acuminatum* apical MT depolymerization is associated with the re-organization of vesicles from a tip-high gradient to an equal distribution along the length of hyphae (Howard and Aist 1980) and disappearance of Spitzenkörper (Howard and Aist 1977). Seiler et al. (1997) also observed that the expression of a mutation in kinesin, a motor protein that runs on MT tracks (reviewed in Bloom and Endow 1995; Brady 1985; Scholey et al. 1985; Vale et al. 1985), in *N. crassa* correlates with the disappearance of the Spitzenkörper and increased branching. The disappearance of the Spitzenkörper could be related to branch formation; displacement of the Spitzenkörper has been shown to alter the direction of hyphal growth (reviewed in Bartnicki-García 2002). As MT depolymerization appears to induce apical branching in a wide range of hyphae, it could be inferred that MTs are involved in the maintenance of growth directionality. Control of hyphal branching is important in that, as hyphae branch, they form a mycelial meshwork, or colony. Branching creates multiple hyphal tips with which the fungus can explore and exploit its environment in multiple directions. Conceivably, this exploration by additional tips could by facilitated by individual tips growing at a variety of rates. Individual hyphae have been shown to grow at a variety of rates (Figs. 2-2, 2-4, 3-6a and b) and Kaminskyj and Heath (1992) have shown that all growing hyphal tips were not

equivalent. Tip growth at a variety of rates in multiple directions could allow new environments (i.e. directions from the colony) to be explored with only a few hyphae per environment at a time. Hyphal tips have been shown to undergo age-related changes in their response to the environment (Kaminskyj and Heath 1992). Thus, if the new environment is favorable, more energy can be devoted to its exploitation, while, if it is unfavorable, the fungus as a whole has lost only a small investment.

4-1.3. MTs and hyphal growth rate variability

The *A. nidulans* hyphae I observed were growing under controlled and reproducible conditions (see Chapter 2, section 2-3., page 20). Despite this, growth rates varied greatly, ranging from zero, to approximately 1.4 µm/min (Figs. 2-2 and 3-6a). This variability of growth rate among hyphae led me to investigate variation in hyphal growth rate over time in individual hyphae. Qualitatively, MTs were observed to vary slightly in terms of lateral intra-hyphal position over seconds to minutes, but overall relative abundance remained consistent (Chapter 2, section 2-4.1., page 23). This time frame is similar to the time frame over which hyphal growth rate variability was observed (Fig. 2-4). I observed the growth rates of *A. nidulans* hyphae to vary over 15-30 s intervals (Fig. 2-4). Hyphal growth rates in many other hyphal species vary over periods as short as 1-5 s (López-Franco et al. 1994; Sampson et al. 2003). It is likely that the growth rates of *A. nidulans* hyphae also vary over time periods shorter than 15 s, although my data does not address this because of constraints on image collection and measurement accuracy. In *N. crassa* some growth rate variations are temporally correlated with *de novo* generation and fusion of satellite Spitzenkörper (López-Franco et al. 1995). However this phenomenon has not been reported for *A. nidulans.*

In *A. nidulans* hyphae, ethanol treatment dramatically increased hyphal growth rate variability (Fig. 2-4). Ethanol could alter membrane permeability to ions such as Ca^{2+} or H^{+}. An increase in Ca^{2+} concentration in the hyphal apex can enhance polarized tipward cytoplasmic contractions in hyphae of the oomycete *S. ferax* (Jackson and Heath 1992, 1993b; Kaminskyj et al. 1992). It is conceivable that polar contractions are induced in *A. nidulans* hyphae by ethanol-induced altered ion homeostasis. Such polar contractions could contribute to hyphal growth rate variability.

The MT and actin cytoskeleton may also contribute to hyphal growth rate variability. Sampson and Heath (2005) suggest that dynamic, predominantly elongating, apical MTs may be responsible for the tipward migration of vesicles, organelles and/or proteins. The depolymerization of either MTs (Fig. 2-4e) or actin (Fig. 2-4f) decreased growth rate variability with respect to the ethanol solvent control. If *A. nidulans* growth rate variability resembles *N. crassa* growth rate variability in that it is temporally correlated with *de novo* generation and fusion of satellite Spitzenkörper (López-Franco et al. 1995), it is possible that there is a link between the actin and/or MT cytoskeleton and the Spitzenkörper. However, there is, as yet, no evidence of such a similarity between *A. nidulans* and *N. crassa* growth rate variability. Actin depolymerization could also reduce hyphal growth variability by reducing cytoplasmic contractions similar to those observed by Jackson and Heath (1992). Both Jackson and Heath (1992) and Bray (1992) suggest that actin is involved in hyphal cytoplasmic contractions. In light of the importance of the cytoplasm in tip growth suggested by Kaminskyj and Heath (1996), it seems reasonable that tipward cytoplasmic contractions could contribute to hyphal growth rate variability.

Fluorescence imaging of taxol treated cells had a notable impact on growth rate variability: the average growth rate in the first 40 s of imaging was significantly faster than for all subsequent intervals, although growth was not halted during the observation period. It is unlikely that growth rate changes were due to drug effects prior to irradiation, so they appear to have been caused by the fluorescence imaging. In addition, hyphal growth rate was not affected by repeated imaging for most of the treatment populations (Fig. 2-4a, b, d-f), suggesting an interaction between irradiation and taxol treatment. The binding of taxol to MTs (Horwitz 1992; Ross and Fygenson 2003) is of considerable interest due to its use in cancer chemotherapy, which is being studied using fluorescent taxol derivatives (Li et al. 2000). Irradiation of cells with visible light, at a wavelength absorbed by GFP, or another fluorescent molecule bound to taxol (see Chapter 2, section 2-5.2., page 38; Fig. A-2) may thus enhance the efficacy of taxol chemotherapy, given the use of fluorescent taxol derivatives. Indeed, taxol has been patented as a radiation sensitizer (Schiff 2000). Treatment could be achieved by treating tissue with a fluorescent taxol derivative followed by appropriate wavelength visible light

irradiation. The fact that an interaction between irradiation and taxol has an impact on hyphal growth rate variability suggests either secondary toxic effects or that MTs are in some way involved in mediating growth rate variability.

The organization of the actin and MT cytoskeletons in *P. infestans* suggested to Temperli et al. (1990) that MTs maintain the spatial organization of hyphae and facilitate intrahyphal movements. Growing hyphae maintain characteristic distributions of organelles (Heath 1994), which could be established and maintained by these intrahyphal movements. As Golgi are important in the processing and sorting of material destined for secretion (e.g. reviewed in Farquhar and Palade 1981, 1998) and secretion is important in polar growth (e.g. reviewed in Bartnicki-Garcia 2002), it seems reasonable to investigate the role(s) of Golgi in tip growth.

4-2. The role of the fungal Golgi in polar growth

Golgi are part of the secretory system (reviewed in Farquhar and Palade 1981, 1998). The Golgi functions in the processing proteins and lipids, which are synthesized in or on the ER (reviewed in Farquhar and Palade 1981, 1998). This processing prepares these proteins and lipids for intra- or extra-cellular use (reviewed in Farquhar and Palade 1981, 1998). When fungal hyphae extend at the tip they require materials, such as wall components in order to grow (Bartnicki-Garcia and Lippman 1977; Bartnicki-Garcia 2002). These wall components are supplied by what Bartnicki-Garcia (2002) termed basically a polarization of the secretory apparatus of the cells. As fungal Golgi are part of the secretory apparatus, I set out to explore their contribution to polar growth.

In order to focus this work, six goals were set for investigating the roles of fungal Golgi in polar growth of *Aspergillus nidulans*. First, to 1) determine whether the Golgi marker α-2,6-sialyltransferase (ST) (Munro 1991) co-localizes with α-COPI-GFP. After having established that α-COPI-GFP does co-localize with the Golgi marker ST-RFP (Fig. 3-2), this thesis 2) investigates the impact of BFA on α-COPI-GFP and ST-RFP morphology. Both ST-RFP and α-COPI-GFP responded to BFA in similar ways. The observed changes were consistent with the changes that might be expected of proxies for fungal Golgi, based on previously observed impacts of BFA treatment on fungi (Cole et al. 2000; Sciaky et al. 1997; Fig. 3-4). These data provide a strong case to

argue that α-COPI-GFP can be used as proxy for fungal Golgi and that α-COPI-GFP particles can be referred to as fungal Golgi. Next I 3) investigated the distribution of α-COPI-GFP in the hyphae of an *A. nidulans* strain with a genetic background including the temperature sensitive morphological mutant, *hypA1*. Subsequently, I 4) explored the relationship between the temperature at which *hypA1 A. nidulans* are grown and the average forward velocity of fungal Golgi and growth rate in the same cells. Finally, this thesis 5) investigates the relationship between hyphal growth rate and forward velocity of fungal Golgi and 6) the impact of MT and actin targeting drugs on the average forward velocity of fungal Golgi and hyphal growth in the same cells.

4-2.1. Spatial distribution and motility of fungal Golgi and polar growth

Golgi are part of the secretory system (reviewed in Farquhar and Palade 1981, 1998). Because of the contribution of Golgi to secretion and the role of secretion in polar growth (reviewed in Bartnicki-Garcia 2002) it seems reasonable that the spatial distribution and/or movement of fungal Golgi might be related to polar growth. Prior to this thesis, little research had been done in hyphal organisms on the relationship between polar growth and the spatial distribution of fungal Golgi relative to the hyphal tip in living cells. *A. nidulans* fungal Golgi have a tip-high distribution gradient in wildtype phenotype hyphae (Fig. 3-5). Consistent with my observations in *A. nidulans*, *C. albicans* Golgi have also been observed to posses a tip-high gradient (Rida et al. 2006). It seems reasonable that organelles involved in secretion, which are needed at the tip for polar growth (Bartnicki-Garcia 2002) would be more abundant near the tip than subapically. However, in the oomycete *S. ferax,* Heath and Kaminskyj (1989) did not observe Golgi or mitochondria in the apical 5 μm. Heath and Kaminskyj (1989) did observe a tip high vesicle gradient in *S. ferax*. The tip-high fungal Golgi gradient was not entirely unexpected in *A. nidulans*. Because living hyphae are dynamic, intrahyphal movements of Golgi presumably maintain the tip-high Golgi distribution observed in *A. nidulans* and *C. albicans*.

The intrahyphal movement of fungal Golgi, independent of tip extension, have not been observed in fungi prior to the work presented in this thesis Chapter 3, section 3-4.1., page 50) in *A. nidulans*. It also shows a clear correlation between the rate of

forward movement of fungal Golgi and hyphal growth rate (Fig 3-6). Movements of Golgi-derived vesicles have also been observed in the cylindrical tip-growth cells of *Chara* rhizoids (Bartnik et al. 1990). Golgi derived vesicles in *Chara* are up to 1 μm in diameter (Bartnik et al. 1990), meaning they are of similar size to fungal Golgi in *A. nidulans* (Chapter 3, section 3-4.1., page 50). Bartnik et al. (1990) observed *Chara* Golgi-derived vesicles to be highly dynamic, undergoing movement in all directions relative to the tip. The most rapid movements of *Chara* Golgi derived vesicles were observed between the ER and the elongating tip as opposed to other trajectories (Bartnik et al. 1990). This is consistent with my observation that forward (Fig. 3-1) fungal Golgi movement in *A. nidulans* was generally more rapid than backwards or sideways movement under the same conditions (Chapter 3, section 3-4.4., page 57; Fig A-3). The ER aggregate (observed at the rhizoid tip by *in vivo* DIC microscopy) to tip movements of *Chara* Golgi derived vesicles took place at speeds up to five times as great as did movements on other trajectories (Bartnik et al. 1990). This suggests that *Chara* Golgi derived vesicles are involved directly in secretion and polar growth by shuttling and processing material from the ER to the growing tip. In addition, Bartnik and Sievers (1988) show that the *Chara* Spitzenkörper is composed of an aggregation of ER and Golgi derived vesicles. If the positioning of the *Chara* Spitzenkörper (ER and Golgi derived vesicle aggregate) correlates with the direction of polar growth as it does in filamentous fungi (Bartnicki-Garcia 2002; Bracker et al. 1997; Riquelme et al. 2000), it could be inferred that Golgi also contribute to tip growth directionality. An indication that forward fungal Golgi movement is tied to the rate of polar growth, if not the direction, is the fact that actin depolymerization eliminates all observable hyphal growth and also significantly reduces the average forward velocity of fungal Golgi (Fig. 3-7g).

Consistent with the movement of fungal Golgi being related to polarity, I observed a link between polar morphology and fungal Golgi movement. In *A. nidulans* hyphal with a *hypA1* temperature sensitive morphological mutant allele, I observed that, as hyphal morphology became increasingly polarized with increased time at the permissive temperature for *hypA1* (28 °C), the average forward velocity of fungal Golgi increased (Fig. 3-6a). The link I observed between establishment of polar morphology and a component of the secretory system, fungal Golgi, is consistent with the findings of

Bartnicki-Garcia and Lippman (1969, 1977) in *Mucor rouxii.* Bartnicki-Garcia and Lippman (1969, 1977) found in *M. rouxii* that during germination (which requires polarity establishment) secretion of cell wall constituents occurred much more frequently at the point of germ tube emergence than in other locations. The observations of Bartnicki-Garcia and Lippman (1969, 1977) in *M. rouxii* and the tip-high gradient of Golgi distribution observed in *A. nidulans* (Fig. 3-4) and *C. albicans* (Rida et al. 2006) during polarity establishment could be interpreted as showing a correlation between Golgi-mediated targeted secretion and the establishment of hyphal polar morphology.

4-2.2. Relationship between MTs and fungal Golgi

The intrahyphal spatial distribution and movement of fungal Golgi in *A. nidulans* hyphae is clearly non-random, as discussed above. Non-random distribution of fungal Golgi appears to require some kind of structural framework, or 'scaffolding'. The cytoskeleton could provide such a scaffolding framework. The MT and/or actin cytoskeleton could thus be involved in the positioning and/or movement of fungal Golgi. In *A. nidulans* hyphae, fungal Golgi were roughly equally abundant at 0-5, 5-10, 10-15, 15-20 and 20-25 μm from the tip (Fig. 3-5), while MTs were less abundant in the apical 5 μm (Chapter 2, section 2-4.2., page 25) and actin is more abundant (Bartnicki-Garcia 2002; Heath 1994; Heath et al. 2003; Torralba et al. 1998), suggesting that actin may play a larger role in fungal Golgi positioning than MTs. Actin depolymerization led to a decrease in the average rate of forward fungal Golgi movement (Fig. 3-7g). In contrast, MT depolymerization did not alter fungal Golgi movement (Fig. 3-7g). This suggests that actin may play a larger role in fungal Golgi movement than MTs. However, taxol-induced stabilization of the MT cytoskeleton does increase the average forward velocity of fungal Golgi (Fig. 3-7g), suggesting either that there is some association between fungal Golgi movement and MTs or that MT stabilization facilitates fungal Golgi movement in some other way, such as enhancing the fungal Golgi movement-related functions of actin.

My observations are consistent with observations in other hyphal organisms. For example, in the basidiomycete *S. commune*, Golgi seem to appear in association with cytoplasmic MTs (Rupeš et al. 1995). However, Rupeš et al. (1995) did not note any

alteration in Golgi intrahyphal arrangement associated with MT depolymerization. Consistent with the observations of Rupeš et al. (1995) in *S. commune*, Heath and Kaminskyj (1989) found no association between *S. ferax* Golgi and MTs. In *Candida albicans* the positioning of Golgi have been shown to be dependant on formin (Rida et al. 2006). Formin is associated with the actin cytoskeleton (Evangelista et al. 2002; Pruyne et al. 2002; Sharpless and Harris 2002), suggesting that, in *C. albicans*, Golgi are at least indirectly associated with actin, rather than MTs. Taken together, observations of the association of fungal Golgi with the cytoskeleton in *A. nidulans, S. commune* (Rupeš et al. 1995)*, S. ferax* (Heath and Kaminskyj 1989) and *C. albicans* (Rida et al. 2006) suggest an association between fungal Golgi and actin, rather than MTs.

4-3. Future research

Viewing the organization of *A. nidulans* MTs with electron tomography could provide information about the association of MTs with the plasma membrane (as shown in *S. pombe* by Höög et al. (2007)) or with the Spitzenkörper (as suggested indirectly via observations in dynein mutants in *A. nidulans* by Inoue et al. 1998). An association of *A. nidulans* MTs with the Spitzenkörper could suggest a mechanism by which MTs mediate the direction of hyphal growth (Fig. A-4).

It appears that fungal Golgi primarily utilize the actin cytoskeleton for intrahyphal motility (Fig. 3-7g). However, increased MT-stabilization may increase the forward velocity of fungal Golgi. This information could be used to develop a model for ER-to-Golgi export in fungal system. In order to develop such a model, it would be helpful to gather data on the movement and distribution of the ER in *A. nidulans.* For example, the response(s) of *A. nidulans* ER morphology, distribution and rate of movement could be observed in untreated and actin- and MT-inhibitor treated hyphae. The morphology of GFP-tagged ER (in a strain currently available) could be described qualitatively in terms of shape and/or degree of tubulation. Potentially, ER distribution could be characterized in terms of the percent hyphal area GFP-tagged ER fills in a single optical section at various set distances from the tip. The degree of mobility of GFP-tagged *A. nidulans* ER could potentially be assessed using fluorescent recovery after photobleaching. If an *A. nidulans* strain containing GFP-tagged ER were transformed

with ST-RFP, the relative positioning of the fungal Golgi and ER could be observed. For example, it could be determined whether the fungal Golgi were frequently in contact with the ER, or appeared to associate preferentially with specific morphological features in the ER. In addition, observations similar to those made in *Chara*, in which the movements of the Golgi with respect to the ER were noted (Bartnick et al. 1990), could be made in *A. nidulans*. Furthermore, the dependency of Golgi-ER interactions on the actin and MT cytoskeleton could potentially be examined by treating *A. nidulans* hyphae containing GFP-tagged ER and RFP-tagged fungal Golgi with MT and/or actin targeting drugs. For example, it could be noted whether inhibition of the actin and/or MT cytoskeleton reduced (or increased) the proximity of GFP-tagged ER and RFP-tagged fungal Golgi. It is also possible that, during contact and/or vesicle tracking between GFP-tagged ER and RFP-tagged fungal Golgi, some RFP fluorescence might be observed co-distributed with the GFP-tagged ER. The occurrence of such co-distribution might be influenced by the nature of the RFP and GFP fusion proteins. For example, if the Golgi marker employed was RFP tagged α-COPI, which is peripheral to the membrane (Fig. 1-3), it might be more likely to be observed intermingled with the ER than would ST-RFP, which localizes to the Golgi via a transmembrane domain. If co-distribution of the ER and fungal Golgi was observed, the proximity of the association could potentially be assessed using fluorescence resonance energy transfer. In fluorescence resonance energy transfer a fluorophore absorbs energy at a specific wavelength and subsequently emitts energy at a longer wavelength. If a second flourophore, whose excitation spectrum matches the emission spectrum of the first fluorophore, is sufficiently close to the first fluorophore (1-9nm) it will absorb the emitted energy and subsequently emitt energy at a still longer wavelength. For example, if fungal Golgi were tagged with GFP and the ER were tagged with yellow fluorescent protein, cells could be irradiated at 488nm (the wavelength absobed by GFP) and yellow, rather than green, fluorescence would be observed in regions where the two fluorophores came into close contact.

Studies of the maturation of *A. nidulans* Golgi, inspired by those conducted in *S. cerevisae* by Losev et al. (2006) and Matsuura-Tokita et al. (2006) could be conducted using three-dimensional time-lapse confocal microscopy. Such experiments might investigate whether individual *A. nidulans* fungal Golgi mature during their lifetime by

changing their complement of resident proteins, or, alternatively, maintain a constant complement of resident proteins. In order to differentiate between these two models, an early Golgi protein (such as α-COPI) could be tagged with GFP and a late Golgi protein could be tagged with RFP (based on a method suggested by Losev et al. 2006). If individual fungal Golgi are stable, the relative amounts of GFP and RFP should remain constant, but, if individual fungal Golgi mature over time, the relative amounts of GFP would be expected to decrease and RFP would be expected to increase.

CHAPTER 5: References

Abe K, Gomi K, Hasegawa F and Machida M (2006) Impact of *Aspergillus oryzae* genomics on industrial production of metabolites. Mycopathologia 162: 143-153.

Adams TH, Wieser JK and Yu, J-H (1998) Asexual sporulation in *Aspergillus nidulans*. Microbiol Mol Biol Rev 62: 35-54.

Aist JM and Berns MW (1981) Mechanics of chromosome separation during mitosis in *Fusarium* (Fungi imperfecti); new evidence from ultrastructural and laser microbeam experiments. J Cell Biol 91: 446-458.

Akao T, Yamaguchi M, Yahara A, Yoshiuchi K, Fujita H, Yamada O, Akita O, Ohmachi T, Asada Y and Yoshida T (2006) Cloning and expression of 1,2-alpha-mannosidase gene (fmanIB) from filamentous fungus *Aspergillus oryzae*: in vivo visualization of the FmanIBp-GFP fusion protein. Bioscience Biotech Biochem 70: 471-479.

Akashi T, Kanbe T and Tanaka K (1994) The role of the cytoskeleton in the polarized growth of the germ tube in *Candida albicans*. Microbiology (Reading) 140: 271-280.

Ali S (2006) Application of kaolin to improve citric acid production by a thermophilic *Aspergillus niger.* Applied Microbiol Biotech 73: 755-762.

Bachewich C and Heath IB (1997) Differential cytoplasm-plasma membrane-cell wall adhesion patterns and their relationships to hyphal tip growth and organelle motility. Protoplasma 200: 71-86.

Bachewich C and Heath IB (1998) Radial F-actin arrays precede new hypha formation in *Saprolegnia*: implications for establishing polar growth and regulating tip morphogenesis. J Cell Sci 111: 2005-2016.

Bachewich C and Heath IB (1999) Cytoplasmic migrations and vacuolation are associated with growth recovery in hyphae of *Saprolegnia*, and are dependent on the cytoskeleton. Mycol Res 103: 849-858.

Baird GS, Zacharias DA and Tsien RY (2000) Biochemistry, mutagenesis, and oligomerization of DsRed, a red fluorescent protein from coral. Proc Natl Acad Sci USA 97: 11984-11989.

Bartnicki-Garcia S (2002) Hyphal tip growth: outstanding questions. In Osiewacz HD (ed) *Molecular Biology of Fungal Development*. Marcel Dekker Inc, New York, pp 29-58.

Bartnicki-Garcia S and Lippman E (1969) Fungal morphogenesis cell wall construction in *Mucor rouxii*. Science (Washington D C) 165: 302-304.

Bartnicki-Garcia S and Lippman E (1977) Polarization of cell wall synthesis during spore germination of *Mucor rouxii*. Exp Mycol 1: 230-240.

Bartnik E, Hejnowicz Z and Sievers A (1990) Shuttle-like movements of Golgi vesicles in the tip of growing *Chara* rhizoids. Protoplasma 159: 1-8.

Bartnik E and Sievers A (1988) *In vivo* observations of a spherical aggregate of endoplasmic reticulum and of Golgi vesicles in the tip of fast-growing *Chara* rhizoids. Planta (Heidelberg) 176: 1-9.

Beckett A, Heath IB and McLaughlin DJ (1974) An Atlas of Fungal Ultrastructure. Longman.

Bentivoglio M and Mazzarello P (1998) The pathway to the cell and its organelles: one hundred years of the Golgi apparatus. Endeavour (Cambridge) 22: 101-105.

Bessey EA (1950) *Morphology and Taxonomy of Fungi*. The Blakiston Co. Philadelphia.

Bloom GS and Endow SA (1995) Motor proteins 1: kinesins. Protein Profile 2: 1105-1171.
Boehm J, Letourneur F, Ballensiefen W, Ossipov D, Demolliere C and Schmitt HD (1997) Sec12p requires Rer1p for sorting to coatomer (COPI)-coated vesicles and retrieval to the ER. J Cell Sci 110: 991-1003.
Boevink P, Oparka K, Cruz SS, Martin B, Betteridge A and Hawes C (1998) Stacks on tracks: the plant Golgi apparatus traffics on an actin/ER network. Plant J 15: 441-447.
Bracker CE, Murphy DJ and López-Franco R (1997) Laser microbeam manipulation of cell morphogenesis in growing fungal hyphae. In Farkas DL and Tromberg BJ (eds) *Functional Imaging and Optical Manipulation of Living Cells*. Bellingham, WA. SPIE – The International Society of Optical Engineering 2983: 67-80.
Brady ST (1985) A novel brain ATPase with properties expected for the fast axonal transport motor. Nature 317: 73-75.
Brandizzi F, Irons SL, Johansen J, Kotzer A and Neumann U (2004) GFP is the way to glow: bioimaging of the plant endomembrane system. J Microscopy (Oxford) 214: 138-158.
Bray D (1992) *Cell Movements*. Garland Publishing, New York and London.
Broad Institute: http://www.broad.mit.edu/
Buller AHR (1933) The translocation of protoplasm through the septate mycelium of certain pyrenomycetes discomycetes, and hymenomycetes. Hafner Publication Co. New York Res Fungi 5: 75-167.
Burkhardt JK (1998) The role of microtubule-based motor proteins in maintaining the structure and function of the Golgi complex. Biochim Biophys Acta 1404: 113-126.
Cai H, Zhang Y, Pypaert M, Walker L and Ferro-Novick S (2005) Mutants in *trs120* disrupt traffic from the early endosome to the late Golgi. J Cell Biol 171: 823-833.
Campbell RE, Tour O, Palmer AE, Steinbach PA, Baird BS, Zacharias DA and Tsien RY (2002) A monomeric red fluorescent protein. Proc Natl Acad Sci USA 99: 7877-7882.
Carlier MF (1991) Actin protein structure and filament dynamics. J Biol Chem 266: 1-4.
Caro CG and Palade GE (1964) Protein synthesis, storage, and discharge in the pancreatic exocrine cell: an autoradiographic study. J Cell Biol 20: 473-495.
Cavalier-Smith T (1985) *The Evolution of Genome Size*. Wiley, New York.
Champe SP, Nagle DL and Yager LN (1994) Sexual sporulation. Martinelli SD and Kinghorn JR (eds) In Aspergillus: *50 years on. Progress Industrial Microbiol* 29.
Chang F, Feierbach B and Martin S (2005) Regulation of actin assembly by microtubules in fission yeast cell polarity. Novartis Foundation Symposium 269: 59-66.
Chow VTK and Quek HH (1996) HEP-COP, a novel human gene whose product is highly homologous to the α-subunit of the yeast coatomer complex. Gene 169: 223-227.
Cole L, Davies D, Hyde GJ and Ashford AE (2000) Brefeldin A affects growth, endoplasmic reticulum, Golgi bodies, tubular vacuole system, and secretory pathway in *Pisolithus tinctorius*. Fung Genet Biol 29: 95-106.
Collinge AJ and Trinci APJ (1974) Hyphal tips of wild-type and spreading colonial mutants of *Neurospora crassa*. Archives Microbiol 99: 353-368.

Combeau C, Commercon A, Mioskowski C, Rousseau B, Aubert F and Goeldner M (1994) Predominant labeling of beta- over alpha-tubulin from porcine brain by a photoactivatable taxoid derivative. Biochemistry 33: 6676-6683.
Cormack B (1998) Green fluorescent protein as a reporter of transcription and protein localization in fungi. Curr Opin Microbiol 1: 406-410.
Crampin H, Finley K, Gerami-Nejad M, Court H, Gale C, Berman J and Sudbery P (2005) *Candida albicans* hyphae have a Spitzenkorper that is distinct from the polarisome found in yeast and pseudohyphae. J Cell Sci 118: 2935-2947.
DaSilva LLP, Snapp EL, Denecke J, Lippincott-Schwartz J, Hawes C and Brandizzi F (2004) Endoplasmic reticulum export sites and Golgi bodies behave as single mobile secretory units in plant cells. Plant Cell 16: 1753-1771.
Davidse LC (1986) Benzimidole fungicides: mechanisms of action and biological impact. Ann Rev Phytopathol 24: 43-65.
Davidse LC and Flach W (1977) Differential binding of methyl benzimidazol-2-yl carbamate to fungal tubulin as a mechanism of resistance to this antimitotic agent in mutant strains of *Aspergillus nidulans*. J Cell Biol 72: 174-193.
Davidse LC and Flach W (1978) Interaction of thiabendazole with fungal tubulin. Biochimica et Biophysica Acta 543: 82-90.
Denning DW (1998) Invasive aspergillosis. Clin Infect Dis 26: 781-803.
Díaz JF and Andreu JM (1993) Assembly of purified GDP-tubulin into microtubules induced by taxol and taxotere: reversibility, ligand stoichiometry, and competition. Biochemistry 32: 2747–2755.
Donaldson JG, Finazzi D and Klausner RD (1992) Brefeldin A inhibits Golgi membrane-catalysed exchange of guanine nucleotide onto ARF protein. Nature 360: 350-352.
Donaldson J, Lippincott-Schwartz J, Bloon GS, Kreis TE and Klausner RD (1990) Dissociation of a 110-kD peripheral membrane protein from the Golgi apparatus is an early event in brefeldin A action. J Cell Biol 111: 2295-2306.
Donaldson J, Lippincott-Schwartz J and Klausner RD (1991) Guanine nucleotides modulate the effects of brefeldin A in semipermeable cells: regulation of the association of 110-kD peripheral membrane proteins with the Golgi apparatus. J Cell Biol 12: 579-588.
Doonan JH (1994) Control of cell growth. In Martinelli SD and Kinghorn JR (eds) Aspergillus: *50 years on. Progress in Industrial Microbiol* 29.
Dou X, Wu D, An W, Davies J, Hashmi SB, Ukil L and Osmani SA (2003) The *PHOA* and *PHOB* cyclin-dependent kinases perform as essential function in *Aspergillus nidulans.* Genetics 165: 1105-1115.
Egea G, Lazaro-Dieguez F and Vilella M (2006) Actin dynamics at the Golgi complex in mammalian cells. Curr Opin Cell Biol 18: 168-178.
Evangelista M, Pruyne D, Amberg DC, Boone C and Bretscher A (2002) Formins direct Arp2/3-independent actin filament assembly to polarize cell growth in yeast. Nature Cell Biol 4: 32-41.
Food and Agriculture Organization/World Heath Organization (1987) Committee on food additives. 31.

Farah CA, Perreault S, Liazoghli D, Desjardins M, Anton A, Lauzon M, Paiement J and Leclerc N (2006) Tau interacts with Golgi membranes and mediates their association with microtubules. Cell Motil Cytoskel 63: 710-724.

Farquhar MG and Palade GE (1981) The Golgi apparatus (complex) - (1954-1981) - from artifact to center stage. J Cell Biol 91: 77s-103s.

Farquhar MG and Palade GE (1998) The Golgi apparatus: 100 years of progress and controversy. Trends Cell Biol 8: 2-10.

Faulstich D, Auerbach S, Orci L, Ravaolla M, Wegehingel S, Lottspeich F, Stenbeck G, Harter C, Wieland FT and Tschochner H (1996) Architecture of coatomer: molecular characterization of δ-COP and protein interaction within the complex. J Cell Biol 135: 53-61.

Felenbok B (1991) The ethanol utilization regulon of *Aspergillus nidulans*: the *alc*A-*alc*R system as a tool for the expression of recombinant proteins. Gene Express Filament Fung 17: 11-17.

Fernández-Ábalos JM, Fox F, Pitt C, Wells B and Doonan JH (1998) Plant-adapted green fluorescent protein is a versatile vital reporter for gene expression, protein localization and mitosis in the filamentous fungus, *Aspergillus nidulans*. Mol Microbiol 27: 121-130.

Fidel S, Doonan JH and Morris NR (1988) *Aspergillus nidulans* contains a single actin gene which has unique intron locations and encodes a γ-actin. Gene 70: 283-293.

Freitag M, Hickey PC, Raju NB, Selker EU and Read ND (2004) GFP as a tool to analyze the organization, dynamics and function of nuclei and microtubules in *Neurospora crassa*. Fung Genet Biol 41: 897-910.

Fuchs U, Manns I and Steinberg G (2005) Microtubules are dispensable for the initial pathogenic development but required for long-distance hyphal growth in the corn smut fungus *Ustilago maydis.* Mol Biol Cell 16: 2746-2758.

Fujiwara T, Oda K, Yokota S, Takatsuki A and Ikehara Y (1988) Brefeldin A causes disassembly of the Golgi complex and accumulation of secretory proteins in the endoplasmic reticulum. J Biol Chem 263: 18545-18552.

Gatherar IM, Pollerman S, Dunn-Coleman N and Turner G (2004) Identification of a novel gene *hbrB* required for polarized growth in *Aspergillus nidulans.* Fung Genet Biol 41: 463-471.

Gaynor EC, Graham TR and Emr SD (1998) COPI in ER/Golgi and intra-Golgi transport: do yeast COPI mutants point the way? Biochimica Biophysica Acta 1404: 33-51.

Gems D, Johnstone IL and Clutterbuck J (1991) An autonomously replicating plasmid transforms *Aspergillus nidulans* at high frequency. Gene 98: 61-68.

Gerich B, Orci L, Tschochner H, Lottspeich F, Ravazolla M, Amhert M, Wieland F and Harter C (1995) Non-clathrin coat protein a is a conserved subunit of coatomer and in *Saccharomyces cerevisiae* is essential for growth. Proc Natl Acad Sci USA 92: 3229-3233.

Girbardt M (1957) Der Spitzenkörper von *Polystictus versicolor.* Planta 50: 47-59.

Guo W, Sacher M, Barrowman J, Ferro-Novick S and Novick P (2000) Protein complexes in transport vesicle targeting. Trends Cell Biol 10: 251-255.

Gupta GD and Heath IB (1997) Actin disruption by latrunculin B causes turgor-related changes in tip growth of *Saprolegnia* hyphae. Fung Genet Biol 21: 64–75.

Gupta GD and Heath IB (2000) A tip-high gradient of a putative plasma membrane SNARE approximates the exocytotic gradient in hyphal apices of the fungus *Neurospora crassa*. Fung Genet Biol 29: 187-199.
Harris SD (2006) Cell polarity in filamentous. Jeon KW (ed) Int Rev Cyt 251: 41-77.
Harris SD, Hoffman AF, Tedford HW and Lee MP (1999) Identification and characterization of genes required for hyphal morphogenesis in the filamentous fungus *Aspergillus nidulans*. Genetics 151: 1015-1025.
Harris SD, Morrell JL and Hamer JE (1994) Identification and characterization of *Aspergillus nidulans* mutants defective in cytokinesis. Genetics 136: 517-532.
Hawes C and Satiat-Jeunemaître B (2005) The plant Golgi apparatus - going with the flow. Biochimica et Biophysica Acta 1744: 93-107.
Heath IB (1981) Nucleus-associated organelles in fungi. Intl Rev Cytol 69: 191-221.
Heath IB (1988) Evidence against a direct role for cortical actin arrays in saltatory organelle motility in hyphae of the fungus *Saprolegnia ferax*. J Cell Sci 91: 41-47.
Heath IB (Ed.) (1990a) *Tip Growth in Plant and Fungal Cells*. Academic Press, Toronto.
Heath IB (1990b) The role of actin in tip growth of fungi. Intl Rev Cytol 123: 95-127.
Heath IB (1994) The cytoskeleton in hyphal growth, organelle movements, and mitosis. In Wessels J and Meinhardt F (eds) *The Mycota. I: Growth, Differentiation and Sexuality*. Springer-Verlag, Berlin and Heidelberg, pp 43-65.
Heath IB (1995) The cytoskeleton. In *The Growing Fungus* (Gow NAR and Gadd GM eds): Chapman and Hall, London and New York, pp 99-124.
Heath IB, Bonham M, Akram A and Gupta GD (2003) The interrelationships of actin and hyphal tip growth in the ascomycete *Geotrichum candidum.* Fung Genet Biol 38: 85-97.
Heath IB, Gupta G and Bai S (2000) Plasma membrane-adjacent actin filaments, but not microtubules, are essential for both polarization and hyphal tip morphogenesis in *Saprolegnia ferax* and *Neurospora crassa*. Fung Genet Biol 30: 45-62.
Heath IB and Kaminskyj SGW (1989) The organization of tip-growth-related organelles and microtubules revealed by quantitative analysis of freeze-substituted oomycete hyphae. J Cell Sci 93: 41-52.
Helms JB and Rothman JE (1992) Inhibition by brefeldin A of a Golgi membrane enzyme that catalyses exchange of guanine nucleotide bound ARF. Nature 360: 352-354.
Hirt H, Kögl M, Murbacher T and Heberle-Bors E (1990) Evolutionary conservation of transcriptional machinery between yeast and plants as shown by the efficient expression from the CaMV 35S promoter and 35S terminator. Curr Genet 17: 473-479.
Hohmann-Marriott MF, Uchida M, van de Meene AML, Garret M, Hjelm BE, Kokoori S and Roberson RW (2006) Application of electron tomography to fungal ultrastructure studies. New Phytologist 172: 208-220.
Höög JL, Schwartz C, Noon AT, O'Toole ET, Mastronarde DN, McIntosh JR and Antony C (2007) Organization of interphase microtubules in fission yeast analyzed by electron tomography. Dev Cell 12: 349-361.
Horio T and Oakley BR (2005) The role of microtubules in rapid hyphal tip growth in *Aspergillus nidulans*. Mol Biol Cell 16: 918-926.

Horio T, Uzawa S, Jung MK and Oakley BR (1991) The fission yeast γ-tubulin is essential for mitosis and is localized at two different microtubule organizing centers. J Cell Sci 99: 693-700.
Horwitz SB (1992) Mechanism of action of taxol. Trends Pharmacol Sci 13: 134-136.
Howard RJ and Aist JR (1977) Effects of methyl benzimidazole-2-ylcarbamate on hyphal tip organization growth and mitosis of *Fusarium acuminatum* and their antagonism by deuterium oxide. Protoplasma 92: 195-210.
Howard RJ and Aist JR (1980) Cytoplasmic microtubules and fungal morphogenesis: ultrastructural effects of methyl benzimidazole-2-ylcarbamate determined by freeze-substitution of hyphal tips. J Cell Biol 87: 55-64.
Howard J and Hyman A (2003) Dynamics and mechanics of the microtubule plus end. Nature 422: 753-758.
Ichinomiya M, Yamada E, Yamashita S, Ohta A and Horiuchi H (2005) Class I and class II chitin synthases are involved in septum formation in the filamentous fungus *Aspergillus nidulans*. Euk Cell 4: 1125-1136.
Inoue S, Turgeon BG, Yoder OC and Aist JR (1998) Role of fungal dynein in hyphal growth, microtubule organization, spindle pole body motility and nuclear migration. J Cell Sci 111: 1555-1566.
Jackson SL and Heath IB (1990a) Evidence that actin reinforces the extensible hyphal apex of the oomycete *Saprolegnia ferax*. Protoplasma 157: 144-153.
Jackson SL and Heath IB (1990b) Visualization of actin arrays in growing hyphae of the fungus *Saprolegnia ferax*. Protoplasma 154: 66-70.
Jackson SL and Heath IB (1992) UV microirradiation implicates F-actin in reinforcing growing hyphal tips. Protoplasma 175: 67-74.
Jackson SL and Heath IB (1993a) The dynamic behavior of cytoplasmic F-actin in growing hyphae. Protoplasma 173: 23-34.
Jackson SL and Heath IB (1993b) Roles of calcium ions in hyphal tip growth. Microbiol Rev 57: 367-382.
Jefferson RA, Kavanagh TA and Bevan MW (1987) GUS fusions: beta-glucuronidase as a sensitive and versatile gene fusion marker in higher plants. EMBO J 6**:** 3901-3907.
Jung MK and Oakley BR (1990) Identification of an amino acid substitution in the *benA,* β-tubulin, gene of *Aspergillus nidulans* that confers thiabenazole resistance and benomyl supersensitivity. Cell Motil Cytoskel 17: 87-94.
Jung MK, Wilder IB and Oakley BR (1992) Amino acid alterations in the *benA* (β-tubulin) gene of *Aspergillus nidulans* that confer benomyl resistance. Cell Motil Cytoskel 22: 170-174.
Kaminskyj SGW (2000) Septum position is marked at the tip of *Aspergillus nidulans* hyphae. Fung Genet Biol 31: 105-113.
Kaminskyj SGW (2001) Fundamentals of growth, storage, genetics and microscopy in *Aspergillus nidulans*. Fung Genet Newsletter 48: 25-31.
Kaminskyj SGW and Boire MR (2004) Ultrastructure of the *Aspergillus nidulans hypA1* restrictive phenotype shows defects in endomembrane arrays and polarized wall deposition. Can J Bot 82: 807-814.
Kaminskyj SGW and Hamer JE (1998) *hyp* loci control cell pattern formation in the vegetative mycelium of *Aspergillus nidulans.* Genetics 148: 669-680.

Kaminskyj SGW and Heath IB (1992) Age-dependent differential responses of *Saprolegnia* hyphal tips to a helical growth-inducing factor in the agar substitute, gellan. Exp Mycol 16: 230-239.
Kaminskyj SGW and Heath IB (1994) A comparison of techniques for localizing actin and tubulin in hyphae of *Saprolegnia ferax*. J Histochem Cytochem 42: 523-530.
Kaminskyj SGW and Heath IB (1995) Integrin and spectrin homologues, and cytoplasm-wall adhesion in tip growth. J Cell Sci 108: 849-856.
Kaminskyj SGW and Heath IB (1996) Studies on *Saprolegnia ferax* suggest the importance of the cytoplasm in determining hyphal morphology. Mycologia 88: 20-37.
Kaminskyj S, Jackson S and Heath IB (1992) Fixation induces differential polarized translocations in hyphae of *Saprolegnia ferax*. J Microscopy 167:153-168.
Kaminskyj SGW, Yoon KS and Heath IB (1989) Cytoskeletal interactions with post-mitotic migrating nuclei in the oyster mushroom fungus, *Pleurotus ostreatus*: evidence against a force-generating role for astral microtubules. J Cell Sci 94: 663-674.
Kashman Y, Groweiss A and Shmueli U (1980) LatrunculinA new 2-thiazolidinone macrolide from the marine sponge *Latrunculia magnifica.* Tetrahedron Letters 21: 3629-3632.
Kendrick B (2000) *The Fifth Kingdom*. 3rd ed. Waterloo, ON. Mycologue Publications.
Khalaj V, Brookman JL and Robson GD (2001) A study of the protein secretory pathway of *Aspergillus niger* using a glucoanmylase-GFP fusion protein. Fung Genet Biol 32: 55-65.
Kim YG, Raunser S, Munger C, Wagner J, Song YL, Cygler M, Walz T, Oh BH and Sacher M (2006) The architecture of the multisubunit TRAPP I complex suggests a model for vesicle tethering. Cell 127: 817-830.
Klausner RD, Donaldson JG and Lippincott-Schwartz J (1992) Brefeldin A insights into the control of membrane traffic and organelle structure. J Cell Biol 116: 1071-1080.
Konzack S, Rischitor PE, Enke C and Fischer R (2005) The role of the kinesin motor *KipA* in microtubule organization and polarized growth of *Aspergillus nidulans*. Mol Biol Cell 16: 497-506.
Korn ED (1982) Actin polymerization and its regulation by proteins from nonmuscle cells. Physiol Rev 62: 672-737.
Ladinsky MS, Mastronarde DN, McIntosh JR, Howell KE and Staehelin LA (1999) Golgi structure in three dimensions: functional insights from the normal rat kidney cell. J Cell Biol 144: 1135-1149.
Lazaro-Dieguez F, Jimenez N, Barth H, Koster AJ, Renau-Piqueras J, Llopis JL Burger KNJ and Egea G (2006) Actin filaments are involved in the maintenance of Golgi cisternae morphology and intra-Golgi pH. Cell Motil Cytoskel 63: 778-791.
Ledbetter MC and Porter KR (1964) Morphology of microtubules of plant cells. Science 144: 872-874.
Lee HH, Park JS, Chae SK, Maeng PJ and Park HM (2002) *Aspergillus nidulans* sod^{VI}*C1* mutation causes defects in cell wall biogenesis and protein secretion. FEMS 208: 253-257.
Lee MCS, Miller EA, Goldberg J, Orci L and Schekman R (2004) Bi-directional protein transport between the ER and Golgi. Annu Rev Cell Devel Biol 20: 87-123.

Letourneur F, Gaynor EC, Hennecke S, Demoltere C, Duden R, Emr SC, Riezman H and Cosson P (1994) Coatomer is essential for retrieval of dilysine-tagged proteins to the endoplasmic reticulum. Cell 79: 1199-1207.

Li A, Altosaar I, Health MC and Horgen PA (1993) Transient expression of the beta-glucuronidase gene delivered into urediniospores of *Uromyces appendiculatus* by particle bombardment. Canadian J Plant Pathol 15: 1-6.

Li Y, Edsall R Jr, Jagtap PG, Kingston DGI and Bane S (2000) Equilibrium studies of a fluorescent taxol derivative binding to microtubules. Biochemistry 39: 616-623.

López-Franco R, Bartnicki-Garcia S and Bracker CE (1994) Pulsed growth of fungal hyphal tips. Proc Natl Acad Sci USA 91: 12228-12232.

López- Franco R and Bracker CE (1996) Diversity and dynamics of the Spitzenkörper in growing hyphal tips of higher fungi. Protoplasma 195: 90-111.

López-Franco R, Howard RJ and Bracker CE (1995) Satellite Spitzenkörper in growing hyphal tips. Protoplasma 188: 85-103.

Losev E, Reinke CA, Jellen J, Strongin DE, Bevis BJ and Glick BS (2006) Golgi maturation visualized in living yeast. Nature 44: 1002-1006.

Lui H and Bretscher A (1992) Characterization of TMP1 disrupted yeast cells indicates an involvement of tropomyosin in directed vesicular transport. J Cell Biol 118: 285-300.

Malavazi I, Semighini CP, von Zeska Kress MR, Harris SD and Goldman GH (2006) Regulation of hyphal morphogenesis and the DNA damage response by the *Aspergillus nidulans* ATM homolog AtmA. Genetics 173: 99-109.

Martinelli SD (1994) *Aspergillus nidulans* as an experimental organism. Martinelli SD and Kinghorn JR (eds) In Aspergillus: *50 years on. Progress in Industrial Microbiol* 29.

Matsuura-Tokita K, Takeuchi M, Ichihara A, Mikuriya K and Nakano A (2006) Live imaging of yeast Golgi cisternal maturation. Nature 441: 1007-1010.

Maytum R, Geeves MA and Konrad M (2000) Actomyosin regulatory properties of yeast tropomyosin are dependent upon N-terminal modification. Biochemistry 39: 11913-11920.

McDaniel DP and Roberson RW (1998) Gamma tubulin is a component of Spitzenkörper and centrosomes in hyphal tip cells of *Allomcyes macrogynus*. Protoplasma 203: 118-123.

McDaniel DP and Roberson RW (2000) Microtubules are required for vesicle and mitochondrial motility and positioning in hyphal tip cells of *Allomcyes macrogynus.* Fung Genet Biol 31: 233-244.

McGoldrick CA, Gruver C and May GS (1995) *myoA* of *Aspergillus nidulans* encodes an essential myosin I required for secretion and polarized growth. J Cell Biol 128: 577-587.

Meyer S, Kaminskyj S and Heath IB (1987) Nuclear migration in a *nud* mutant of *Aspergillus nidulans* is inhibited in the presence of a quantitatively normal population of cytoplasmic microtubules. J Cell Biol 106: 773-778.

Mitchison T and Kirschner M (1984) Dynamic instability of microtubule growth. Nature 312: 237-242.

Mogelsvang S and Howell KE (2006) Global approaches to study Golgi function. Curr Opin Cell Biol 18: 438-443.

Momany M and Hamer JE (1997) Relationship of actin, microtubules, and crosswall synthesis during septation in *Aspergillus nidulans*. Cell Motil Cytoskel 38: 373-384.
Momany M, Westfall PJ and Abramowsky G (1999) *Aspergillus nidulans swo* mutants show defects in polarity establishment, polarity maintenance and hyphal morphogenesis. Genetics 151: 557-567.
Moore RT and McAlear JH (1962) Fine structure of mycota. 7. Observations on septa of Ascomycetes and Basidiomycetes. Amer J Bot 49: 86-94.
Morinaga N, Tsai SC, Moss J and Vaughan M (1996) Isolation of a brefeldin A-inhibited guanine nucleotide-exchange protein for ADP ribosylation factor (ARF) 1 and ARF3 that contains a Sec7-like domain. Proc Natl Acad Sci USA 93: 12856-12860.
Morris NR and Enos AP (1992) Mitotic gold in a mold: *Aspergillus* genetics and the biology of mitosis. Trends Genet 8: 32-37.
Morris NR, Xiang X and Beckwith SM (1995) Nuclear migration advances in fungi. Trends Cell Biol 5: 278-282.
Morton WM, Ayscough KR and McLaughlin PJ (2000) Latrunculin alters the actin-monomer subunit interface to prevent polymerization. Nature Cell Biol 2: 376-378.
Moss MO (1998) Recent studies of mycotoxins. J Applied Microbiol Symposium Suppl 84: 62S-72S.
Mouriño-Pérez RR, Roberson RW and Bartnicki-García S (2006) Microtubule dynamics and organization during hyphal growth and branching in *Neurospora crassa*. Fung Genet Biol 43: 389-400.
Munro S (1991) Sequences within and adjacent to the transmembrane segment of alpha-2,6-sialyltransferase specify Golgi retention. EMBO J 10: 3577–3588.
Nebenfuhr A, Gallagher LA, Dunahay TG, Frohlick JA, Mazurkiewicz AM, Meehl JB and Staehelin LA (1999) Stop-and-go movements of plant Golgi stacks are mediated by the acto-myosin system. Plant Physiol 121: 1127-1141.
Nèeman I, Fishelson L and Kashman Y (1975) Isolation of a new toxin from the sponge *Latrunculia magnifica* in the Gulf of Aqaba, Red sea. Marine Biol 30: 293-296.
Nikolaev I, Mathieu M, van de Vondervoort PJI, Visser J and Felenbok B (2002) Heterologous expression of the *Aspergillus nidulans alcR-alcA* system in *Aspergillus niger*. Fung Genet Biol 37: 89-97.
Nogales E, Wolf SG**,** Khan IA, Ludueña RF and Downing KH (1995) Structure of tubulin at 6.5 Å and location of the taxol-binding site. Nature 375: 424-427.
Novick P and Botstein D (1985) Phenotypic analysis of temperature-sensitive yeast actin mutants. Cell 40: 405-416.
Oakley BR and Morris NR (1980) Nuclear movement is β-tubulin dependent in *Aspergillus nidulans*. Cell 51: 255-262.
Oakley BR and Morris NR (1981) A β-tubulin mutation in *Aspergillus nidulans* that blocks microtubule function without blocking assembly. Cell 24: 837-845.
Oakley BR, Oakley CE, Yoon Y and Jung MK (1990) γ-tubulin is a component of the spindle-pole-body that is essential for microtubule function in *Aspergillus nidulans.* Cell 61: 1289-1301.
Odell JT, Nagy F and Chua NH (1985) Identification of DNA sequences required for activity of the cauliflower mosaic virus 35S promoter. Nature 313: 810-812.

Osmani SA, May GS and Morris NR (1987) Regulation of the messenger RNA levels of *nimA*, a gene required for the G2-M transition in *Aspergillus nidulans.* J Cell Biol 104: 1495-1504.

Ovechkina Y, Maddox P, Oakley CE, Xiang X, Osmani SA, Salmon ED and Oakley BR (2003) Spindle formation in *Aspergillus* is coupled to tubulin movement into the nucleus. Mol Biol Cell 14: 2192-2200.

Palade GE (1975) Intracellular aspects of the processing of protein synthesis. Science. 189: 347-354.

Palmer DRJ, Balogh H, Ma G, Zhou X, Marko M and Kaminskyj SGW (2004) Synthesis and antifungal properties of compounds which target the alpha-aminoadipate pathway. Die Pharmazie 59: 93-98.

Papoulas O, Hays TS and Sisson JC (2005) The golgin *Lava lamp* mediates dynein-based Golgi movements during *Drosophila* cellularization. Nature Cell Biol 7: 612-618.

Patterson TF, Kirkpatrick WR, White M, Hiemenz JW, Wingard JR, Dupont B, Rinaldi MG Stevens DA and Graybill JR (2000) Invasive aspergillosis: disease spectrum, treatment practices, and outcomes. Medicine (Baltimore) 79: 250-260.

Payne GA Nierman WC Wortman JR, Pritchard BL, Brown D, Dean RA, Bhatnagar D, Cleveland TE, Machida M and Yu J (2006) Whole genome comparison of *Aspergillus flavus* and *A. oryzae*. Medical Mycology 44 (Suppl. 1): S9-S11.

Peyroche A, Paris S and Jackson CL (1996) Nucleotide exchange on ARF mediated by yeast Gea1 protein. Nature 384: 479-481.

Plamann M, Minke PF, Tinsley JH and Bruno KS (1994) Cytoplasmic dynein and actin related protein *Arp1* are required for normal nuclear distribution in filamentous fungi. J Cell Biol 127: 139-149.

Pollard TD, Selden SC and Maupin P (1984) Interaction of actin filaments with microtubules. J Cell Biol 99: 33s-37s.

Prendergast F and Mann K (1978) Chemical and physical properties of aequorin and the green fluorescent protein isolated from *Aequorea forskålea*. Biochemistry 17: 3448-3453.

Pruyne D, Evangelista M, Yang C, Bi E, Zigmond S, Bretscher A and Boone C (2002) Role of formins in actin assembly: Nucleation and barbed-end association. Science 297: 612-615.

Pushalker S and Rao KK (1995) Production of β-glucosidase by *Aspergillus terreus.* Curr Microbiol 30: 255-258.

Pushalker S and Rao KK (1998) Ethanol fermentation by a cellulolytic fungus *Aspergillus terreus*. World J Microbiol Biotech 14: 289-291.

Rao S, Horwitz B and Ringel I (1992) Direct photoaffinity labeling of tubulin with taxol. J Natl Cancer Inst 84: 785-788.

Rao S, Krauss NE, Heerding JM, Swindell CS, Ringel I, Orr GA and Horwitz SB (1994) 3'-(p-azidobenzamido) taxol photolabels the N-terminal 31 amino acids of beta-tubulin. J Biol Chem 269: 3132-3134.

Raper KB and Fennel DI (1965) *The Genus* Aspergillus. The Williams & Wilkins Co. Baltimore.

Raudaskoski M, Mao WZ and Yli-Mattila T (1994) Microtubule cytoskeleton in hyphal growth: Response to nocodazole in a sensitive and a tolerant strain of the homobasidiomycete *Schizophyllum commune*. Eur J Cell Biol 64: 131-141.

Raudaskoski M, Rupeš I and Timonen S (1991) Immunofluorescence microscopy of the cytoskeleton in filamentous fungi after quick-freezing and low-temperature fixation. Exp Mycol 15: 167-173.
Rida PCC, Nishikawa A, Won GY and Dean N (2006) Yeast-to-hyphal transition triggers formin-dependent Golgi localization to the growing tip in *Candida albicans*. Mol Biol Cell 17: 4364-4378.
Riquelme M, Fischer R and Bartnicki-Garcia S (2003) Apical growth and mitosis are independent processes in *Aspergillus nidulans*. Protoplasma 222: 211-215.
Riquelme M, Gierz G and Bartnicki-Garcia S (2000) Dynein and dynactin deficiencies affect the formation and function of the Spitzenkörper and distort hyphal morphogenesis of *Neurospora crassa.* Microbiology 146: 1743-1752.
Riquelme M, Reynaga-Peña CG, Gierz G and Bartnicki-García S (1998) What determines growth direction in fungal hyphae? Fung Genet Biol 24: 101-109.
Riquelme M, Roberson RW, McDaniel DP and Bartnicki-Garcia S (2002) The effects of *ropy-1* mutation on cytoplasmic organization and intracellular motility in mature hyphae of *Neurospora crassa*. Fung Genet Biol 37: 171-179.
Ritzenthaler C, Nebenfuhr A, Movafeghi A, Stussi-Garaud C, Behnia L, Pimpl P, Staehelin LA and Robinson DG (2002) Reevaluation of the effects of brefeldin A on plant cells using tobacco Bright Yellow 2 cells expressing Golgi-targeted green fluorescent protein and COPI antisera. Plant Cell 14: 237-261.
Robinson MS and Kreis TE (1992) Recruitment of coat proteins onto Golgi membranes in intact and permeabilized cells: effects of brefeldin A and G-protein activators. Cell 69: 129-138.
Romero B, Turner G, Olivas I, Laborda F and De Lucas JR (2003) The *Aspergillus nidulans alcA* promoter drives tightly regulated conditional gene expression in *Aspergillus fumigatus* permitting validation of essential genes in this human pathogen. Fung Genet Biol 40: 103-114.
Ross JL and Fygenson DK (2003) Mobility of taxol in microtubule bundles. Biophysical J 84: 3959-3967.
Rothman JE (1996) The protein machinery of vesicle budding and fusion. Protein Sci 5: 185-194.
Rothman JE and Wieland FT (1996) Protein sorting by transport vesicles. Science 272: 227-234.
Rupeš I, Mao WZ, Astrom H and Raudaskoski M (1995) Effects of nocodazole and brefeldin A on microtubule cytoskeleton and membrane organization in the homobasidiomycete *Schizophyllum commune*. Protoplasma 185: 212-221.
Saint-Jore-Dupas C, Gomord V and Paris N (2004) Protein localization in the plant Golgi apparatus and the trans-Golgi network. Cell Mol Life Sci 61: 159-171.
Sampson K and Heath IB (2005) The dynamic behaviour of microtubules and their contributions to hyphal tip growth in *Aspergillus nidulans*. Microbiology (Reading) 151: 1543-1555.
Sampson K, Lew RR and Heath IB (2003) Time series analysis demonstrates the absence of pulsatile hyphal growth. Microbiology (Reading) 149: 3111-3119.
Satiat-Jeunemaître B, Steele C and Hawes C (1996) Golgi-membrane dynamics are cytoskeleton dependent: A study on Golgi stack movement induced by brefeldin A Protoplasma 191: 21-33.

Schiff PB (2000) Taxol as a radiation sensitizer. Patent: The Trustees of Columbia University in the City of New York, Patent Class: 514-449.
Schiff PB, Fant J and Horwitz SB (1979) Promotion of microtubule assembly *in-vitro* by taxol. Nature 277: 665-667.
Scholey JM, Porter ME, Grisson PM and McIntosh JR (1985) Identification of kinesin in sea urchin eggs, and evidence for its localization in the mitotic spindle. Nature 318: 483-486.
Schuchardt I, Abmann D, Thines E, Schuberth C and Steinberg G (2005) Myosin-V, kinesin-1, and kinesin-3 cooperate in hyphal growth of the fungus *Ustilago maydis*. Mol Bio Cell 16: 5191-5201.
Schwientek T, Lorenz C and Ernst JF (1995) Golgi localization in yeast is mediated by the membrane anchor region of rat liver sialyltransferase. J Biol Chem 270: 5483-5489.
Sciaky N, Presley J, Smith C, Zaal KJM, Cole N, Moreira JE, Terasaki M, Siggia E and Lippincott-Schwartz J (1997) Golgi tubule traffic and the effects of brefeldin A visualized in living cells. J Cell Biol 139: 1137-1155.
Seiler S, Nargang FE, Steinberg G and Schliwa M (1997) Kinesin is essential for cell morphogenesis and polarized secretion in *Neurospora crassa*. EMBO J 16: 3025-3034.
Serafini T, Orci L, Amherdt M, Brunner M, Kahn RA and Rothman JE (1991) ADP-ribosylation factor is a subunit of the coat of Golgi-derived COP-coated vesicles: A novel role for a GTP-binding protein. Cell 67: 239-253.
Sharpless KE and Harris SD (2002) Functional characterization and localization of the *Aspergillus nidulans* formin SEPA. Mol Biol Cell 13: 469-479.
Shaw BD and Upadhyay S (2005) *Aspergillus nidulans swoK* encodes an RNA binding protein that is important for cell polarity. Fung Genet Biol 42: 862-872.
Shepherd VA, Orlovich DA and Ashford AE (1993) A dynamic continuum of pleomorphic tubules and vacuoles in growing hyphae of a fungus. J Cell Sci 104: 495-507.
Shi X, Sha Y and Kaminskyj SGW (2004) *Aspergillus nidulans hypA* regulates morphogenesis through the secretion pathway. Fung Genet Biol 41: 75-88.
Silverman-Gavrila LB and Lew RR (2000) Calcium and tip growth in *Neurospora crassa*. Protoplasma 213: 203-217.
Silverman-Gavrila LB and Lew RR (2001) Regulation of the tip-high [Ca^{2+}] gradient in growing hyphae of the fungus *Neurospora crassa*. Eur J Cell Biol 80: 379-390.
Silverman-Gavrila LB and Lew RR (2003) Calcium gradient dependence of *Neurospora crassa* hyphal growth. Microbiology (Reading) 149: 2475-2485.
Spector I, Shocket NR, Kashman Y and Groweiss A (1983) Latrunculins: novel toxins that disrupt micro filament organization in cultured cells. Science 219: 493-495.
Steinberg G, Wedlich-Soeldner R, Brill M and Schulz I (2001) Microtubules in the fungal pathogen *Ustilago maydis* are highly dynamic and determine cell polarity. J Cell Sci 114: 609-622.
Suelmann R and Fischer R (2000a) Mitochondrial movement and morphology depend on an intact actin cytoskeleton in *Aspergillus nidulans*. Cell Mot Cytoskel 45: 42-50.
Suelmann R and Fischer R (2000b) Nuclear migration in fungi – different motors at work. Res Microbiol 151: 247-254.

Suelmann R, Sievers N and Fischer R (1997) Nuclear traffic in fungal hyphae: *in vivo* study of nuclear migration and positioning in *Aspergillus nidulans*. Mol Microbiol 25: 757-769.

Sun L, Cai H, Xu W, Hu Y and Lin Z (2002) CaMV 35S promoter directs beta-glucuronidase expression in *Ganoderma lucidum* and *Pleurotus citrinopileatus*. Mol Biotech 20: 239-244.

Temperli E, Roos UP and Hohl HR (1990) Actin and tubulin cytoskeleton in germlings of the oomycete fungus *Phytophthora infestans*. Eur J Cell Biol 53: 75-88.

Temperli E, Roos UP and Hohl HR (1991) Germ tube growth and the microtubule cytoskeleton in *Phytophthora infestans* effects of antagonists of hyphal growth microtubule inhibitors and ionophores. Mycol Res 95: 611-617.

That TCCT, Rossier C, Barja F, Turian G and Roos UP (1988) Induction of multiple germ tubes in *Neurospora crassa* by antitubulin agents. Eur J Cell Biol 46: 68-79.

Timberlake WE and Clutterbuck AJ (1994) Genetic regulation of conidiation. In Martinelli SD and Kinghorn JR (eds) Aspergillus: *50 years on. Progress in Industrial Microbiol* 29.

Toews MW, Warmbold J, Konzack S, Rischitor P, Veith D, Vienken K, Vinuesa C, Wei H and Fischer R (2004) Establishment of mRFP1 as a fluorescent marker in *Aspergillus nidulans* and construction of expression vectors for high-throughput protein tagging using recombination in vitro (GATEWAY). Curr Genet 45: 383-389.

Torralba S and Heath IB (2000) Cytoskeletal and Ca^{2+} regulation of hyphal tip growth and initiation. Curr Top Dev Biol 51: 135-187.

Torralba S, Pisabarro AG and Ramirez L (2004) Immunofluorescence microscopy of the microtubule cytoskeleton during conjugate division in the dikaryon *Pleurotus ostreatus* N001. Mycologia 96: 41-51.

Torralba S, Raudaskoski M, Pedregosa AM and Laborda F (1998) Effect of cytochalasin A on apical growth, actin cytoskeleton organization and enzyme secretion in *Aspergillus nidulans.* Microbiology (Reading) 144: 45-53.

Trinci APJ (1973) The hyphal growth unit of wild type and spreading colonial mutants of *Neurospora crassa*. Arch Microbiol 91: 127-136.

Trinci APJ and Morris NR (1979) Morphology and growth of a temperature sensitive mutant of *Aspergillus nidulans* which forms aseptate mycelia at non-permissive temperature. J Gen Microbiol 114: 53-59.

Tsien R (1998) The green fluorescent protein. Annu Rev Biochem 67: 509-544.

Uchida M, Roberson RW, Chun S-J and Kim D-S (2005) *In vivo* effects of the fungicide ethaboxam on microtubule integrity in *Phytophthora infestans*. Pest Management Sci 61: 787-792.

Vale RD, Reese TS and Sheetz MP (1985) Identification of a novel force-generating protein, kinesin, involved in microtubule-based motility. Cell 42: 39-50.

Verweij PE, Meis JFGM, van den Hurk P, Zoll J, Samsom RA and Melchers WJG (1995) Phylogenetic relationships of five species of *Aspergillus* and related taxa as deduced by comparison of sequences of small subunit ribosomal RNA. J Med Vet Mycol 33: 185-190.

Virag A and Griffiths AJF (2004) A mutation in the *Neurospora crassa* actin gene results in multiple defects in tip growth and branching. Fung Genet Biol 41: 213-225.

Waters MG, Serafini T and Rothman JE (1991) 'Coatomer': a cytosolic protein complex containing subunits of non-clathrin-coated Golgi transport vesicles. Nature 349: 248-251.

Weber I, Assmann D, Thines E and Steinberg G (2006) Polar localizing class V myosin chitin synthases are essential during early plant infection in the plant pathogenic fungus *Ustilago maydis*. Plant Cell 18: 225-242.

Wee EGT, Sherrier DJ, Prime TA and Dupree P (1998) Targeting of active sialyltransferase to the plant Golgi apparatus. Plant Cell 10: 1759-1768.

Weinberger A, Kamena F, Kama R, Spang A and Gerst JE (2005) Control of Golgi morphology and function by Sed5 t-SNARE phosphorylation. Mol Biol Cell 16: 4918-4930.

Weresub LK and Pirozynski KA (1979) Pleomorphism of fungi as treated in the history of mycology and nomenclature. In Kendrick WB (ed) *The Whole Fungus*. National Museum of Natural Sciences. Ottawa ON. 17-25.

Whittaker SL, Lunness P, Milward KJ, Doonan JH and Assinder SJ (1999) *sod*^{VI}*C* is an α-COP-related gene that is essential for establishing and maintaining polarized growth in *Aspergillus nidulans*. Fung Genet Biol 26: 236-252.

Williamson RE (1991) Observations of cortical microtubules in plant cells. Intl Rev Cytol 129: 135-206.

Xu X-J, Jhang J, Li X, Yu M-M and Ru B-G (2004) Expression of human intestinal trefoil factor (hITF) in transgenic *Pleurotus ostreatus* and its ELISA assay. Weishengwu Xuebao 44: 609-612.

Yang Y (2003) Cloning and analysis of an *Aspergillus nidulans* Sec7 domain coding gene. Univ of Saskatchewan, MSc Thesis.

Yokoyama K, Kahi H, Nishimura K and Miyaji M (1990) The role of microfilaments and microtubules in apical growth and dimorphism of *Candida albicans*. J Gen Microbiol 136: 1067-1076.

Yoon Y and Oakley BR (1995) Purification and characterization of assembly competent tubulin from *Aspergillus nidulans*. Biochemistry 34: 6373-6381.

Yuste R (2005) Fluorescence microscopy today. Nat Methods 2: 902-904.

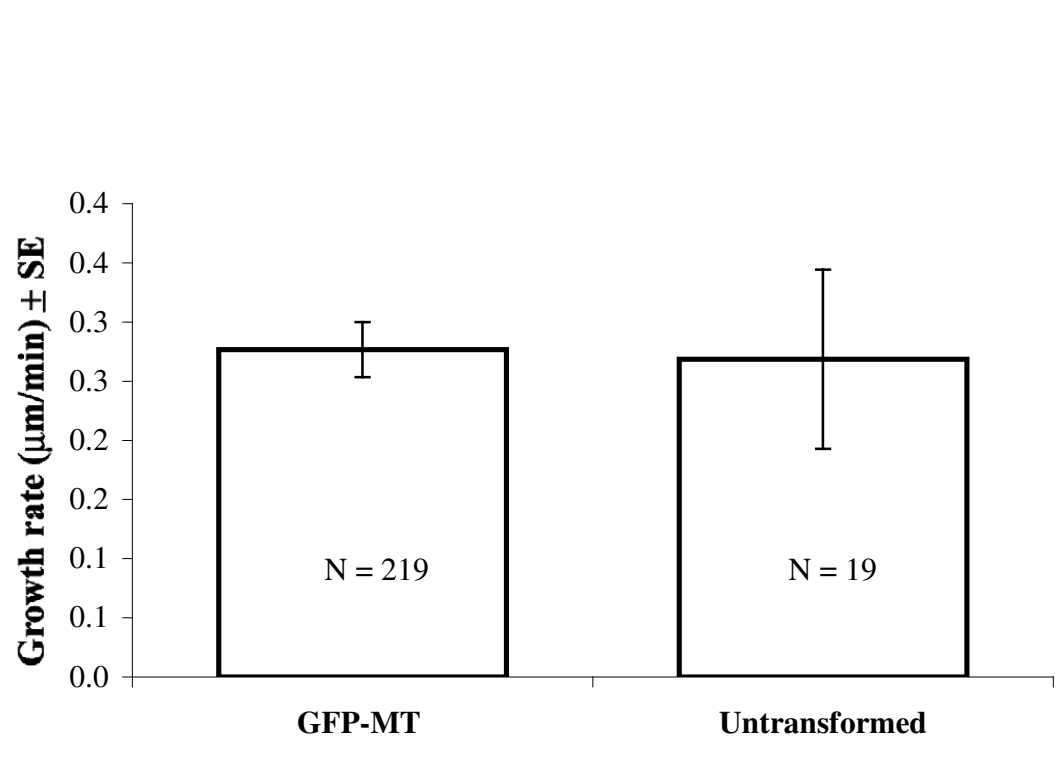

Figure A-1. Tagging of α-tubulin with GFP does not alter hyphal growth rate. The growth rates of *Aspergillus nidulans* hyphae transformed with GFP-α-tubulin (labeled GFP-MT) do not differ significantly compared to the hyphal growth rates of A28 (labeled untransformed), a wildtype *A. nidulans* strain not transformed with α-tubulin tagged with GFP ($P > 0.1$). N = number of hyphae.

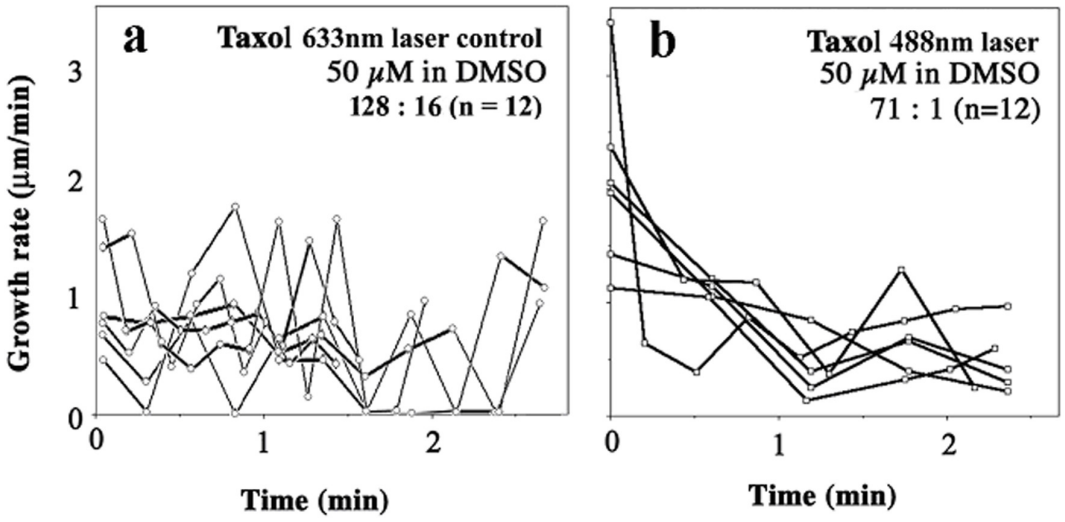

Figure A-2. Taxol induces sensitivity to 488 nm, but not 633 nm irradiation in *Aspergillus nidulans* hyphae with GFP tagged α-tubulin. Growth rates are calculated for 15-30 s intervals. Both graphs use the same y-axis. Each line represents a different hyphae; only a representative subset from each treatment is shown for visual clarity. A tally of growing : non-growing intervals from a larger number of cells (n) is shown for both treatment populations. a) Repeated irradiation of taxol-treated *A. nidulans* hyphae with 633nm radiation (a wavelength not absorbed by GFP) does not appear to reduce hyphal growth rate during imaging. b) However, repeated irradiation of taxol-treated *A. nidulans* hyphae with 488nm radiation (the wavelength that is absorbed maximally by GFP) does appear to reduce hyphal growth rate during imaging. The overall average hyphal growth rate of taxol treated hyphae imaged with 633nm radiation does not differ significantly from that of taxol treated hyphae imaged with 488nm radiation in Figure 2-3d ($P = 0.5$).

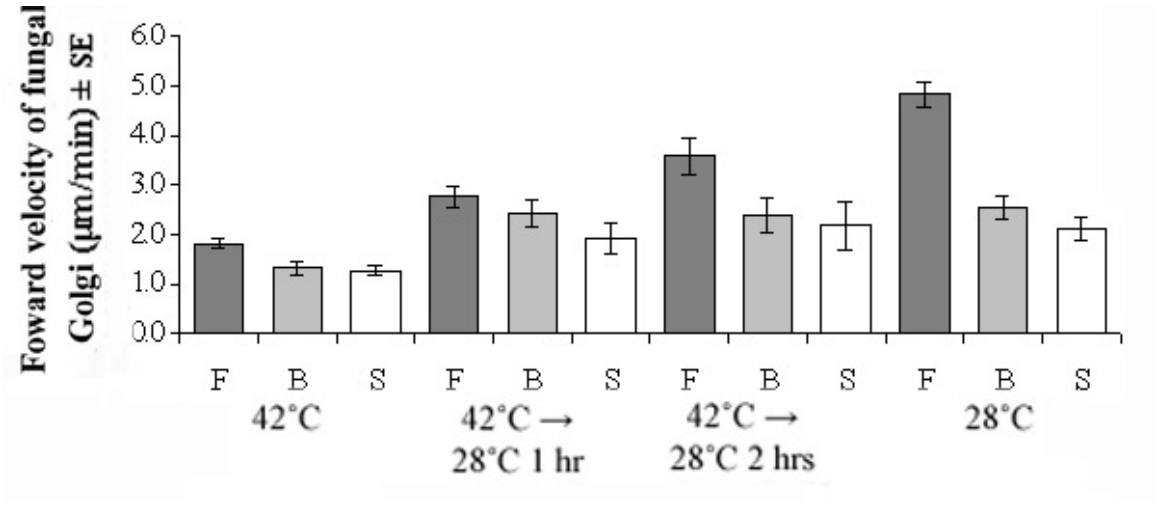

F = Forward, B = Backward, S = Sideways

Figure A-3. Forward, backward and sideways fungal Golgi movement in *Aspergillus nidulans* hyphae. Forward fungal Golgi movement was faster than backwards or sideways under all conditions observed *A. nidulans* hyphae. In addition, the relationship between the rate of forward fungal Golgi movement and hyphal polarity (as determined by growth temperature, 28 ºC and 42 ºC) was not observed found to be significant for the relationship between the rate of backwards or sideways fungal Golgi movement and hyphal polarity.

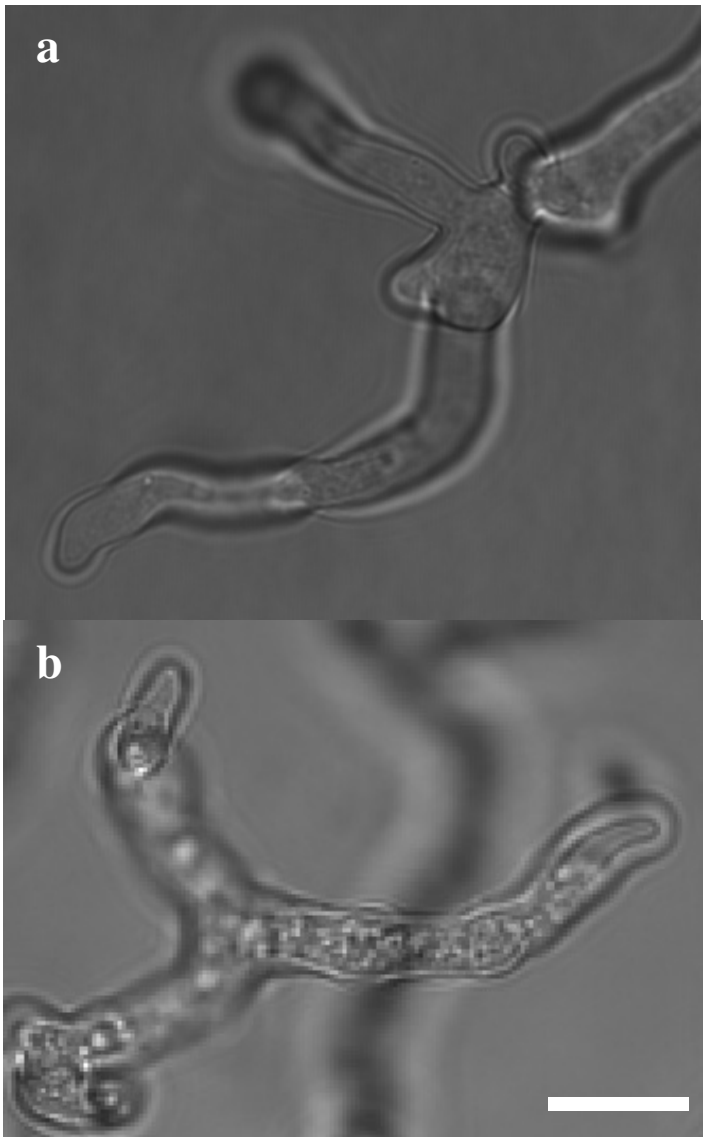

Figure A-4. Morphological impact of overnight treatment of *Aspergillus nidulans* hyphae with 1 and 2.5 µg/mL benomyl. a) A representative *A. nidulans* hypha grown overnight in a moist chamber in liquid media containing 1 µg/mL benomyl. b) A representative *A. nidulans* hypha grown overnight in a moist chamber in liquid media containing 2.5 µg/mL benomyl. Bar = 5 µm.